

Addendum:

- Page 47** The paragraph pasted at the back of page 46 should be read before paragraph 2 in page 47.
- Page 106** The paragraph pasted at the back of page 105 should be read before viewing Figure 5.7.
- Page 118** The paragraph marked "1" pasted at the back of page 117 should be read instead of the paragraph starting with "*Titration curves of humic substances...*" in line 5 paragraph 1, page 118.
- The paragraph marked "2" pasted at the back of page 117 should be read instead of the sentence starting with: "*The initial size...*" in line 5 of paragraph 3, page 118.
- Page 135** The paragraph pasted at the back of page 134 should be read after the first paragraph in the conclusion section.
- Page 180** The paragraph pasted at the back of page 179 should be read after the third paragraph in page 180.

Errata:

- Abstract** In page 2 paragraph 3 line 5 "SRFA" should read "*Suwannee River Fulvic Acid (SRFA)*"
- Page 3** In paragraph 2 line 6 "*ranges from*" should read "*ranges for size are from*"
- Page 5** In paragraph 2 line 5 "*Suwannee River fulvic acid*" should read "*Suwannee River fulvic acid (SRFA)*"
- Page 25** In paragraph 2 line 8 "*molecular*" should read "*molecular weight*"
- Page 25** In paragraph 3 line 5 "*Polystyrenesulphonates*" should read "*Poly styrenesulphonates (PSS)*"
- Page 26** In paragraph 1 line 6 "*resembled the humic substances more*" should read "*more closely resembled the humic substances*"
- Page 37** In reference 24 "*a.s. M*" should read "*and Schnitzer, M.,*"
- Page 122** In paragraph 2 line 1 "*A decrease is noted...*" should read "*A decrease at high ionic strength is noted...*"
- Page 126** In paragraph 4, line 1 "*Cameron, Swift and Hayes*" should read "*Cameron et al., Hayes and Swift and Swift*"

H24/3108

MONASH UNIVERSITY
THESIS ACCEPTED IN SATISFACTION OF THE
REQUIREMENTS FOR THE DEGREE OF
DOCTOR OF PHILOSOPHY

ON..... 11 December 2001

.....
by Sec. Research Graduate School Committee

Under the copyright Act 1968, this thesis must be used only under the normal conditions of scholarly fair dealing for the purposes of research, criticism or review. In particular no results or conclusions should be extracted from it, nor should it be copied or closely paraphrased in whole or in part without the written consent of the author. Proper written acknowledgement should be made for any assistance obtained from this thesis.

USE OF FLOW FIELD-FLOW
FRACTIONATION
FOR THE CHARACTERISATION OF
HUMIC SUBSTANCES

BY

SHOELEH ASSEMI

BACHELOR OF SCIENCE

MASTER OF SCIENCE

A THESIS SUBMITTED IN FULFILMENT OF THE REQUIREMENTS
FOR THE DEGREE OF DOCTOR OF PHILOSOPHY

COOPERATIVE RESEARCH CENTRE FOR FRESHWATER ECOLOGY AND
WATER STUDIES CENTRE
DEPARTMENT OF CHEMISTRY
MONASH UNIVERSITY
MELBOURNE
AUSTRALIA

DECEMBER 2000

STATEMENT

This thesis contains no material which I have presented for any other degree or diploma at any university, and to the best of my knowledge and belief, no material previously published or written by any other person, except where due reference is made in the text of this thesis.



Shoeleh Assemi

CRC for Freshwater Ecology and

Water Studies Centre

Department of Chemistry

Monash University

Melbourne

Australia

ACKNOWLEDGEMENTS

I would like to extend my sincere thanks towards my supervisors Dr Ron Beckett and Professor Barry Hart for their assistance, encouragement and support throughout this work. I am particularly indebted to my main supervisor Ron for letting me pursue my ideas, his advice, constructive criticism and efforts for establishing collaboration with other groups where possible.

I gratefully acknowledge the scholarships provided by Monash University and CRC for Freshwater Ecology to support this study.

So many people have helped me throughout this thesis. I thank Drs Iko Burgar (CSIRO manufacturing science), Patrick Hartley (CSIRO molecular science) and Peter Nichols for their help in NMR, atomic force microscopy and Biosym II modelling software, respectively. I am indebted to Dr Ian McKelvie for lending me his computer in the writing up stage. I am also thankful to Dr Don McGilvery for his valuable assistance with the computer and printing problems. Comments of Dr Mike Grace on Chapter 8 are much appreciated. I would like to thank everyone in the Water Studies Centre, especially the FFF group members for their friendship, help and support and to FIA group for their joyful company. Special thanks to Rod Ferdinands for proofreading various chapters.

I would like to thank my parents, my sister and my bother for their ongoing, unstinting support, believing in me and respecting my goals and decisions throughout my life.

Heartful thanks to my husband Soheyl for his invaluable help and support throughout. For always encouraging me and for taking care of all the responsibilities to enable me complete this thesis.

Last but not least, I thank my son Arash, for being so supportive, encouraging and understanding. His drawings and notes about Mummy s thesis and his warm hugs every time a chapter was completed, will always remain among the best memories of this period of my life.

**This thesis is gratefully dedicated to my parents
for their endless support**

∞

ABSTRACT

Humic substances are ubiquitous in the environment. They are complex mixtures of organic compounds resulting from the breakdown of vegetable and animal material in the environment and usually comprise about 50% of the organic matter in natural aquatic systems [1]. Their size and structure depend on their origin. In general aquatic humic substances are known to be less polydisperse and smaller in size than terrestrial humic substances.

Although many studies have been reported on the relative size of humic substances, their sizes and molecular weights still remain open to conjecture. One major reason for this debate is the polydispersity of humic substances. What is often measured is an average size or weight of the whole set of molecules. Each technique measures a different parameter and hence may give a different average. Most of the methods are not absolute and need calibration. To achieve a better understanding of the size and molecular weight of humic substances a separation technique is desirable that can provide a distribution of these parameters.

This thesis uses flow field-flow fractionation (FIFFF) as a separation technique to determine distributions of diffusion coefficient, size and molecular weight of humic substances. Results obtained from FIFFF have been compared to those obtained from several other techniques, namely fluorescence correlation spectroscopy, pulsed field gradient NMR, high pressure size exclusion chromatography and atomic force

microscopy. The results obtained from these techniques fall within the same range and are also close to the values obtained from colligative properties.

FIFFF was used to measure the size and molecular weight distributions of natural organic matter fractions separated by ultrafiltration (UF). UF is still one of the most commonly used techniques for isolation and fractionation of humic substances, despite the disadvantages frequently mentioned in the literature [2, 3]. The results of this study suggest that separation of natural organic matter by UF membranes is based on molecular structure as well as size.

FIFFF was used to measure the size of several humic substances in solutions of different pH and salt concentration. The results indicate that humic substances aggregate and thus increase in size with increasing salt concentration and with decreasing pH. It was found that the presence of the cellulose acetate membrane used to cover the accumulation wall in the FIFFF channel limits the analysis to moderate solution pH and salt concentrations. As a result it is recommended that different membranes and/or other FIFFF run strategies be tested to extend the analysis range of FIFFF for humic substances.

Atomic force microscopy is another new technique that has great potential for the characterisation of humic substances. In this thesis atomic force microscopy was used for imaging humic substances both in moist and solution conditions. AFM was also used to measure the interactive forces between a silica probe and a goethite surface. The effect of introducing SRFA onto the goethite substrate was also studied. Thus the forces between humic coated surfaces can be measured directly.

Interactions of orthophosphate with a sediment humic acid was studied using solid state ^{13}C NMR and solution ^{31}P NMR spectroscopy. The results suggest that there might be a direct interaction between humic acid and orthophosphate, possibly through an esterification reaction.

The subject of humic substances is so complex that after several decades of systematic study and characterisation attempts, certain questions have never changed and we ask the same fundamental questions as the newcomers did forty years ago, as commented by Steelink [4]. This thesis has attempted to explore the use of several new techniques to characterise humic substances. The main focus has been the study of their size and molecular weight using FIFFF. It is hoped that the results of this study will provide the basis for further exploration of the issues discussed here.

1. Thurman, E.M., Organic Geochemistry of Natural Waters, Martinus Nijhoff/Dr W. Junk publishers. Dordrecht, 1985 .
2. Aiken, G.R., Evaluation of ultrafiltration for determining molecular weight of fulvic acid., *Environmental Science and Technology*, 18 (1984) 978-981 .
3. Buffle, J., Perret, D., and Newman, M., The use of filtration and ultrafiltration for size fractionation of aquatic particles, colloids and macromolecules, in. Buffle J. and H.P. Van Leeuwen (Ed.), *Environmental Particles*, Lewis Publishers, Michigan. 1984, pp. 171-230 .
4. Steelink, C., What is humic acid? A perspective of the past forty years., in Davis, G. and Ghabbour, E.A, (Ed.), *Understanding Humic Substances*, The Royal Society of Chemistry, Cambridge. 1999, pp. 1-8 .

PUBLICATIONS AND PRESENTATIONS BASED ON THE CONTENTS OF THIS THESIS

Publications:

1. Newcombe, G., Drikas, M., Assemi, S., and Beckett, R., The influence of the characterised natural organic material on activated carbon adsorption:1. Characterisation of concentrated reservoir NOM., *Water Research*, 31 (1997) 965-972.
2. Pelekani, C., Newcombe, G., Snoeyink, V.L., Hepplewhite, C., Assemi, S., and Beckett, R., Characterisation of natural organic matter using high performance size exclusion chromatography, *Environmental Science and Technology*, 33 (1999) 2807-2813.
3. Lead, J.R., Wilkinson, K. J., Balnois, E., Cutak, B. J., Larive, C. K., Assemi, S. and Beckett, R., Diffusion coefficients and polydispersities of the Suwannee River fulvic acid: Comparison of fluorescence correlation spectroscopy, pulsed-field gradient nuclear magnetic resonance, and flow field-flow fractionation, *Environmental Science and Technology*, 34 (2000) 3508-3513.
4. Assemi, S., Newcombe, G., Heplewhite, C., and Beckett R., Characterisation of natural organic matter fractions separated by ultrafiltration using flow field-flow fractionation, *Water Research* (submitted).

Conference presentations:

1. Assemi, S., and Beckett, R. Use of flow field-flow fractionation in characterisation of humic substances, *Humic Substances: Science and Commercial Applications*, Monash University, Melbourne, February 2000.

2. Assemi, S., Lead, J.R., Wilkinson, K.J., Cutak, B., Larive, C., Buffle, J., and Beckett, R. Study of the effect of solution pH and salt concentration on the diffusion coefficient of Suwannee River fulvic acid, International Symposium of Field-Flow Fractionation , FFF-99, Paris, France. September 1999.
3. Assemi, S., Newcombe G, Hepplewhite C., Pelekani, C., and Beckett, R. Evaluation of performance of ultrafiltration membranes for characterisation of natural organic matter using flow field-flow fractionation and SEC, 9th International Meeting of the Humic Substances Society, Adelaide, Australia, September 1998.
4. Assemi, S. Hartley, P.G., Scales, P.J., and Beckett, R.. Investigation of adsorbed humic substances using atomic force microscopy, 9th International meeting of the humic Substances Society, Adelaide, Australia, September 1998.
5. Assemi, S., Newcombe, G., Hepplewhite, C., and Drikas, M., Use of flow field-flow fractionation to characterise natural organic matter separated by ultrafiltration, International Symposium on Refractory Organic Matters in the Environment (ROSE), Karlsruhe, Germany, October 1997.
6. Assemi, S and Beckett, R. Characterisation of humic substances separated by membrane ultrafiltration using flow field-flow fractionation., International Symposium of Field-Flow Fractionation , FFF-96, Ferrara, Italy. September 1996.

TABLE OF CONTENTS

CHAPTER 1		
OVERVIEW OF THE THESIS		1
<hr/>		
1.1	INTRODUCTION	1
1.2	ENVIRONMENTAL SIGNIFICANCE OF HUMIC SUBSTANCES	2
1.3	SIZE AND MOLECULAR WEIGHT OF HUMIC SUBSTANCES	2
1.4	USE OF FLOW FIELD-FLOW FRACTIONATION (FIFFF) IN CHARACTERISATION OF HUMIC SUBSTANCES	4
1.5	RESEARCH OBJECTIVES	4
1.6	STRUCTURE OF THE THESIS	5
1.7	REFERENCES	7
 CHAPTER 2		
DETERMINATION OF SIZE AND MOLECULAR WEIGHT OF HUMIC SUBSTANCES. A LITERATURE REVIEW		12
<hr/>		
2.1	INTRODUCTION	12
2.2	ABSOLUTE METHODS FOR MEASUREMENT OF SIZE AND MOLECULAR WEIGHT OF HUMIC SUBSTANCES	14
2.2.1	Colligative properties	14
2.2.2	Ultracentrifugation	16
2.2.3	Small angle x-ray scattering	19
2.2.4	Light scattering techniques	21
2.2.5	Field-flow fractionation	23
2.2.6	Imaging techniques	23
2.3	METHODS THAT REQUIRE CALIBRATION FOR SIZE AND/OR MOLECULAR WEIGHT CALCULATION	24
2.3.1	Size exclusion chromatography	24
2.3.2	Ultrafiltration	26
2.4	METHODS THAT USE MATHEMATICAL APPROXIMATIONS	26
2.4.1	Potentiometric titrations	26
2.5	CONCLUSIONS	33
2.6	REFERENCES	34

CHAPTER 3

FLOW FIELD-FLOW FRACTIONATION 42

3.1	INTRODUCTION	42
3.2	FIELD-FLOW FRACTIONATION	42
3.3	DATA TREATMENT	46
3.3.1	Conversion of fractogram to size and MW distribution	46
3.3.2	Relationship between the UV signal and the molar concentration	48
3.3.3	Calculation of M_n and M_w utilising the UV signal	49
3.3.4	Calculation of d_n and d_w utilising the UV signal	50
3.3.5	Calculation of D_n and D_w from FIFFF results	51
3.4	EXPERIMENTAL	52
3.4.1	FIFFF instrumentation	52
3.4.2	FIFFF channel	53
3.4.3	Membrane synthesis	60
3.4.4	Void volume measurement	60
3.4.5	Carrier	62
3.5	CONCLUSIONS	63
3.6	REFERENCES	63

CHAPTER 4

DETERMINATION OF DIFFUSION COEFFICIENT OF SUWANNEE RIVER FULVIC ACID: COMPARISON OF FLOW FIELD-FLOW FRACTIONATION WITH SOME OTHER NEW TECHNIQUES 66

4.1	INTRODUCTION	66
4.2	THEORY	68
4.2.1	Fluorescence correlation spectroscopy (FCS)	68
4.2.2	Pulsed-field gradient NMR (PFG-NMR)	70
4.3	EXPERIMENTAL	70
4.3.1	Flow field-flow fractionation	71
4.3.2	Atomic force microscopy	71
4.3.3	FCS and PFG-NMR	71
4.4	RESULTS AND DISCUSSION	72
4.4.1	FIFFF results	72
4.4.2	Comparison of the FIFFF results with those obtained from FCS	75
4.4.3	Comparison of the FIFFF results with those obtained from PFG-NMR	77
4.4.4	Comparison of the FIFFF results with the size obtained from AFM	79
4.5	COMPARISON OF THE TECHNIQUES	81
4.6	CONCLUSIONS	83
4.7	REFERENCES	83

CHAPTER 5
USE OF FLOW FIELD FLOW FRACTIONATION TO CHARACTERISE
NATURAL ORGANIC MATTER SEPARATED BY ULTRAFILTRATION **86**

5.1	INTRODUCTION	86
5.2	EXPERIMENTAL	89
5.2.1	NOM preparation and ultrafiltration	89
5.2.2	Materials	90
5.2.3	Flow field-flow fractionation experiments	91
5.2.4	Mobility measurements	91
5.3	RESULTS AND DISCUSSION	92
5.3.1	FIFFF fractograms	92
5.3.2	Size distributions	94
5.3.3	Molecular weight distributions	97
5.3.4	Mobility measurements	100
5.3.5	Solid state ¹³ C NMR spectra of the NOM fractions	101
5.3.6	Comparison of the molecular weight data with those obtained from HPSEC	105
5.4	CONCLUSIONS	107
5.5	REFERENCES	108

CHAPTER 6
EFFECT OF SOLUTION PH AND IONIC STRENGTH ON SIZE AND
DIFFUSION COEFFICIENT OF HUMIC SUBSTANCES **114**

6.1	INTRODUCTION	114
6.1.1	Chemical processes involved in the aggregation of HS	115
6.1.2	Methods used in the study of HS aggregation	116
6.2	MATERIALS AND METHODS	116
6.2.1	Sample preparation	116
6.2.2	FIFFF run conditions	117
6.3	RESULTS AND DISCUSSION	117
6.3.1	Effect of the pH on aggregation of humic samples	117
6.3.2	Effect of the ionic strength on aggregation of humic samples	122
6.4	SIMULATION OF THE EFFECT OF PH ON CONFORMATION OF A MODEL FULVIC ACID	126
6.5	CONCLUSIONS	135
6.6	REFERENCES	136

CHAPTER 7

ADSORPTION OF SUWANNEE RIVER FULVIC ACID ON GOETHITE, STUDIED BY DIRECT FORCE MEASUREMENT IN ATOMIC FORCE MICROSCOPY

140

7.1	INTRODUCTION	140
7.2	ATOMIC FORCE MICROSCOPY	142
7.2.1	Contact mode	143
7.2.2	Non-contact mode(constant height mode)	143
7.2.3	Tapping mode™	144
7.2.4	Force measurements	145
7.3	EXPERIMENTAL	147
7.3.1	Atomic force microscopy measurements	147
7.3.2	Preparation of goethite coated mica surface	148
7.3.3	Adsorption of SRFA on goethite for AFM force measurements	149
7.4	RESULTS AND DISCUSSION	149
7.4.1	Characterisation of the goethite coated mica surface	149
7.4.2	Incubation of the goethite coated mica surface in 100 ppm SRFA	152
7.4.3	Image of the adsorbed fulvic acid	156
7.5	CONCLUSIONS	157
7.6	REFERENCES	158

CHAPTER 8

USE OF ^{31}P NMR IN INVESTIGATING THE BINDING OF ORTHOPHOSPHATE TO A HUMIC ACID

162

8.1	INTRODUCTION	162
8.1.1	Previous application of ^{31}P NMR to humic substances	164
8.1.2	NMR spectroscopy	166
8.1.3	Brief overview of the theory of NMR spectroscopy	167
8.2	EXPERIMENTAL	170
8.2.1	Samples	170
8.2.2	NMR instrument and run conditions	171
8.2.3	Sample preparation	172
8.3	RESULTS AND DISCUSSION	173
8.3.1	Solid state ^{31}P NMR spectra of Chaffey HA before and after addition of orthophosphate	173
8.3.2	Solid state ^{13}C NMR spectra of Chaffey HA before and after addition of orthophosphate	175
8.3.3	Solution ^{31}P NMR experiments	177
8.3.4	Effect of Fe	180
8.4	CONCLUSIONS	181
8.5	REFERENCES	183

CHAPTER 9

CONCLUSIONS AND RECOMMENDATIONS FOR FUTURE WORK 187

9.1	MAJOR OUTCOMES OF THE THESIS	188
9.2	RECOMMENDATIONS FOR FUTURE WORK	189
9.3	OVERVIEW OF THE THESIS	190
9.4	REFERENCES	191

APPENDICES 192

1	SOME PROPOSED STRUCTURES FOR HUMIC SUBSTANCES	192
2	ISOLATION AND CHARACTERISATION OF CHAFFEY HA	197
3	INFORMATION ON SOME COMMONLY USED ULTRAFILTRATION MEMBRANES	201

LIST OF TABLES

Table 2.1	Comparison of some results obtained on molecular size and weight of humic substances in the literature.	28
Table 3.1	Parameters that can be obtained from commonly used FFF techniques.	44
Table 4.1	Comparison of the diffusion coefficients of SRFA obtained by FIFFF at different solution pH and ionic strength (I).	75
Table 4.2	Functional groups corresponding to each spectral region in PFG-NMR results.	77
Table 4.3	Comparison of the diffusion coefficients obtained from FIFFF with some other data collected from the literature.	82
Table 5.1	Concentration of the NOM in UF fractions as determined by total organic carbon (TOC) and UV absorbance measurements.	90
Table 5.2	Comparison of the hydrodynamic diameter ranges and averages obtained by FIFFF for the UF fractions.	96
Table 5.3	FIFFF calibration constants found in this study, together with some literature values.	98
Table 5.4	Comparison of the nominal molecular weight ranges of the fractions with the MW ranges and averages obtained from FIFFF.	98

Table 5.5	Electrophoretic mobility of goethite and goethite coated with NOM fractions from Myponga Reservoir.	101
Table 5.6	Polydispersity and molecular weight ranges of Myponga Reservoir and Hope Valley NOM fractions, obtained by HPSEC.	105
Table 6.1	Size parameters of the humic substances determined by FIFFF. diameter at the peak maximum (d_p), number and weight average diameters (d_n and d_w), and the diffusion coefficient at the peak maximum (D_p), number and weight average diffusion coefficients (D_n and D_w) are given.	119
Table 8.1	^{31}P NMR chemical shifts of the pure HA and $\text{HA}+10^{-7} \text{ M PO}_4^{3-}$ in different solution pH. The chemical shifts have been assigned from the data available in the literature.	177

LIST OF FIGURES

Figure 2.1	Plot of some selected molecular weight data of humic substances reported in the literature at various times between 1970 and 1995.	33
Figure 3.1	Representation of the separation mechanism in a field-flow fractionation channel ((a), (b) and (c)) and the concentration profile along the channel of an eluting sample zone (d).	43
Figure 3.2:	Scheme for calculation of size and molecular weight from the retention volume in FIFFF.	46
Figure 3.3	Experimental layout of an FFF system.	52
Figure 3.4	The FIFFF system used in this thesis.	53
Figure 3.5	Schematic diagram of a FIFFF channel.	54
Figure 3.6	Plumbing of the FIFFF system used in this thesis.	55
Figure 3.7	Schematic diagram of a FIFFF system illustrating how the back pressures and flow rates are balanced.	57
Figure 4.1	Distribution of diffusion coefficients of SRFA at different pH (5.5, 7, 8.5) and ionic strengths (0.005 and 0.05 M). Hydrodynamic diameters corresponding to the diffusion coefficients are given on the top x- axis.	72
Figure 4.2	Comparison of the diffusion coefficient at the peak maximum obtained by FIFFF with the most probable diffusion coefficient obtained from FCS at similar conditions.	76

Figure 4.3	Comparison of the diffusion coefficients at the peak maxima obtained from FIFFF with the diffusion coefficients at the peak maxima obtained from PFG-NMR at different solution pH values. The ionic strength was 0.03 M for NMR experiments and 0.05 M for FIFFF runs.	78
Figure 4.4	(a) Tapping mode AFM image of the SRFA on mica in air (PH=6, I=0.0007) and (b) section analysis of two points on the image for measurement of the vertical size of the SRFA molecules.	80
Figure 5.1	FIFFF fractograms of (a) Myponga Reservoir and (b) Hope Valley NOM samples.	93
Figure 5.2	FIFFF Size distributions of (a) Myponga Reservoir and (b) Hope Valley NOM samples.	94
Figure 5.3	Calibration line obtained with poly(styrenesulphonate) MW standards used to calculate MW distributions of the NOM fractions.	97
Figure 5.4	FIFFF molecular weight distributions of (a) Myponga Reservoir and (b) Hope Valley NOM fractions obtained by ultrafiltration.	99
Figure 5.5	Solid state ¹³ C NMR spectra of ultrafiltration fractions of Hope Valley NOM.	102
Figure 5.6	¹³ C NMR spectra of ultrafiltration fractions of Myponga Reservoir NOM. (Figure from Ref. [32].)	103
Figure 5.7	Comparison of the molecular weight ranges calculated from molecular weight distributions obtained by FIFFF and HPSEC (a) Myponga Reservoir and (b) Hope Valley NOM,. The range was calculated by excluding 10% of the peak area from each side of the	106

MW distribution.

Figure 6.1	Effect of the solution pH on size distribution of humic samples in 0.04 M TRIS buffer.	120
Figure 6.2	Effect of pH on the (a) number average and (b) weight average diameters of humic samples in 0.04 M TRIS buffer.	121
Figure 6.3	Effect of the ionic strength on the size distribution of humic samples in TRIS buffer.	123
Figure 6.4	Effect of the ionic strength on (a) d_n and (b) d_w of the humic samples (carrier TRIS buffer), pH =7.9.	124
Figure 6.5	A model polyelectrolyte structure proposed for humic substances (Figure from Ref.[25]).	127
Figure 6.6	Two adjacent statistical segments of a chain with three charges per segment (Figure from Ref.[33]).	128
Figure 6.7	Stealink humic acid structure (Figure adopted from Ref.[31]).	129
Figure 6.8	Simulation of Stealink structure in a vacuum. No charge effects are considered. Maximum end to end distance: 1.5 nm.	130
Figure 6.9	Simulation of Stealink structure in a vacuum. A hydrogen atom is removed from each carboxyl group. Maximum end to end distance: 1.4 nm.	131
Figure 6.10	Simulation of Stealink structure in a vacuum. Hydrogen atoms on all the phenolic and carboxyl groups are removed. Maximum end to end distance is 2.1 nm.	132

Figure 6.11	Simulation of Steelink structure in vacuum. All the carboxyl, phenolic and amine groups are charged. Maximum end to end distance: 2.4 nm	133
Figure 6.12	Simulation of Steelink structure in vacuum, with the amine group protonated. Maximum end to end distance: 1.5 nm.	134
Figure 7.1	Schematic diagram of the optical scanning system in AFM (Adapted from Nanoscope III manual -Digital Instruments, Santa Barbara, CA).	142
Figure 7.2	Illustration of the operating modes of AFM.	144
Figure 7.3	A silica sphere glued to an AFM cantilever tip (Figure from Ref.[13]).	145
Figure 7.4	Illustration of "jump into contact" in a force versus probe-surface separation (Figure from Ref. [15]).	146
Figure 7.5	Tapping mode AFM image of the goethite coated mica surface. (a) scan size $1\mu\text{m} \times 1\mu\text{m}$, (b) scan size $300\text{ nm} \times 300\text{ nm}$ and (c) section analysis of the surface.	150
Figure 7.6	AFM force measurements between a silica colloid probe and goethite coated mica surface in different solution pH values.	151
Figure 7.7	The effect of introduction of 100 ppm SRFA, on the electrostatic forces between the surface and the silica probe.	153
Figure 7.8	The electrostatic forces between the goethite surface and the silica probe as a result of introduction of SRFA at pH 5.6. The	154

electrostatic repulsion in the absence of SRFA is replaced by attraction. The deviation from an exponential function at short separations suggest the presence of an steric layer in the repulsion case.

- Figure 7.9** Illustration of the effect of introduction of SRFA on the interactions between goethite and the silica probe at pH below 7. (a) The goethite surface is positively charged and the silica probe is negatively charged (IEP~ pH 3), resulting in attraction between the surfaces. (b) Coating goethite with SRFA, results in the surface being negatively charge and the electrostatic repulsion being the dominant force. 155
- Figure 7.10** Effect of incubation time in 100 ppm SRFA on forces between silica probe and the goethite surface at pH 9.4. 156
- Figure 7.11** Tapping mode AFM image in fluid of SRFA adsorbed to the goethite coated mica surface. The goethite colloid is visible under the SRFA layer. 157
- Figure 8.1** Schematic diagram illustrating the possible role of humic substances in binding orthophosphate. 163
- Figure 8.2** Chemical shift assignments for phosphorus forms present in peat, soil and humic acid. (Figure from Ref. [12]). 165
- Figure 8.3** Solid state ^{31}P NMR spectra of (a) Chaffey HA with added orthophosphate (a) Chaffey HA with added orthophosphate and dialysed, and (b) Pure Chaffey HA with same amount as in (b). 174
- Figure 8.4** Solid state ^{13}C NMR spectrum of Chaffey humic acid (a) before and (b) after addition of orthophosphate 175

- Figure 8.5** Possible reactions that might have occurred between orthophosphate and some functional groups in Chaffey HA (a) reaction with alcohol groups to yield alkyl phosphates (b) reaction with amide groups [7]. 176
- Figure 8.6** Solution ^{31}P NMR spectrum of Chaffey humic (a) Pure HA, pH=8 179
(b) HA after addition of 1×10^{-7} M orthophosphate pH=8, (c) HA after addition of 1×10^{-7} M orthophosphate pH=9.3 and (d) HA after addition of 1×10^{-7} M orthophosphate pH=4.6
- Figure 8.7** Solution ^{31}P NMR spectrum of a solution of 10^{-7} M PO_4^{3-} and 10^{-4} M Fe^{3+} (Fe:P ratio of 1:10000). 181

CHAPTER 1

OVERVIEW OF THE THESIS

1.1 INTRODUCTION

Humic substances are yellow-brown coloured complex mixtures of organic compounds isolated from natural waters, soils, sediments and coal. They have been known to soil scientists for about 200 years [1, 2]. Alkaline soil extracts were acidified to form a precipitate, which was named humic acid. The remaining solution was named fulvic acid and the insoluble part, humin. Today the same operational definitions are used for these fractions of humic substances, but they are not only characterised by their solubility and colour, but also by their functional groups determined by various spectroscopic techniques [3-5], size [6, 7], molecular weight [8], environmental interactions [9-13] and various applications [14-16].

Humic substances are present dissolved in natural waters at concentrations typically in the range 1-50 mg L⁻¹ [17]. They usually comprise about 40-60% of the total dissolved organic carbon (DOC). This value can go up to 70-90% for highly coloured waters [18]. About 70-80% of the soil organic matter is also attributed to humic substances [19].

1.2 ENVIRONMENTAL SIGNIFICANCE OF HUMIC SUBSTANCES

Humic substances can be considered to be polyelectrolytes with anionic functional groups and hydrophobic components [20]. At the pH of most natural environments they have a negative charge and can be adsorbed to suspended particulate matter, altering their surface charge [21]. As a result heavy metals and other contaminants can become associated with the particulate matter. This association affects the transport and fate of the contaminants in natural water systems [22]. They can also act as buffers, solubilise insoluble organic compounds and generate trihalomethanes during chlorination of natural waters [9, 16].

In the terrestrial environments, humic substances influence the concentration and availability of metal ions [23-25], organic pollutants (such as pesticides) [13] and plant nutrients. In agriculture, humic substances can be used as a soil additive for water and nutrient retention [15] and plant growth enhancement [14, 26, 27]. It has been proposed that aquatic solutions of humic substances can be used to remedy contaminated soils through hydrophobic binding of organic contaminants [28]. Some biological and medical applications of humic substances as virus inhibitors and heavy metal chelators are being explored [19, 29].

1.3 SIZE AND MOLECULAR WEIGHT OF HUMIC SUBSTANCES

In the previous section the environmental importance of humic substances was highlighted. Humic substances can enhance or retard contaminant transport in the environment, based on their origin (aquatic or terrestrial) and their affinity for that contaminant. Knowledge of the structure and also molecular size of the humic substances is highly desirable in order to understand and model various interactions of humic substances in the environment.

Some controversy exists on the size and molecular weight of the humic substances. Eventually with the emergence of new and reliable methods agreement on certain properties of humic substances should be achieved. It should be mentioned here that the structure or molecular size obtained for one fraction (humic acid, fulvic acid or humin) gives an average of perhaps millions of molecules with different structures and sizes in that fraction. So it is fair to say that there is still a lot of work to do in order to be able to resolve the fundamental issues of structure and size of the humic substances. One approach to characterise humic substances is to isolate, fractionate and characterise the fractions as much as possible.

The research on size and molecular properties of humic substances has been actively pursued in the past few decades (see Chapter 2). However, it has proven to be a difficult task as humic substances are not pure compounds. The molecular composition and properties of the humic substances can vary depending on their origin and method of isolation. The data in the literature on the size and molecular weight of humic substances is not consistent and ranges from orders of one nanometer (a single molecule) to few microns. This is the result of several factors such as:

- (1) *Use of rather improper calibration material*
- (2) *Wide range of the used solution conditions*
- (3) *Different parameters and averages obtained by different techniques*

These issues will be discussed in detail in Chapter 2.

1.4 USE OF FLOW FIELD-LOW FRACTIONATION (FIFFF) IN CHARACTERISATION OF HUMIC SUBSTANCES

FIFFF is a chromatography like technique, which separates humic substances on the basis of their diffusion coefficient. It has been used for the characterisation of humic substances since 1987 [7, 30, 31]. FIFFF has the following advantages when compared with other techniques:

- the system does not have a stationary phase. This ensures that the separation is achieved solely by physical forces. These forces can be formulated and used to calculate the size distribution of the sample.
- measures the diffusion coefficient from the first principles, which can be converted to a hydrodynamic size.
- gives a distribution, from which different averages can be calculated.

FIFFF was the main technique used in this thesis and is discussed in detail in Chapter 3.

1.5 RESEARCH OBJECTIVES

The main objectives of this thesis are as follows:

- To validate the data obtained from FIFFF by comparing the results with those obtained from other techniques.
- To apply FIFFF to study the aggregation of humic substances.
- To explore the capabilities of atomic force microscopy (AFM) for investigation of the properties of humic substances.
- To use NMR spectroscopy to test the hypothesis that there is some direct interaction between humic acid and orthophosphate.

1.6 STRUCTURE OF THE THESIS

Chapter 2 gives an overview of the techniques normally used for the characterisation of humic substances. Some advantages of FIFFF in comparison to some commonly used techniques will be mentioned there. The technique itself and the data processing methods will be discussed in detail in Chapter 3.

FIFFF results will be compared to those obtained by fluorescence correlation spectroscopy (FCS) and pulse-field gradient NMR (PFG-NMR) in Chapter 4. For complex molecules such as humic substances it is beneficial to use several techniques simultaneously. This chapter also gives an insight into the size of a very commonly used humic standard, Suwannee River fulvic acid and its aggregation behaviour in water.

Size of the humic substances isolated from aquatic, sediment and coal have been analysed in different solution conditions. These results will be presented in Chapter 5 along with a computer simulation on a model humic acid. The aim was to simulate the effect of solution pH on the size and conformation of humic molecules.

In Chapter 6, FIFFF has been used to determine the size and molecular weights of two natural organic matter samples, isolated and fractionated by ultrafiltration (UF). Separation and isolation of humic substances is a very important issue especially in the water industry. Although ultrafiltration is very commonly used for separation of humic substances, the results obtained should be handled with caution [32-34].

The size and molecular weight of the UF isolates were also analysed by HPSEC (independently by another group). This gave an opportunity to compare the FIFFF results with another commonly used technique.

Chapter 7 presents the results of another relatively new and exciting technique, atomic force microscopy (AFM). It will be demonstrated that AFM can be used as a force measurement technique as well as an imaging tool for humic substances. The use of goethite with adsorbed SRFA, as a model for natural particles will be examined in this chapter.

The interactions of orthophosphate with a humic acid will be investigated in Chapter 8. Phosphorus is often a major limiting nutrient in the environment. Excess phosphorus can cause eutrophication, leading to algal blooms. In modelling the interactions and transport mechanisms of nutrients, it is important to determine the role of natural organic matter. Humic acid isolated from Chaffey Reservoir sediment (NSW, Australia) was treated with orthophosphate. The binding sites on the humic were investigated using ^{13}C and ^{31}P NMR spectroscopy.

The overall conclusion of the thesis is presented in Chapter 9. Appendices contain some background information on humic substances from the literature and details of some experimental methods used in this thesis. These sections are placed in appendices as they are not part of the work presented for examination in this thesis.

1.7 REFERENCES

1. Achard, F.K., *Chemische untersuchung der torfs*, *Crell's Chem. Ann.*, 2 (1786) 391-403.
2. Berzelius, J.J., *Sur deux acides organiques qu'on trouve dans les eaux minerales*, *Annals de Chimie et de Physique*, 54 (1833) 219-231.
3. Preston, C., *Applications of NMR to soil organic matter analysis: History and prospects*, *Soil Science*, 161 (1996) 144-166.
4. Steenlink, C., Wershaw, R.L., Thorn, K.A., Wilson, M.A., *Application of liquid-state NMR spectroscopy to humic substances*, in M.H.B. Hayes, MacCarthy, P., Malcolm, R.L., and Swift, R., (Eds.), *Humic Substances II, In Search of Structure*, John Wiley & Sons, Chichester, 1989, 281-308.
5. Wilson, M.A., *Techniques and Applications of Nuclear Magnetic Resonance Spectroscopy in Geochemistry and Soil Science*, Pergamon Press. Oxford, 1987.
6. Thurman, E.M., Wershaw, R.L., Malcolm, R.L and Pinckney, D.J., *Molecular size of aquatic humic substances*, *Organic Geochemistry*, 4 (1982) 27-35.
7. Beckett, R., Zhang J., and Giddings C., *Determination of molecular weight distributions of fulvic and humic acids, using flow field-flow fractionation*, *Environmental Science and Technology*, 21 (1987) 289-295.
8. Aiken, G.R., and Malcolm, R.L., *Molecular weights of aquatic fulvic acids by vapor pressure osmometry*, *Geochimica et Cosmochimica Acta*, 51 (1987) 2177-2184.
9. Schnitzer, M., and Khan, S.U., *Humic Substances in the Environment*, Dekker., New York, 1972 .

10. Senesi, N., Molecular and quantitative aspects of the chemistry of fulvic acid and its interactions with metal ions and organic chemicals Part I, The electron spin resonance approach, *Analytica Chimica Acta*, 232 (1990) 51-75.
11. Hayes, M.H.B., and Wilson, W.S., (Eds.), *Humic Substances in Soils, Peats and Waters, Health and Environmental Aspects*. The Royal Society of Chemistry, Cambridge, 1997.
12. Buffle, J., Wilkinson, K.J., Stoll, S., Filella, J., and Zhang J., A generalised description of aquatic colloidal interactions: the three colloidal component approach, *Environmental Science and Technology*, 32 (1998) 2887-2899.
13. Spark, K.M. and R.S. Swift, Investigation of the interaction between pesticides and humic substances using fluorescence spectroscopy, *Science of the Total Environment* 152 (1994) 9-17.
14. Chen, Y., Magen, H., and Riov, J., Humic substances originating from rapidly decomposing organic matter: properties and effects on plant growth, in N. Senesi, and Miano, T.M., (Eds.), *Humic Substances in the Global Environment and Implications on Human Health*, Elsevier, Amsterdam, 1994.
15. MacCarthy, P., and Rice, J., Industrial applications of humus: An overview, in N. Senesi, and Miano, T.M., (Eds.), *Humic substances in the global environment and implications on human health : Proceedings of the 6th international meeting of the international humic substances society, Monopoli (Bari), Italy, September 20-25, 1992*, Elsevier, Amsterdam. 1994.
16. Ubbelohde, G.A., Chipman, K.J., Moody, G., Marsh, J.W. and Hayes, M.H.B., Hepatic protective factors against mutagens from chlorinated humic substances, in N. Senesi, and Miano, T.M., (Eds.), *Humic substances in the global environment and implications on human health: Proceedings of the 6th international meeting of*

- the international humic substances society, Monopoli (Bari), Italy, September 20-25, 1992, Elsevier, Amsterdam. 1994.
17. Thurman, E.M., *Organic Geochemistry of Natural Waters*, Martinus Nijhoff/Dr W. Junk publishers, Dordrecht, 1985 .
 18. Beckett, R., and Le, N.P., The role of organic matter and ionic composition in determining the surface charge of suspended particles in natural waters, *Colloids and Surfaces*, 44 (1990) 35-49 .
 19. Hayes, M.H.B., Humic substances: progress towards more realistic concepts of structures, in Ghabour, E.A and G.Davis (Eds.), *Humic Substances: Structures, Properties and Uses*, The Royal Society of Chemistry, Cambridge. 1998, pp. 1-2.
 20. Wershaw, R.L. and Pinckney D.J., NMR characterisation of humic acid fractions from different Philippine soils and sediments, *Analytica Chimica Acta*, 232 (1990) 31-42.
 21. Beckett, R., The composition and surface properties of suspended particulate matter, in B.T. Hart, (Ed.), *Water Quality Management: The role of particulate matter in the transport and fate of contaminants*, Chisholm Institute of Technology, Melbourne. 1986, 113-142.
 22. Beckett, R., The surface chemistry of humic substances in aquatic systems. *Surface and Colloid Chemistry in Natural Waters and Water Treatment*, R. Beckett (Ed.), Plenum Press, New York, 1990 .
 23. Schnitzer, M., Metal-organic matter interactions in soils and waters, in : *Organic Compounds in Aquatic Environment*, 5th Rudolfs Research Conference, 1971, 297-315.
 24. Finger, W., Post B., and. Klamberg H., Interaction between soil humic substances and metal ions. Part 2. Investigation of soil humic substances by gel-permeation

- chromatography and vapor pressure osmometry, in *Z. Pflanzenernaehr. Bodenkd.*, 154 (1991) 287-91.
25. Spark, K.M., J.D. Wells, and B.B. Johnson, The interaction of a humic acid with heavy metals, *Australian Journal of Soil Research*, 35 (1997) 89-101.
 26. Clapp, C.E., Liu, R., Cline, V.W, Chen, Y., and Hayes, M.H.B, Humic substances for enhancing turfgrass growth, in G.Davis, E.A. Ghabbour, (Eds.), *Humic Substances: Structures, Properties and Uses*, The Royal Society of Chemistry: Cambridge, 1998, 228-233.
 27. Schnitzer, M., A lifetime perspective on the chemistry of soil organic matter, *Advances in Agronomy* 68 (2000) 1-58.
 28. Rebhun, M., De Smedt, F, and Rwetabula, J., Dissolved humic substances for remediation of sites contaminated by organic pollutants. Binding-Desorption model predictions, *Water Research*, 30 (1996) 2027-38.
 29. Klocking, R., Humic substances as potential therapeutics, in N. Senesi, and Miano, T.M., (Eds.), *Humic Substances in the Global Environment*, Elsevier Science B.V., Amsterdam. 1994, 1245-1257.
 30. Dycus, P.J.M., Healy, K., Stearman, G.K., and Wells, M., Diffusion coefficients and molecular weight distributions of humic and fulvic acids determined by flow field-flow fractionation, *Separation Science and Technology*, 30 (1995) 1435-1453.
 31. Schimpf, M.E., and Petteys, M.P., Characterisation of humic materials by flow field-flow fractionation, *Colloids and Surfaces A*, 120 (1997) 87-100.
 32. Aiken, G.R., Evaluation of ultrafiltration for determining molecular weight of fulvic acid, *Environmental Science and Technology*, 18 (1984) 978-981 .

33. Buffle, J., Deladoey P. and Haerdi W., The use of ultrafiltration for the separation and fractionation of organic ligands in fresh waters, *Analytica Chimica Acta*, 101 (1978) 339-357.
34. Buffle, J., Perret, D., and Newman, M., The use of filtration and ultrafiltration for size fractionation of aquatic particles, colloids and macromolecules, in Buffle J., and van Leeuwen, H.P, (Eds.), *Environmental Particles*, Lewis Publishers, Michigan. 1984, 171-230 .

CHAPTER 2

A REVIEW OF THE METHODS FOR DETERMINATION OF SIZE AND MOLECULAR WEIGHT OF HUMIC SUBSTANCES

2.1 INTRODUCTION

Characterisation of humic substances in terms of size, molecular weight and structure is necessary in order to understand their behaviour in the environment. Two important points should be considered when comparing molecular parameters of the humic substances:

a) The solution conditions in which the sample is measured.

Humic substances can aggregate or dissociate depending on the concentration, solution pH or concentration of salts present. It is thus necessary to note the experimental conditions

when comparing size and MW data obtained from different experiments. Measurements perform in extreme conditions of sample concentration, solution pH and high salt contents may in fact present the aggregate properties of humic substances rather than their molecular properties.

b) The technique used and its limitations.

Different techniques have been used to determine the size and molecular weight of humic substances. As it was stated before each technique is based on a different principle and thus measures a different property. They will also be subject to their own limitations and approximations. This might lead to different molecular weight data for the same sample.

Molecular weights of polydisperse systems like humic substances are commonly expressed as "the number average" and "the weight average" molecular weight. The number average molecular weight (M_n) can be determined by methods that depend on the total number of molecules present, regardless of size (such as collegative properties). M_n can be expressed mathematically as:

$$M_n = \frac{\sum_i n_i M_i}{\sum_i n_i} \quad (2.1)$$

Where n_i is the number of molecules with molecular weight M_i .

The weight average molecular weight (M_w) can be measured by methods, which depend on the masses of material in different fractions. M_w can be expressed as:

$$M_w = \frac{\sum_i w_i M_i}{\sum_i w_i} = \frac{\sum_i n_i M_i^2}{\sum_i n_i M_i} \quad (2.2)$$

M_w is weighted more by the heavier fraction of the sample and is larger than M_n . M_w/M_n can be used as an indication of polydispersity. For a monodispersed system $M_n=M_w$.

M_n can be measured from colligative property measurements (vapor pressure osmometry, osmotic pressure), which depend on the number of molecules in solution. Methods that depend on the masses of material in different fractions, such as light scattering can be used to determine M_w . Some methods like small angle X-ray scattering and FFFF produce data based on molecular size. To obtain data on MW, molecular weight standards of known size, weight and composition should be used to convert the size data to MW data. In methods like high performance size exclusion chromatography (HPSEC) and ultrafiltration, calibration with size or MW standards is necessary to provide information on any of these parameters.

In this chapter some of the common methods used to measure size and MW of humic substances will be reviewed. These methods have been explained under three different sections: a) absolute methods of size or molecular weight measurement, where the molecular parameter can be calculated from the first principles, b) methods that need calibration with standards of known molecular parameters to be able to provide any information, c) methods that use mathematical approximations

2.2 ABSOLUTE METHODS FOR MEASUREMENT OF SIZE AND MOLECULAR WEIGHT OF HUMIC SUBSTANCES

2.2.1 COLLIGATIVE PROPERTIES

By definition, colligative properties are thermodynamic properties that depend on the

number of particles in solution (i.e. concentration or mole fraction) and not on the nature of the particle. Of the four colligative properties, vapour pressure osmometry and freezing point depression (cryoscopy) have been used most often for determination of number average molecular weight of humic substances. These methods measure the activity of the solvent in solution relative to the activity of the pure solvent. The temperature change is measured to equalise the activity of the solvent in the pure phase with the activity of the solvent in the solution of interest. For humic substances, which are polydisperse the following equation is used to determine the molecular weight [1]:

$$\theta = \theta_0 + aW + bW_2 + cW_3 \quad (2.3)$$

The first virial coefficient (a), is related to the molecular weight (M) by the following equation:

$$a = \frac{1000K}{M} \quad (2.4)$$

Where θ is change in the temperature of solvent, W is weight of solute per unit gram of solvent and K is calibration constant of the apparatus ($\theta/\text{mol} \cdot 1000 \text{ g of solvent}$). Thus the molecular weight can be calculated from a plot of θ versus W . For an ideal system it should pass the zero point and should be a straight line. The second virial coefficient, b , is not directly related to the molecular weight. It however does affect the value of a . The value of K is determined for a given solvent and osmometer system by determining first virial coefficients of known molecular weight.

One serious problem that can result in misleading M_n values from colligative property measurements is the dissociation of the organic acids in solvents with dielectric constants greater than 15 [2] in which case the dissociated protons are counted absolute molecules. Several methods have been suggested to correct for dissociation of solvents [2-5].

Another problem is the possibility of error due to aggregation of humic substances, which can occur in high concentrations.

2.2.2 ULTRACENTRIFUGATION

In this method the humic sample is spun inside an analytical UV-scanning ultracentrifuge so that the humic samples sediment towards the bottom of the centrifuge. The cells have quartz windows, which allow a beam of UV light to be passed through the cell. The concentration profile of the sample along the length of the column can be determined while the centrifuge is spinning. It can be performed using three different techniques:

(a) sedimentation velocity, (b) sedimentation equilibrium and (c) approach to sedimentation equilibrium (Archibald method)

SEDIMENTATION VELOCITY:

In this method the centrifuge is run at very high speed (up to 60000 rpm [6] and the sedimentation coefficient (S) of the sample is determined from the position of the sedimentation front, the sedimentation time and the rotor speed (Equation 2.5).

$$M = \frac{RTS^0}{(1 - \bar{V}\rho_s)D^0} \quad (2.5)$$

Where D^0 and S^0 are values obtained by extrapolation of the measured values to zero concentration. R is the gas constant, T is the absolute temperature, \bar{V} is the partial specific volume of the solute, ρ_s is the density of the solution. S is the sedimentation coefficient defined as the radial velocity of the solute molecules divided by the centrifugal field ($r\omega^2$):

$$S = \frac{1}{r\omega^2} \cdot \frac{dr}{dt} = \frac{d \ln r}{\omega^2 dt} \quad (2.6)$$

SEDIMENTATION EQUILIBRIUM

In this method the sample is spun at lower speed (15000-20000 rpm) until the concentration profile becomes stable [7]. The concentration of solute at any point x in the cell can be determined spectrophotometrically and the MW at that point is calculated using equation 2.7:

$$M = \frac{2RT}{(1 - \nabla\rho_s)\omega^2} \cdot \frac{d \ln C}{dr^2} \quad (2.7)$$

Where M is the molecular mass, ω is the angular velocity, C is the solute concentration and r is the distance from the axis of rotation.

To calculate the weight average molecular weight, the MW must be averaged over the length of the column. One limitation of sedimentation equilibrium is that for higher molecular mass samples the results are dependent on the force field used ($r\omega^2$). Thus for high force fields material can be lost from the measurable concentration gradient in the ultracentrifuge cell so that the average masses obtained relate to only a part of the molecular mass distribution [8]. The approach to sedimentation equilibrium (Archibald method) method can be used to overcome this problem.

APPROACH TO SEDIMENTATION EQUILIBRIUM (ARCHIBALD METHOD)

This method depends on the fact that the conditions of sedimentation equilibrium are realised at all times at the ends of the fluid column in the ultracentrifuge cell. If a measurement of the concentration and concentration gradient can be made at the meniscus (m) or base (b) of the cell, the weight average mass can be calculated after a short period of

centrifugation during the approach to equilibrium. Weight average molecular weight (M_w) of the sample can be calculated using the following equation:

$$M_w = \frac{RT}{(1 - \nabla\rho_s)\omega^2} \frac{1}{r_m c_m} \left(\frac{dc}{dr} \right)_m \quad (2.8)$$

Where r_m is the radius at the meniscus and c_m is the concentration at the meniscus. If the measurements are made early in the run, before any material is lost from the gradient, the weight average molecular weight obtained should be very close to that of the whole sample. In practice it is found that M_w calculated using equation (2.8) were dependent on time for lower molecular mass samples and dependent on both force field and time for higher molecular mass material [8]. Scans of the concentration distributions are made at frequent intervals after reaching a chosen speed and are fitted to a second degree polynomial of absorbance as a function of r :

$$A = A_r = r_m + \left(\frac{\delta A}{\delta r} \right)_m r + \text{constant } r^2 \quad (2.9)$$

Ultracentrifugation experiments can be performed with sample concentrations as low as 45 mg/L [7], therefore minimising the solute-solute interactions and aggregation. In all the ultracentrifuge techniques it is assumed that: (a) the extinction coefficient is constant through the range of the molecular weight, (b) the partial specific volumes of all solutes in a mixture are independent of molecular weight and can be represented by the average values obtained for the mixture as a whole, and (c) there are no charge effects between molecules of the solute [9]. Apart from these limitations a major drawback is the long acquisition time (> 72 hours to reach equilibrium) [7, 8].

2.2.3 SMALL ANGLE X-RAY SCATTERING

Small angle X-ray scattering measures the radius of gyration (R_g). R_g is defined as the root-mean square distance of the electrons in the particle from the centre of charge. In this method the sample is irradiated by X-rays. The X-ray will scatter as a function of the size and shape of the humic molecule. It was shown by Guinier and Fournet [10] that for an ensemble of randomly oriented identical particles, in which there is no long range order, the scattered radiation $I(h)$, can be represented to a close approximation by the following equation:

$$I(h) = I_e(h) N n^2 e^{\left(\frac{-h^2 R_g^2}{3}\right)} \quad (2.10)$$

where $I_e(h)$ is the scattered intensity that would result if a single electron were substituted for one of the scattering particles, N is the total number of particles in the ensemble, n is the number of electrons per particle, and $h=2\pi(\sin 2\theta)/\lambda$, with θ being the scattering angle, λ the wavelength of the impinging X-ray, and R_g , the radius of gyration. This equation can be written as follows:

$$\ln I(h) = \frac{(-h^2) R_g^2}{3} + \text{constant} \quad (2.11)$$

R_g can be calculated from the slope of the plot on $\ln I(h)$ versus h^2 which is called a Guinier plot. The Guinier plot is a straight line for a monodisperse system in which all of the scattering particles are of the same molecular size. The plot is concave upward for a polydisperse system.

Wershaw *et al.* [11] found that the Guinier plots for unfractionated humic samples were concave, indicating the polydispersity of the sample. They reported radii of gyration of

3.6 to 13.7 nm. Guinier plots of the humic acid fractions isolated by adsorption on Sephadex gels, gave different results for each fraction. Some of the fractions appeared to be monodispersed in a range of pH from 3.5 to 7. Other fractions appeared to be polydisperse in the same pH range. Thurman *et al.* [4] reported a linear Guinier plot for the fulvic acid at pH 12.5 in tap water with a radius of gyration of 0.62 nm. The humic acid of the same sample in the same pH, resulted in a concave Guinier plot, with radii of gyration from 1.1 to 3.3 nm. Aiken *et al.* [12] also found that the Guinier plot for the Suwannee River fulvic acid was linear and reported a radius of gyration of 0.88–0.06 nm for that sample. However other methods like ultracentrifugation or FIFFF have shown that these samples are not mono dispersed. While small angle X-ray scattering may not be sensitive enough to report the polydispersities of smaller size samples, the radii of gyration generally agrees with those obtained from methods like FIFFF and HPSEC (see Table 2.1).

MW data can be obtained by comparing the radii of standards of known molecular weight with the radii of the unknown material. Aiken *et al.* [12] have used aquatic fulvic acids with known M_n , polyacrylic and polyglycol acids, as standards and obtained M_n values about 645-816 daltons for a fulvic acid sample and 1055-1066 daltons for a humic acid sample. Small angle X-ray scattering does not actually measure the distribution of sizes within a system, but gives a range of sizes. Even this is limited by the slits chosen for the measurements because the entire range of measurements cannot be covered with a single set of slits.

Because of the small electron density difference between the humic substances and water, the scattering intensity can be weak and the measurement often requires long counting

times. This long counting time can cause problems due to stability considerations of the X-ray generator. Measurements of the radii of gyration of 0.4-0.5 nm can incur an error of up to 10%. [11]. It seems that sample concentration does not interfere with the measurements. Thurman *et al.* [4] have reported radii of gyration of 0.47 nm to 2.6 nm for a range of humic acid fractions isolated from waters with different DOC content.

2.2.4 LIGHT SCATTERING TECHNIQUES

Light scattering measures the same parameters of an ensemble of scattering particles as small angle X-ray scattering. The resolution of light scattering is lower than that of small angle X-ray scattering, because of the longer wavelengths used. The light induces an oscillating dipole between electrons and nucleus. If the particle dimensions of the emitting light is smaller than 1/20 of the wavelength λ the light is scattered isotropically (Rayleigh scattering). With increasing the particle size destructive interference occurs between the particle which causes a decreasing scattering intensity at increasing angle (Debye scattering). When the molecular size is larger than the wavelength, constructive and destructive interference are observed (Mie scattering).

Rayleigh and Debye scattering can be described by the equation:

$$R_{\theta} = KCMP_{\theta} \quad (2.12)$$

Where R_{θ} is the reduced scattering intensity at angle θ , K is the optical constant, C is the concentration and M is the molar mass. P_{θ} is the scattering function, which describes the decrease in intensity at increasing angle and depends on the size and shape of the particle.

In practice, a linear approach is used where the shape is neglected and only the radius of gyration is included, using the equation:

$$\frac{KC}{R_{\theta}} = \frac{1}{M} + \frac{4\pi n}{3M\lambda_0} (R_g^2 \sin^2(\frac{\theta}{2})) \quad (2.13)$$

KC/R_{θ} can be plotted against $\sin^2(\theta/2)$ to obtain the molar mass from the intercept and the radius of gyration (R_g) from the slope. Light scattering can be used in two modes, (a) static and (b) dynamic light scattering (also called photon correlation spectroscopy). Both techniques require high concentration (2 g/L) [13] compared to the concentration of humic substances in natural waters (2-40 mg/L) [14]. This relatively high concentration may lead to formation of large aggregates. On the other hand light scattering techniques are usually biased towards the higher mass and determine the z average mass or diffusion coefficient. Reid *et al.* [15] measured the z average diffusion coefficients of an aquatic humic sample as a function of scattering angle and humic concentration. Extrapolation to zero angle gave D_z values of the order of 3×10^{-12} . This value corresponds to a z-average radius of gyration (using the Stokes-Einstein equation) of 81 nm and a molecular mass of 10^9 g.mol⁻¹ [13]. The ultracentrifugation of the same sample resulted in a molecular mass of 3750 and the mass measured by light scattering would correspond to an aggregate of 300000 units. Wagoner *et al.* [16, 17] have reported root mean square radii of 30-60 nm for SRFA NOM and 25-156 nm for aquatic NOM.

Other values reported for humic substances using light scattering are also very large compared to the values found from other analytical techniques (see Table 2.1). This size range probably corresponds to aggregate structures rather than molecules. Aggregation can

be induced by the high concentration used and the bias of light scattering towards larger size may generate anomalously larger molecular weight value.

2.2.5 FIELD-FLOW FRACTIONATION

Field-flow fractionation is a group of chromatography-like separation techniques, in which a field is used to bring the sample species close to an accumulation wall in a thin channel. After a certain period of time which allows the particles to relax under the applied field, the laminar channel flow elutes the smaller components first and the larger ones last. The field can be gravitational, thermal gradient, electrical or in case of flow field-flow fractionation (FIFFF), a crossflow. The detailed theory of field-flow fractionation can be found in Giddings [18], Giddings and Caldwell [19] and Beckett and Hart [20].

The separation in FFF is mainly due to physical interaction of the sample species with the applied field. The diffusion coefficient is obtained directly from the first principles and can be converted to the hydrodynamic diameter using the Stokes-Einstein equation. Molecular weight of the sample species can only be obtained after calibration with appropriate standards. Beckett *et al.* [21] reported that for humic substances, polystyrene sulphonates (PSS) were more appropriate as molecular weight standards than globular proteins. Although humic molecules probably have more side chains and are more polydisperse in structure. FIFFF has been explained in detail in Chapter 3.

2.2.6 IMAGING TECHNIQUES

Imaging techniques such as SEM, TEM and AFM have been used extensively for characterisation of humic substances. Previous attempts at imaging humic substances with TEM and AFM [22-26] usually show long strands, which indicate aggregation. These

aggregated structures could be related to the sample preparation which usually requires freeze drying, filtering or embedding in a resin (for sectioning purposes) and most of times high concentration of the sample.

TEM and SEM measurements are conducted in vacuum after drying of the humic substances in which case there is an opportunity for crystallisation to occur. Also precipitation of dust can give doubtful results. The same arguments are valid for dry imaging by AFM. But AFM has advantages over TEM and SEM in that it does not require such high concentration and imaging can be done on "moist" samples or in solution (Lead *et al.* [27], also see Chapters 4 and 7). The sizes obtained by AFM using this technique are of the order of a few nanometers.

2.3 METHODS THAT REQUIRE CALIBRATION FOR SIZE AND/OR MOLECULAR WEIGHT CALCULATION

2.3.1 SIZE EXCLUSION CHROMATOGRAPHY (SEC)

Size exclusion chromatography, also known as gel permeation chromatography (GPC), is perhaps one of the most common methods used to determine the molecular weight of humic substance [28-30], references in [14]. SEC is a separation technique where sample species are separated based on their hydrodynamic size. A column is packed with porous material that has a range of pore sizes corresponding to the range of compounds to be separated. The sample is carried into the column by a mobile phase at a certain flow rate. Smaller sample species with low hydrodynamic volume will penetrate deeper into the pores than larger ones. Assuming no interaction between the solute and the solid phase, the largest compounds will elute first, as they will not be able to diffuse into many pores. The smallest molecules that have been diffused into more of the pores, will elute last. The eluent from the column is analyzed by a UV detector as the intensity versus elution

volume (chromatogram). Calibration with suitable size or molecular weight standards is necessary to obtain information on molecular size or masses.

One of the serious problems encountered is interaction (attraction or repulsion) of the solute with the stationary phase. Charge exclusion can^{be} a major problem. In this case, the stationary phase acquires a negative charge as a result of the solution pH or ionic strength, thus the humics are prevented from diffusing into the stationary phase pores by electrostatic repulsion. This makes the optimisation for solution pH and ionic strength a very crucial task. It has also been demonstrated that the wavelength of the UV detector, can affect the obtained molecular weight, specially the M_n . Increasing the detector wavelength resulted in an increase in the molecular [31], a wavelength of 254 nm is recommended [32].

Choice of calibration material is also very important. Use of globular proteins usually gives very misleading results for humic substances. De Nobili and Chen [33] illustrated that molecular weight data for a series of polyphenolic acid, ranging from 200 to 500 daltons, could be drastically overestimated (72000 to 180000), if deduced from a calibration with proteins. Polystyrene sulphonates have proven to be a better choice. Use of organic acids as charged low molecular weight standards is also recommended [32]. Perminova *et al.* [34] compared four sets of standards, polydextrans, polyacrylates, polymethacrylates and polystyrene sulfonates. They found a strong dependence of the estimated molecular weight of the HS on the charge density of the molecules of the standard [34]. Recently Chin *et al.* [35] and Pelekani *et al.* [36] have been able to obtain MW results that are in the same range as data obtained using colligative property measurements, ultracentrifugation and flow field-flow fractionation. Analysis of the humic

fractions obtained from SEC, by multi angle laser light scattering by Wandruszka *et al.*[37] demonstrated that the preparative column separated the humic substances by size. Improvements in the results obtained by SEC is the outcome of the following changes in the system: (1) change of the stationary phase, (2) optimisation of carrier ionic strength and pH (3) replacement of globular proteins as standards, with substances like PSS that resembled the humic substances more [35, 38, 39].

2.3.2 ULTRAFILTRATION

In this method the humic sample is passed through membrane filters with nanometer pore sizes, under pressure or vacuum. The concentration of the humic sample is measured in each fraction and reported using data on the percentage of humic material retained.

$$\% \text{ retained} = \left(1 - \frac{\text{filtrate concentration}}{\text{initial concentration}} \right) \times 100 \quad (2.14)$$

These data can be used to report the "apparent molecular weight distribution" as the percentage of humic material in each fraction. Reported molecular weights can vary from 500-300000 (see Table 2.1). Many authors have investigated the potential problems that can arise in such a system. Problems like humic-membrane interactions, pore hydration, change of conformation of humic substances with experimental conditions, often lead to misleading results. These limitations have been discussed in detail in chapter 5.

2.4 METHODS THAT USE MATHEMATICAL APPROXIMATIONS

2.4.1 POTENTIOMETRIC TITRATIONS

In this method, the humic substances are modelled as either cylinders [40], compact spheres [40], or double layer cylinders or spheres [41] with surface potentials generated

by the ionisation of acidic groups. Based on the acid and base titration data in solutions of different ionic strengths, and numerical solutions of Poisson-Boltzmann equation for surface potentials, the equivalent radius is calculated. The equivalent radius is the radii of ideal charged cylinders or spheres that would display the same titration behaviour in response to humic charge density and ionic strength [40]. The radii calculated by this method are in the range of 0.2 to 4.4 nm depending on the model. ([40, 41] see Table 2.1). Molar mass of the molecules can also be calculated using the equivalent radius and the specific surface area, calculated from the density of the humic molecule [41].

Table 2.1 gives a comparison of the some of the results obtained by different techniques, used to measure size and/or molecular weight of humic substances. Figure 2.1 also illustrates some of the results in the literature on molecular weights of humic substances to illustrate the decrease from orders of 10^5 in 1960's to few thousands in recent years after development of more accurate techniques and improvements in HPSEC.

Table 2.1: Comparison of some results obtained on molecular size and weight of humic substances in the literature. M_n , M_w , M_v are number average, weight average and viscosity average molecular weight. M_p is the molecular weight at the peak maximum and M_{app} is the apparent molecular weight (obtained from ultrafiltration):

Technique	Sample	MW (daltons)	Size (nm)	Comment	Reference
Analytical ultracentrifugation	SRFA	$M_w=1460\pm 80$			[7]
	SRHA	$M_w=4260$			
Sedimentation Velocity	Soil HA extracts	$M_w=53000$		I=0.1 M	[42]
Equilibrium UC		$M_w=24000-230000$			[43]
Multi Angle Laser Light Scattering (MALLS)	Suwannee River NOM	$M_n=16595$	$R_n=56$	I=0.0069 M	[16]
		$M_w=25715$	$R_w=60$		
		$M_n=15050$	$R_n=30$	I=0.275 M	
		$M_w=20185$	$R_w=29$		
Light Scattering	Chernozem HA	$M_w=66200$			[44]
	Sod-podzol HA	$M_w=65800$			
Cryoscopy	Soil FA	$M_n=640$			[45]
	Soil organic matter	$M_n=669-1648$			[46]

Table 2.1, continued,

Technique	Sample	MW (daltons)	Size (nm)	Comment	Reference
Vapor pressure Osmometry	Soil FA	$M_n=951$			[47]
	SRFA	$M_n =829$			[5]
	SRFA	$M_n =734-823$			[12]
	SRHA	$M_n = 824-840$			
	Stream FA	$M_n =943$			[48]
	Marine FA	$M_n =501-792$			[48]
	Coal HA	$M_n=3090-10080$			[49]
		$M_n =600-5370$			
GPC (Sephadex)		$M_{app}=<10K- >100 K$			[28]
		$<700 - <200K$			[50]
High Performance Size Exclusion Chromatogra- phy	FA	$M_n= 839-1360, M_w=1000-2310$			[35]
	HA	$M_n=713-1330$ $M_w=1080-4100$			
	Nordic FA	$M_w=1690$		pH=6.5 I=0.02 M	[51]
	SRFA	$M_w=1340$		pH=6.5 I=0.02 M	

Table 2.1, continued,

Technique	Sample	MW (daltons)	Size (nm)	Comment	Reference
flow field-flow fractionation	SRFA SRHA	$M_n=1150,$ $M_w=1910,$	$d_p=1.06^*$ $d_p=1.35^*$		[21]
	soil/Peat FA:	$M_n=819-840$ $M_w=748-911$			
	HA	$M_n=1980-$ 3253 $M_w=2338-$ 3378			
	SRFA	$M_p=980$			
	SRHA	$M_p=1350-$ 1818	$d_p=1.59^*$		
	Leonardite HA		$d_p=1.54^*$		
	SRFA	$M_p=980$	$d_p=0.93$	pH=8.5	[52]
			$d_p=0.50$	pH=5.0	
			$d_p=<0.4$	pH=3.0	
Viscometry	Soil HA	$M_v=29000$		I=0.1 M	[53]
	SoilHA (Diff. source)	$M_v=110000$		I=0.1 M	
		$M_v=1200$		pH=6	[54, 55]
		$M_v=2700$		pH=7	

* Calculated by the author from published data

Table 2.1, continued,

Technique	Sample	MW (daltons)	Size (nm)	Comment	Reference
Viscometry	FA	$M_v=2300$		pH=6.5 I=5.4	[55]
	HA	$M_v=3700$		pH=6.5 I=7.3	
	FA	$M_w=68000$ $M_n=6200$			
	Soil HA	$M_v =1380, 1430$		pH=7.0	[56]
			$M_v =6370, 8800$		pH=10.5
	HA extracted from fertilised soil	$M_v =1290, 1390$		pH=7.0	
		$M_v =5610, 7240$		pH=10.5	
Electrophoresis	Soil HA	$M_w=2500-2000000$			[57]
Fluorescence Correlation Spectroscopy	NOM (9 samples)		d=1.8- 2.0 nm		[27]
Ultrafiltration	Aquatic	F1: $M_{app} < 1K^{\#}$ F2: $1K < M_{app} < 20K$ F3: $M_{app} > 20K$			[58]
	NOM	F1: $M_{app} < 1K$ F2: $1K < M_{app} < 10K$ F3: $M_{app} > 10K$			[59]
	NOM	F1: $M_{app} < 0.5 K$ F2: $0.5 K < M_{app} < 10 K$ F3: $10 K < M_{app} < 100 K$			[60]
	NOM	F1: $M_{app} < 0.5 K$ F2: $0.5 K < M_{app} < 2 K$ F3: $2 K < M_{app} < 5K$ F4: $5 K < M_{app} < 10 K$ F5: $10 K < M_{app} < 30K$			[61]

K= k daltons

Table 2.1, continued,

Technique	Sample	MW (daltons)	Size (nm)	Comment	Reference
Ultrafiltration	Aldrich HA	F1: $M_{app} < 2 K^{\#}$ F2: $2 K < M_{app} < 10 K$ F3: $10 K < M_{app} < 100 K$			[62]
	Aldrich HA	F1: $1 K < M_{app} < 10 K$ F2: $50 K < M_{app} < 100 K$ F3: $100 K < M_{app} < 300 K$			[63]
Potentiometric titrations	Soil HA			Cylindrical geometry model	[40]
			$r_{eq}^{\oplus} = 0.24$ nm	90% ionisation	
		$r_{eq} = 1.1$ nm	10% ionisation		
	SRFA	$M_{eq}^* = 545$	$r_{eq} = 0.6$ nm	Spherical double layer model	[41]
			$r_{eq} = 0.19$ nm	Cylindrical double layer model	

K : k daltons

$\oplus r_{eq}$: Equivalent radius (radius of ideal charged cylinders(or spheres) that would display the same titration behaviour in response to humic acid charge density and ionic strength.)

* M_{eq} = Molar mass calculated using r_{eq} and specific surface area.

The results gathered in Table 2.1 demonstrate the wide range of the molecular parameters of humic substances given in the literature. Figure 1 gives an indication of how the results on the molecular weight of the humic substances have changed throughout the years. The results obtained with FIFFF gave sizes much smaller than those obtained from UF, GPC and light scattering. Improved GPC (HPSEC) gives results in the range closer to those obtained by FIFFF.

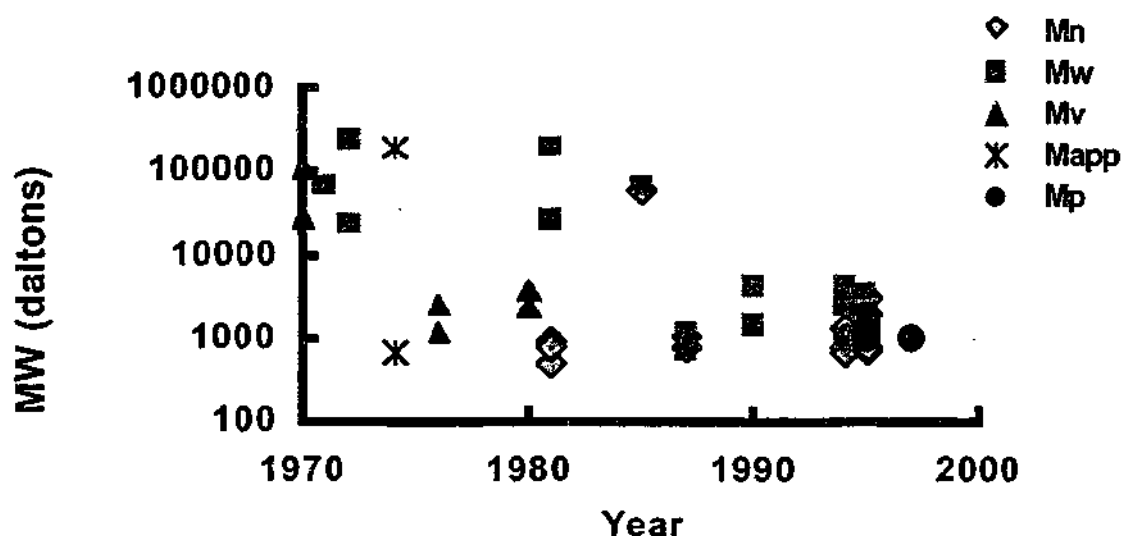


Figure 2.1: Plot of some selected molecular weight data of humic substances reported in the literature at various times between 1970 and 1997. M_n , M_w and M_v are the number average, weight average and viscosity average molecular weights respectively. M_p is the molecular weight at the peak maximum and M_{app} is the apparent molecular weight obtained by UF.

2.5 CONCLUSIONS

In this chapter some of the methods commonly used to measure molecular parameters of humic substances are discussed. A brief evaluation of the advantages and limits of each technique is given. The absolute methods of measurements of size and molecular weight are often very time-consuming (ultracentrifugation) or are unable to measure the size of small molecules (light scattering) like humic substances. Imaging techniques like TEM and AFM can be used to study the size of humic substances but suffer from artefacts due to sample preparation. Improvements are needed for the imaging techniques to be able to give reliable results although from the research carried out in recent years AFM looks promising.

Methods that need calibration, like UF and SEC should be used very carefully. UF does not separate humic substances based on size or MW alone. SEC has been improved in the last decade and the recent results are promising. Special care must be taken in choosing appropriate calibration standards. PSS proves to give better results than globular proteins but still they are not as branched and heterogeneous as humic substances. It is probably better to report the primary parameter obtained by a technique (like size or MW), instead of using standards to generate derived parameters. Flow field-flow fractionation is an absolute method for measurement of the diffusion coefficient of the humic substances. It will be explained in Chapter 3 that there are no stationary phases in FIFFF, the separation is based on the physical (and not chemical) interaction of the sample with the field and above all, because the mathematics have been fully developed, parameters such as diffusion coefficient can be calculated directly from first principles. FIFFF was the main technique used in this thesis for determining molecular size distribution.

2.6 REFERENCES

1. Glover, C.A., Absolute colligative property measurements, in P.E. Slade Jr, (Ed.), *Polymer Molecular Weights, Part I*, Marcel Dekker, New York, 1975, 79-159.
2. Aiken, G.R., and Gilham, A.H, Determination of molecular weight of humic substances by colligative property measurement, in M.H.B. Hayes, MacCarthy, P., Malcolm, R.L., and Swift, R.S., (Eds.), *Humic Substances II, In Search of Structure.*, John Wiley & Sons, Chichester. 1989, 516-544 .
3. Reuter, J.H., and Perdue, E.M., Calculation of molecular weights of humic substances from colligative data: Application to aquatic humus and its molecular size fractions., *Geochimica et Cosmochimica Acta*, 45 (1981) 2017-2022 .

4. Thurman, E.M., Wershaw, R.L., Malcolm, R.L and Pinckney, D.J., Molecular size of aquatic humic substances, *Organic Geochemistry*, 4 (1982) 27-35.
5. Aiken, G.R., and Malcolm, R.L., Molecular weights of aquatic fulvic acids by vapor pressure osmometry, *Geochimica et Cosmochimica Acta*, 51 (1987) 2177-2184.
6. Swift, R.S., Molecular weight, Shape and size of humic substances by ultracentrifugation, in M.H.B. Hayes, MacCarthy, P., Malcolm, R. L., and Swift, R.S., (Eds.), *Humic Substances II: In Search of Structure*, John Wiley&Sons, Chichester, 1989 467-496
7. Reid, P.M., Wilkinson, A.E., Tipping, E. and Jones, M.N., Determination of molecular weights of humic substances by analytical (UV scanning) ultracentrifugation, *Geochimica et Cosmochimica Acta*, 54 (1990) 131-138.
8. Wilkinson, A.E., Hesketh, N., Higgs, J.J.W., Tipping E., Jones, M.N., The determination of the molecular mass of humic substances from natural waters by analytical ultracentrifugation, *Colloids and Surfaces, A: Physicochemical and Engineering Aspects*, 73 (1993) 19-28.
9. Swift, R.S., Molecular weight, size, shape, and charge characteristics of humic substances: some basic considerations, in M.H.B. Hayes, MacCarthy, P., Malcolm, R.L., and Swift, R.S., (Eds.), *Humic Substances II: In Search of Structure*, John Wiley&Sons, 1989, 449-465.
10. Guinier, A., and Fournet, G., *Small-Angle Scattering of X-rays*. Wiley. New York, 1955.
11. Wershaw, R.L., Size and shapes of humic substances by scattering techniques, in M.H.B. Hayes, MacCarthy, P., Malcolm, R.L., and Swift, R., (Eds.), *Humic Substances II, In Search of Structure*, Chichester. 1989, 545-559.

12. Aiken, G.R., Brown, P.A., Noyes, T.I., and Pinckney, D.J., Molecular size and weight of fulvic and humic acids from the Suwannee river, in R.C. Averett, Leenheer, J.A., McKnight, D.M., and Thorn, K.A., (Eds.), *Humic Substances in the Suwannee River, Georgia: Interactions, Properties, and Proposed Structures*, U.S. Geological Survey: Denver. 1995, 89-97.
13. Jones, M.N., and Bryan, N.D., Colloidal properties of humic substances, *Advances in Colloid and Interface Science*, 78 (1998) 1-48.
14. Thurman, E.M., *Organic Geochemistry of Natural Waters*. Martinus Nijhoff/Dr W. Junk publishers. Dordrecht, 1985.
15. Reid, P.M., Wilkinson, A. E., Tipping, E., and Jones, M. N., Aggregation of humic substances in aqueous media as determined by light-scattering methods, *Journal of Soil Science*, 42 (1991) 259-70.
16. Wagoner, D.B., Christman, R.F, Cauchon, G. and Paulson, R., Molar mass and size of Suwannee River natural organic matter using multi-angle laser light scattering, *Environmental Science and Technology*, 31 (1997) 937-941.
17. Wagoner, D.B., and Christman, R.F., Molar mass and size of Norwegian aquatic NOM by light scattering, *Environment International*, 25 (1999) 275-284.
18. Giddings, J.C., Field-flow fractionation, *C & E News*, 66 (1988) 34-45.
19. Giddings, J.C., and Caldwell, K.D., Field-flow fractionation, in B.W. Rositer, and Hamilton, J.F., (Eds.), *Physical Methods of Chemistry*, John Wiley & Sons: New York. 1989, 867-938.
20. Beckett, R., and Hart, B.T., Use of field-flow fractionation techniques to characterize aquatic particles and macromolecules, in J. Buffle, and van Leeuwen, H.P., (Eds.), *Environmental Particles*, Lewis Publishers. 1993, 165-205.

21. Beckett, R., Zhang J., and Giddings C., Determination of molecular weight distributions of fulvic and humic Acids, using flow field-flow fractionation, *Environmental Science and Technology*, 21 (1987) 289-295.
22. Chen, Y., Banin, A, and M. Schnitzer, Use of the scanning electron microscope for structural studies on soils and soil components, *Scanning Electron Microscopy*, 9 (1976) 425-32.
23. De Nobili, M., Baca, M. T.,and Milani, N., Scanning electron microscopy of humic substances produced during cellulose decomposition, *Chemical Ecology*, 11 (1995) 55-66 .
24. Ghosh, K.a.S., M., A scanning electron microscopic study of effects of adding neutral electrolytes to solutions of humic substances, *Geoderma*, 28 (1982) 53-6.
25. Leppard, G.G., Burniston E., and Buffle J., Transmission electron microscopy of the natural organic matter of surface waters, *Analytica Chimica Acta*, 232 (1990) 107-121.
26. Chen, Y., and Schnitzer, M., Sizes and shapes of humic substances by electron microscopy, in P. MacCarthy, Malcolm, R.L., and Swift, R.S., (Ed.), *Humic Substances I, In Search of Structure*, John Wiley & Sons: Birmingham. 1989, pp. 621-638.
27. Lead, J.R., Balnois, M., Hosse, M., Menghetti, R., and Wilkinson, K.J., Characterization of Norwegian natural organic matter: size, diffusion coefficients, and electrophoretic mobilities, *Environment International*, 25 (1999) 245-258.
28. Gjessing, E.T., Use of sephadex gels for estimation of humic substances in natural water, *Nature*, 208 (1965) 1091-1092 .

29. Cameron, R., Swift, R.S., Thornton, B.K. and Posner, A.M., Calibration of gel permeation chromatography materials for use with humic acid, *Journal of Soil Science*, 23 (1972a.) 394-408.
30. Cameron, R., Thornton, B.K., Swift, R.S., and Posner, A.M., Molecular weight and shape of humic acids from sedimentation and diffusion measurements on fractionated extracts, *Journal of Soil Science*, 23 (1972b.) 394-408.
31. O'Loughlin, E., and Chin, Y.P., Effect of detector wavelength on the determination of the molecular weight of humic substances by high pressure size exclusion chromatography, *Water Research*, 35 (2001) 333-338.
32. Zhou, Q., Cabaniss, S. E., and Maurice, P. A., Considerations in the use of high-pressure size exclusion chromatography (HPSEC) for determining molecular weights of aquatic humic substances, *Water Resarch*, 34 (2000) 3505-3514.
33. De Nobili, M., and Chen, Y., Size Exclusion chromatography of humic substances: limits, perspectives and prospects, *soil science*, 164 (1999) 825-833 .
34. Perminova, I. V., Frimmel, F. H., Kovalevskii, D. V., Abbt-Braun, G., Kudryavtsev, A. V., and Hesse, S. Development of a predictive model for calculation of molecular weight of humic substances, *Water Research*, 32 (1998) 872-881 .
35. Chin, Y.P., Aiken, G., and O'Loughlin, E., Molecular weight, polydispersity and spectroscopic properties of aquatic humic substances, *Environmental Science and Technology*, 28 (1994) 1853-1858.
36. Pelekani, C., Newcombe, G., Snoeyink, V.L., Hepplewhite, C., Assemi, S., and Beckett, R., Characterisation of natural organic matter using size exclusion chromatography, *Environmental Science and Technology*, 33 (1999) 2807-2813.

37. von Wandruszka, R., Schimpf, M., Hill, M., and Engebretson, R., Characterization of humic acid fractions by SEC and MALS., *Organic Geochemistry*, 30 (1999) 229-235 .
38. Town, R.M., Powell H.K.J., Limitations of XAD resins for the isolation of the non-colloidal humic fractions in soil extracts and aquatic Samples, *Analytica Chimica Acta*, 271 (1993) 195-202.
39. Chin, Y.P., and Gschwend, P.M., The abundance, distribution and configuration of porewater organic colloids in recent sediments, *Geochimica et Cosmochimica Acta*, 55 (1991) 1309-1317.
40. Barak, P., and Chen, Y., Equivalent radii of humic macromolecules from acid-base titrations, *Soil Science*, 154 (1992) 184-195.
41. de Wit, J.C.M., van Riemsdijk W.H., and Koopal L.K., Proton binding to humic substances 1. Electrostatic effects, *Environmental science and technology*, 27 (1993) 2005-2022.
42. Stevenson, F.J., van Winkle, Q., and Martin, W.P, Physicochemical investigations of clay-adsorbed organic colloids:II., *Soil Science society of America Proceedings*, 17 (1953) 31-34 .
43. Posner, A.M., and Creeth, J.M., A study of humic acid by equilibrium ultracentrifugation, *Journal of Soil Science*, 23 (1972) 333-341 .
44. Orlov, D.S., Ammosova, Ya, M., Glebova, Ye.I., Il'in, N.P., and Kolesnikov, M.P., Molecular weights, sizes, and configurations of humic-acid particles, translated from *Pochvovedeniye*, 11 (1971) 43-56 .
45. Wilson, S.A., and Weber, J.H., A comparative study of number average dissociation-corrected molecular weights of fulvic acids isolated from water and soil., *Chemical Geology*, 19 (1977) 285-293 .

46. Schnitzer, M., and Desjardins, J.G., Molecular and equivalent weights of organic matter of a podzol, *Soil Science Society of America Proceedings*, 26 (1962).
47. Hansen, E.H., and Schnitzer, M., Molecular weight measurements of poly carboxylic acids in water by vapor pressure osmometry, *Analytica Chimica Acta*, 46 (1969) 247-254.
48. Gilam, A.H., and Riley, J.P., Correction of osmometric number-average molecular weights of humic substances for dissociation, *Chemical Geology*, 33 (1981) 355-366 .
49. Wood, J.C., Moschopedis, S.E., and Eloffson, R.M., Studies in humic acid chemistry: 1. Molecular weights of humic acid in sulpholane, *Fuel*, 40 (1961) 193-201.
50. Kemp, A.L.W., and Wong, H.K.T., Molecular weight distribution of humic substances from lakes ontario and erie sediments, *Chemical Geology*, 14 (1974) 15-22.
51. Hongve, D., Baann, J., Becher, G., and Loemo, S., Characterization of humic substances by means of high-performance size exclusion chromatography, *Environment International*, 22 (1996) 489-494.
52. Schimpf, M.E., and Petteys, M.P., Characterization of humic materials by flow field-flow fractionation, *Colloids and Surfaces, A*, 120 (1997) 87-100.
53. Datta, C., and Mukherjee, S.K., Viscosity behavior of natural humic acids isolated from diverse soil types, *Jornal of Indian Chemical society*, 47 (1970) 1105-1108.
54. Chen, Y., and M. Schnitzer., Viscosity measurements on soil humic substances, *Soil Science Society of America Journal*, 40 (1976) 866-872 .
55. Gosh, K., and Schnitzer, M., Macromolecular structuers of humic substances, *Soil Science*, 129 (1980) 266-276.
56. Gonet, S.S., and Wegner, K., Viscometric and chromatographic studies of soil humic acids, *Environmental International*, 22 (1996) 485-488.

57. Kasparov, S.Y., Tikhomirov, F.A., and Fless, A.D., Use of disk electrophoresis to fractionate humic acids, *Soviet Soil Science*, 36 (1981) 21-28.
58. Gjessing, E.T., Ultrafiltration of aquatic humus, *Environmental Science and Technology*, 4 (1970) 437-438.
59. Wilander, A., A study on the fractionation of organic matter in natural water by ultrafiltration techniques., *Schweizerische Zeitschrift für Hydrologie*, 34 (1972) 190-200 .
60. Ogura, N., Molecular weight fractionation of dissolved organic matter in coastal seawater by ultrafiltration, *Marine Biology*, 24 (1974) 305-312.
61. Amy, G.L., Collins M.R., Kuo, C.J. and King P.H., Comparing gel permeation chromatography and ultrafiltration for the molecular weight characterization of aquatic organic matter, *Journal of American Water Works Association*, 79 (1987) 43-49.
62. Kuchler, I.L., Miekeley, N., Ultrafiltration of humic compounds through low molecular mass cut-off level membranes, *The Science of the Total Environment*, 154 (1994) 23-28.
63. Rao, L., and Choppin, G.R., Thermodynamic study of the complexation of Neptunium (V) with humic acids, *Radiochimica Acta*, 69 (1995) 87-95.

CHAPTER 3

FLOW FIELD-FLOW FRACTIONATION

3.1 INTRODUCTION

In this thesis flow field-flow fractionation has been used as the major analytical technique. The FIFFF method, construction of the channel, membrane synthesis and FIFFF data treatment will be explained in this chapter. Other methods have also been used in different chapters of the thesis. These methods will be introduced briefly in the introduction part of each relevant chapter.

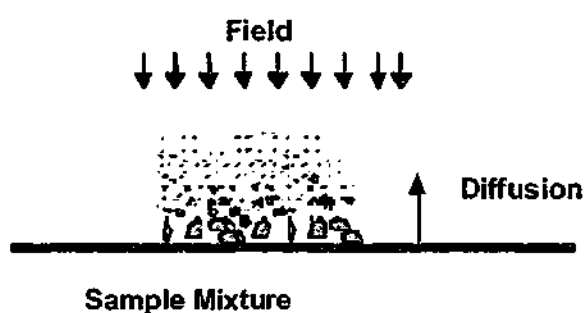
3.2 FIELD-FLOW FRACTIONATION

Field-flow fractionation (FFF) is a chromatography like separation technique in which a field, perpendicular to the channel flow, is used to bring the sample species close to the accumulation wall in a thin channel. After a certain stop flow period of time, which allows the particles to relax under the applied field, the laminar channel flow elutes the smaller components first and the larger ones later (Figure 3.1).

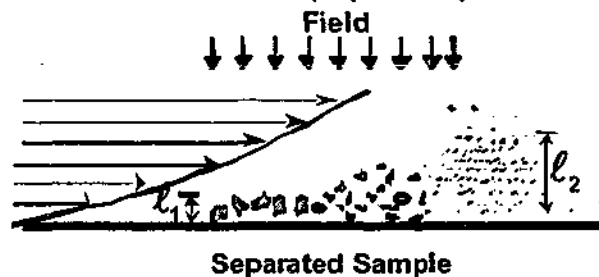
(a) Channel flow and field off (after injection):



(b) Field on and channel flow off (during relaxation):



(c) Channel flow and field on (separation):



(d) Elution Profile

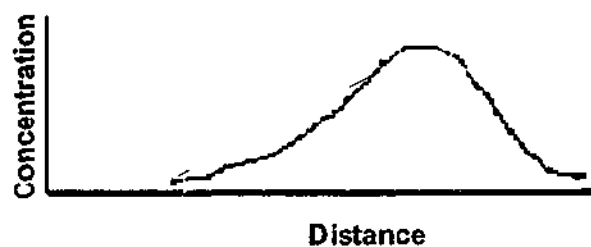


Figure 3.1: Representation of the separation mechanism in a field-flow fractionation channel ((a), (b) and (c)) and the concentration profile along the channel of an eluting sample zone (d).

The field can be gravitational, centrifugal, thermal gradient, electrical or in case of flow field-flow fractionation (FIFFF), a crossflow. The separation in FFF is due to both the physical interaction of the sample species with the applied field and their diffusivity. The detailed theory of field-flow fractionation can be found in Giddings [1], Giddings and Caldwell [2] and Beckett and Hart [3]. Table 3.1 lists different FFF techniques and the particle or molecular parameters that can be found from each technique.

Table 3.1: Parameters that can be obtained from commonly used FFF techniques: k is the Boltzmann constant, T is the temperature, ω is the rotational speed, r is the radius of the centrifuge, $\Delta\rho$ is the density difference between the carrier and the sample, w is the channel thickness, d is the diameter, V^0 is the channel void volume, V_c is the volumetric crossflow rate, D is the diffusion coefficient, D_T is the thermal diffusion coefficient, E_{eff} is the effective charge, μ is the viscosity of the carrier solution.

FFF Technique	Applied Field Gradient	λ	Primary parameter calculated
Sedimentation FFF (SdFFF)	Centrifugal	$\frac{6kT}{\pi\omega^2rw\Delta\rho d^3}$	buoyant mass (diameter, density)
Flow FFF (FIFFF)	Cross Flow	$\frac{DV^0}{w^2V_c}$	diffusion coefficient
Thermal FFF (ThFFF)	Temperature gradient	$\frac{D}{D_T\Delta T}$	D/D_T (thermal diffusion coefficient)
Electrical (EIFFF)	Electrical	$\frac{D}{\mu E_{\text{eff}} w}$	Electrophoretic mobility (charge, diameter)

In the case of constant field and flow runs the retention ratio (R) and the retention parameter (λ) are calculated from the measured retention volume (V_r) and channel void volume (V^0) using the normal mode FFF equation:

$$R = \frac{V^0}{V_r} = 6\lambda \left[\coth \frac{1}{2\lambda} - 2\lambda \right] \quad (3.1)$$

For FIFFF the retention parameter enables calculation of the diffusion coefficient (D) of the sample species (D):

$$D = \frac{\lambda \dot{V}_c w^2}{V^0} \quad (3.2)$$

where \dot{V}_c is the volumetric crossflow rate and w is the channel thickness. The diffusion coefficient obtained from FIFFF can be used to calculate the hydrodynamic size of the sample species using Stokes-Einstein equation:

$$d = \frac{k T}{3 \pi \eta D} \quad (3.3)$$

Where k is the Boltzmann constant, T is the temperature and η the viscosity of water at the given temperature.

Molecular weight (MW) of the sample species can be obtained by using molecular weight standards and an empirical relationship between the diffusion coefficient and molecular weight [4]:

$$D = AM^{-b} \quad (3.4)$$

where A and b are constants for the sample-solvent system and M is the sample MW.

FIFFF has been successfully used for determination of size and MW of humic substances since 1987 [4-6]. The results are within the same range as the values obtained by colligative properties [8], small angle x-ray scattering and recent studies by size exclusion chromatography [9] (see Table 2.1).

3.3 DATA TREATMENT

3.3.1 CONVERSION OF FRACTOGRAM TO SIZE AND MW DISTRIBUTION

In FIFFF, the fractogram is a plot of the detector response versus elution volume or time. The elution time or elution volume is then used to calculate certain molecular parameters (e.g. D , d or M). The path to calculate these parameters from the retention volume is illustrated in Figure 3.2.

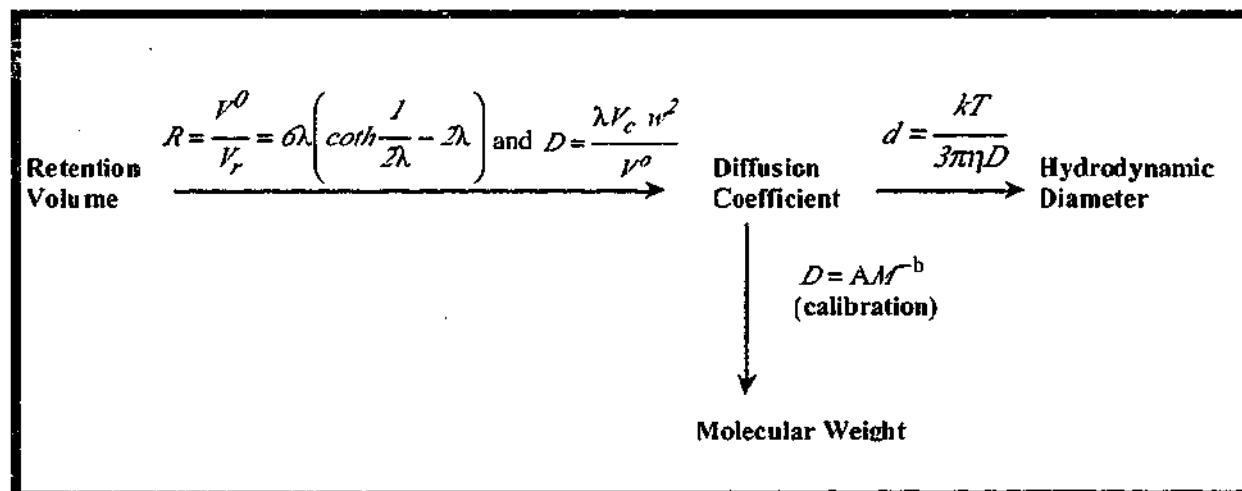


Figure 3.2: Scheme for calculation of size and molecular weight from the retention volume in FIFFF. R is the retention ratio, V^0 is the channel void volume, V_r is the retention volume, λ is the retention parameter, D is the diffusion coefficient of the sample species, V_c is the volumetric crossflow rate, w is the channel thickness, A and b are empirical constants.

The following paragraph should be read before paragraph 2 in page 47.

The UV distribution may be biased according to the distribution of chromophores in the humic molecules across the MW distribution of the humic sample. However, recent studies using both UV and DOC detectors have shown that the retention times at the peak maximum obtained by both detection systems are the same [13,14] but the DOC/UV ratio can be higher for smaller molecules. So it is possible that the values obtained for M_p and M_n using a DOC detector could be slightly less than those obtained by a UV detector.

A size distribution curve is usually defined as a plot in which the area under the curve between specified size limits gives the fraction of the total sample in that size range. In such a distribution, the y -axis is usually referred to as the frequency function by comparison with frequency histogram diagrams. It should be dm^c/dd for a diameter distribution, dm^c/dM for a relative molar mass distribution or dm^c/dD for a distribution of diffusion coefficients. In these distributions, d , M or D will be the x -axis respectively and m^c would be the cumulative mass of eluted sample up to a specific point in the run.

A UV detector is usually used to monitor the mass concentration of sample in the eluent (dm^c/dV). It should be noted that measurement by UV uses the assumption that the chromophores are distributed evenly throughout the whole distribution and hence the molar absorptivity does not change with the size or molecular weight. The frequency function for a size distribution can be written as follows, using the mass concentration:

$$\frac{dm_i^c}{dd} = \frac{dm_i^c}{dV} \cdot \frac{dV}{dd} \quad (3.5)$$

In practice, the differential dm_i^c/dd can be calculated by multiplying each ordinate value (dm_i^c/dV) by $\delta V_i/\delta d$, where δV is the difference between the elution volume for consecutive digitised points and δd is the corresponding difference in the particle diameter for these points. m_i^c is the cumulative mass of sample eluted up to the point V_i and i signifies the i^{th} point in the collected FFF data. Similarly distributions of the molar mass (M) and the diffusion coefficient (D) can be obtained from the fractogram using the following equations:

$$\frac{dm_j^c}{dM} = \frac{dm_j^c}{dV} \cdot \frac{dV}{dM} \quad (3.6)$$

and

$$\frac{dm_j^c}{dD} = \frac{dm_j^c}{dV} \cdot \frac{dV}{dD} \quad (3.7)$$

3.3.2 RELATIONSHIP BETWEEN THE UV SIGNAL AND THE MOLAR CONCENTRATION

The UV signal (S_i) is assumed to indicate the mass based concentration eluted at a certain point (V_i) on the fractogram:

$$\text{UV signal } (S_i) \propto \frac{dm_i^c}{dV_i} \cong \frac{\delta m_i^c}{\delta V_i} \propto \frac{\delta n_i^c M_i}{\delta V_i} \quad (3.8)$$

Where δn_i specifies the number of molecules with mass M_i in the volume increment δV_i .

The number based concentration is represented by $(\delta n_i/\delta v_i)$ and is directly proportional to the molar concentration. Since the volume increment δV_i between digitised points is constant, the UV signal can be assumed to be proportional to the mass of sample transported in this volume. i.e.:

$$S_i \propto \delta n_i M_i \quad (3.9)$$

3.3.3 CALCULATION OF M_n AND M_w UTILISING THE UV SIGNAL

The average molecular weights M_n and M_w can be calculated using the UV detector signal as follows:

By definition the number average (M_n) and weight average (M_w) molecular weights can be written as:

$$M_n = \frac{\sum_i \delta n_i M_i}{\sum_i \delta n_i} \quad (3.10)$$

and

$$M_w = \frac{\sum_i \delta w_i M_i}{\sum_i \delta w_i} = \frac{\sum_i \delta n_i M_i^2}{\sum_i \delta n_i M_i} \quad (3.11)$$

Equation 3.4 showed that the diffusion coefficient can be related to the molecular weight in a given solvent.

$$D = AM^{-b}$$

where A and b are constants.

From FFF measurements the value of b is about 0.5 for humic substances in water [4, 5, 10]. Thus:

$$S_i \propto \delta n_i M_i \propto \frac{\delta n_i}{D^2} \quad (3.12)$$

Thus, from equation 3.9 ($S_i \propto \delta n_i M_i$):

$$M_n = \frac{\sum_i S_i}{\sum_i \frac{S_i}{M_i}} \quad (3.13)$$

and

$$M_w = \frac{\sum_i S_i M_i}{\sum_i S_i} \quad (3.14)$$

3.3.4 CALCULATION OF d_n AND d_w UTILISING THE UV SIGNAL

The number average and weight average diameters can also be written as:

$$d_n = \frac{\sum_i \delta n_i d_i}{\sum_i \delta n_i} \quad (3.15)$$

And

$$d_w = \frac{\sum_i \delta n_i M_i d_i}{\sum_i \delta n_i M_i} \quad (3.16)$$

From equation 3.12 and Stoke's equation:

$$S_i \propto \frac{\delta n_i}{D_i^2} \propto \delta n_i d_i^2 \quad (3.17)$$

Hence d_n and d_w can be written as:

$$d_n = \frac{\sum_i \delta n_i d_i}{\sum_i \delta n_i} = \frac{\sum_i \frac{S_i}{d_i^2} d_i}{\sum_i \frac{S_i}{d_i^2}} = \frac{\sum_i \frac{S_i}{d_i}}{\sum_i \frac{S_i}{d_i^2}} \quad (3.18)$$

and the weight average diameter can be written as:

$$d_w = \frac{\sum_i \delta n_i M_i d_i}{\sum_i \delta n_i M_i} = \frac{\sum_i S_i d_i}{\sum_i S_i} \quad (3.19)$$

3.3.5 CALCULATION OF D_n AND D_w FROM FIFFF RESULTS

By definition the number average and weight average diffusion coefficients can be written as:

$$D_n = \frac{\sum_i \delta n_i D_i}{\sum_i \delta n_i} \quad (3.20)$$

And

$$D_w = \frac{\sum_i \delta n_i M_i D_i}{\sum_i \delta n_i M_i} \quad (3.21)$$

Substitution of δn_i from equation 3.12 into equation 3.20 results in:

$$D_n = \frac{\sum_i S_i D_i^3}{\sum_i S_i D_i^2} \quad (3.22)$$

Similarly from equation 3.21, D_w can be written as:

$$D_w = \frac{\sum_i D_i \cdot S_i}{\sum_i S_i} \quad (3.23)$$

3.4 EXPERIMENTAL

3.4.1 FIFFF INSTRUMENTATION

Field flow fractionation is operated in a similar manner as a chromatography system. The major difference is that the sample does not interact with a stationary phase. Figure 3.3 illustrates the general layout of a FFF system and Figure 3.4 shows the FIFFF system used in this thesis:

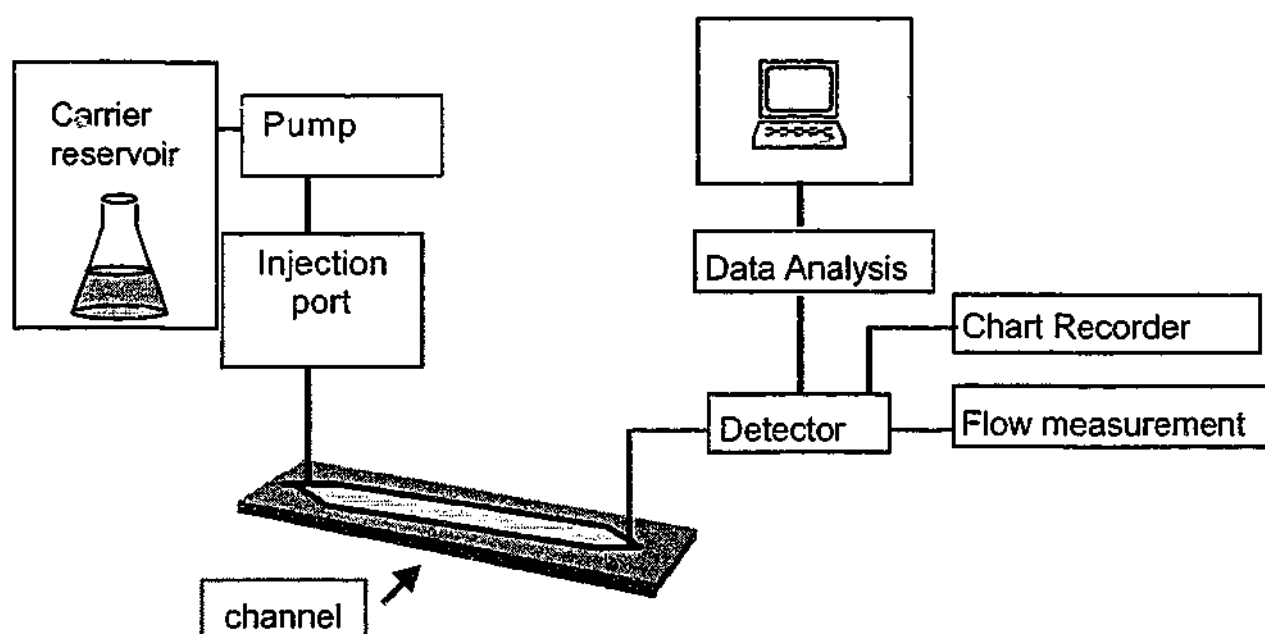


Figure 3.3: Experimental layout of an FFF system

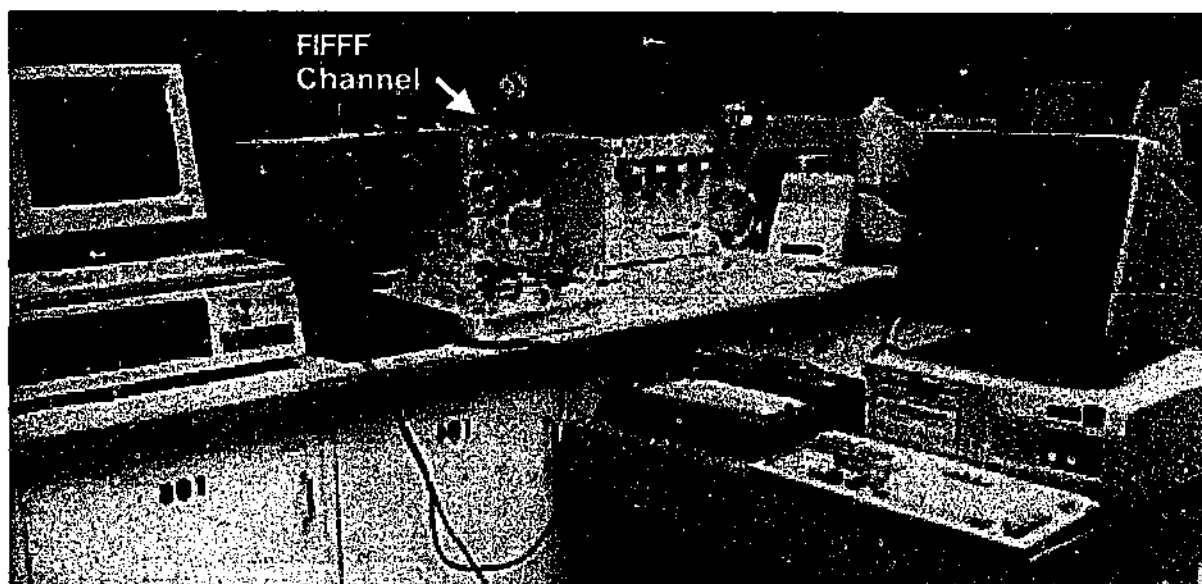


Figure 3.4: The FIFFF system used in this thesis

3.4.2 FIFFF CHANNEL

The FIFFF channel used in this study consists of a thin Teflon spacer (thickness of 0.25 mm) with a hole cut out with shape of the channel. The dimensions of the channel were: length 27.4 cm tip to tip and breadth 2 cm. The ends are triangular with an apex angle of 45° . The channel flow and crossflow were introduced using TEFLON tubing. The spacer sheet is sandwiched between two Lucite blocks. Porous frits (pore size of approximately $5\ \mu\text{m}$) mounted inside these blocks, allow the flow of carrier across the channel. Loss of sample through the lower frit (accumulation wall) is prevented by using a membrane. The FIFFF channel design is shown in Figure 3.5:

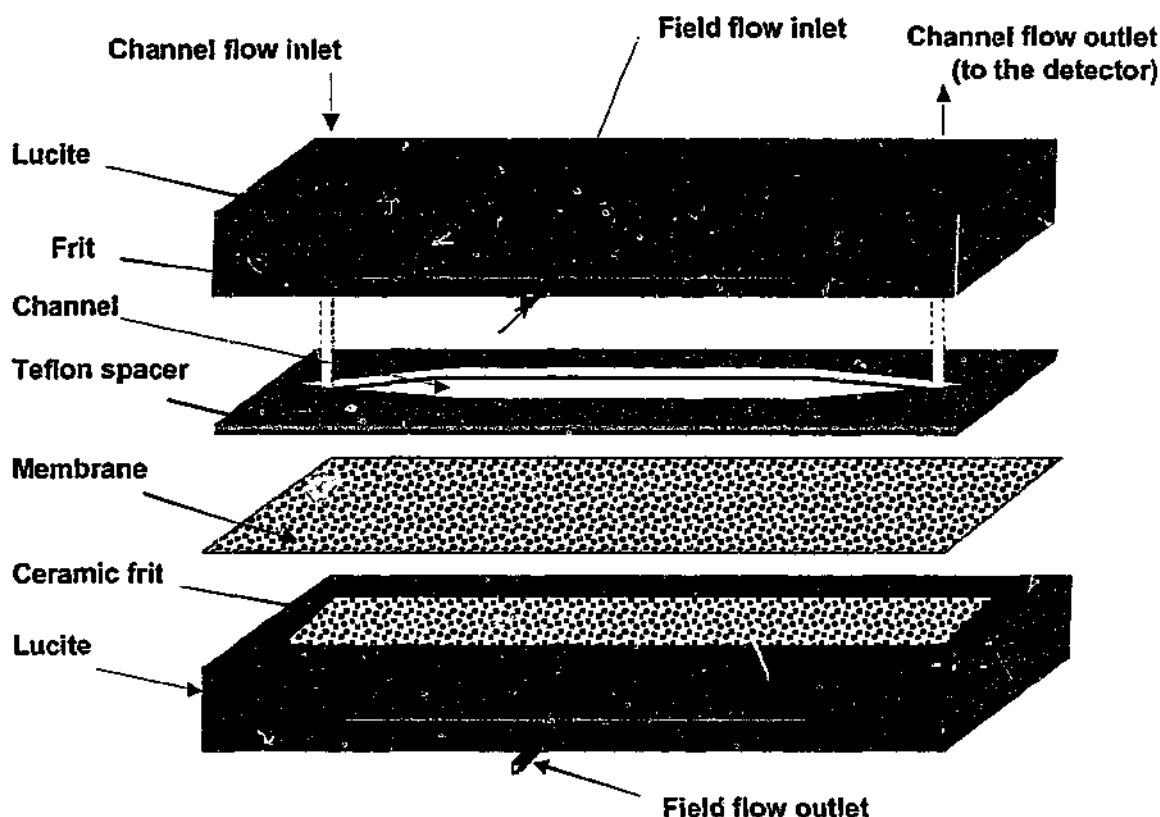


Figure 3.5: Schematic diagram of a FIFFF channel.

The channel and field flow rates were controlled using a 4 channel HPLC pump (Universal fractionator fluid delivery module, FFFractionation, U.S.A). Pressure gauges on the inlets of field and channel were used to measure the inlet flow pressures. The membrane exerted a back pressure of 40-70 psi. A needle valve at the outlet of the detector (see Figure 3.5) was used to bring the back pressure of the channel flow to that of the field flow. One way of the pump was used to draw the flow out of the channel (unpump). The Channel and field flow outlets were directed to flowmeters (built inhouse) and were measured every minute. A Rheodyne® 20 μ L manual injection port (Rheodyne Corporation, Cotati, CA) was used for sample injection. The channel plumbing is illustrated in Figure3.6.

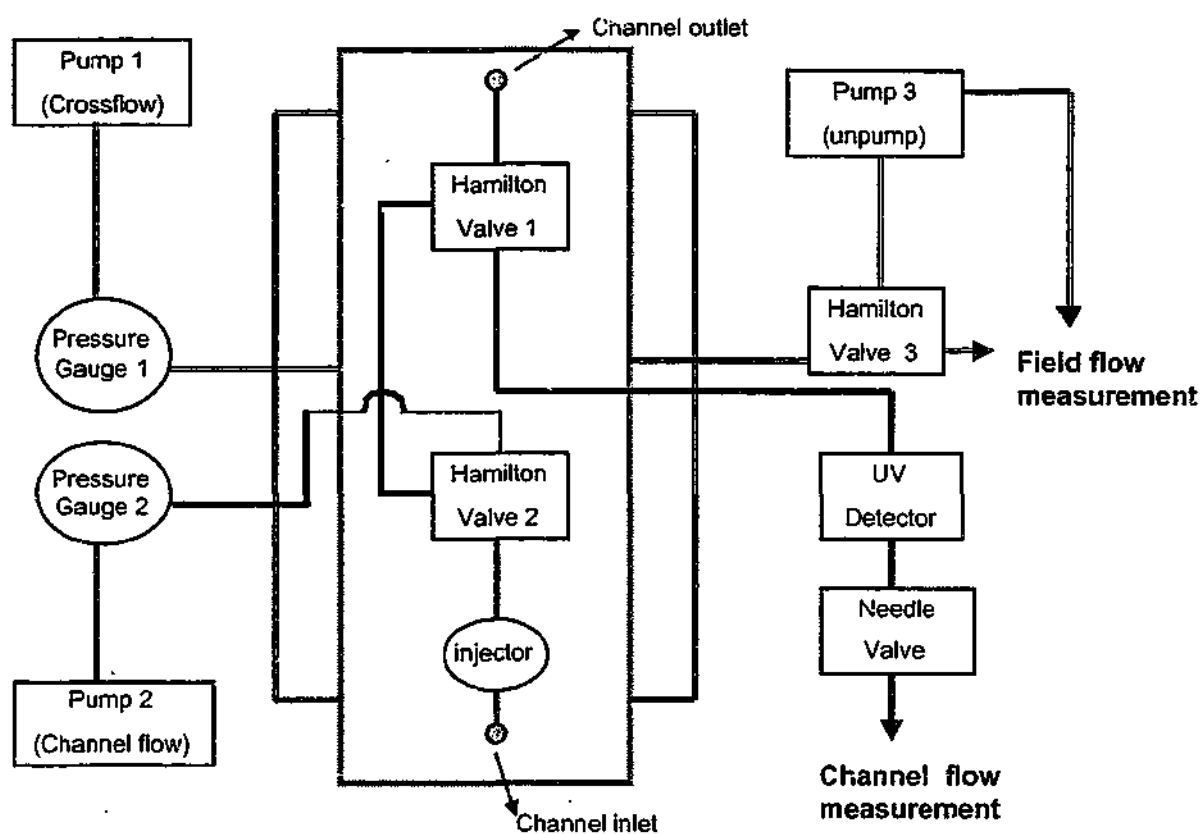


Figure 3.6: Plumbing of the FIFFF system used in this thesis.

After entering the desired channel and field flow rates to the pump software, three steps were followed to balance the back pressures produced by the detector, while the flow equal to the channel flow was going through it (P1 in Figure 3.7), with backpressure produced by the membrane when it had the field flow going through it (P2 in Figure 3.7). This would ensure that the channel flow and the crossflow were not disturbed in the channel and minimised disturbance to the detector signal when the channel bypass was switched on and off.

The steps were as follows:

- 1) The crossflow (field) was passed through the channel. The backpressure (exerted by the membrane) was measured by pressure gauge 2. The crossflow rate was measured by flow meter 2. The channel flow rate was measured without it passing through the channel (channel was bypassed). The backpressure exerted by the detector was measured by pressure gauge 1 and the channel flow rate was measured by flow meter 1. Because of the small pore size of the membrane, the back pressure due to the membrane (P2) was usually higher than the back pressure caused by the the detector (P1). A needle valve after the detector was used to adjust P1 to the same value as P2. The channel and field flowrates and P1 and P2 were then recorded. This step is illustrated in Figure 3.7(a).
- 2) The channel flow was then directed through the channel. This would enable mixing the field and channel flows. The flow rates and pressures were measured again. Ideally there should not be a difference between the pressures (already adjusted in step 1) and the flow rates with the previous stage. This step is illustrated in Figure 3.7(b).
- 3) The crossflow outlet was connected to the unpump using the 3 way valve 2. No adjustment should be necessary to the flow rates and pressures. The average flowrates and pressures were recorded. This step is illustrated in Figure 3.7(c).

The runs could only be started if there was no significant difference between the flow rates measured by flow meters 1 and 2 and the pressures measured by pressure gauges 1 and 2 in the three steps mentioned above. In case of any difference, the FIFFF channel, pumps, detector and fittings should be checked systematically for any leakage and/or blockage.

(a)

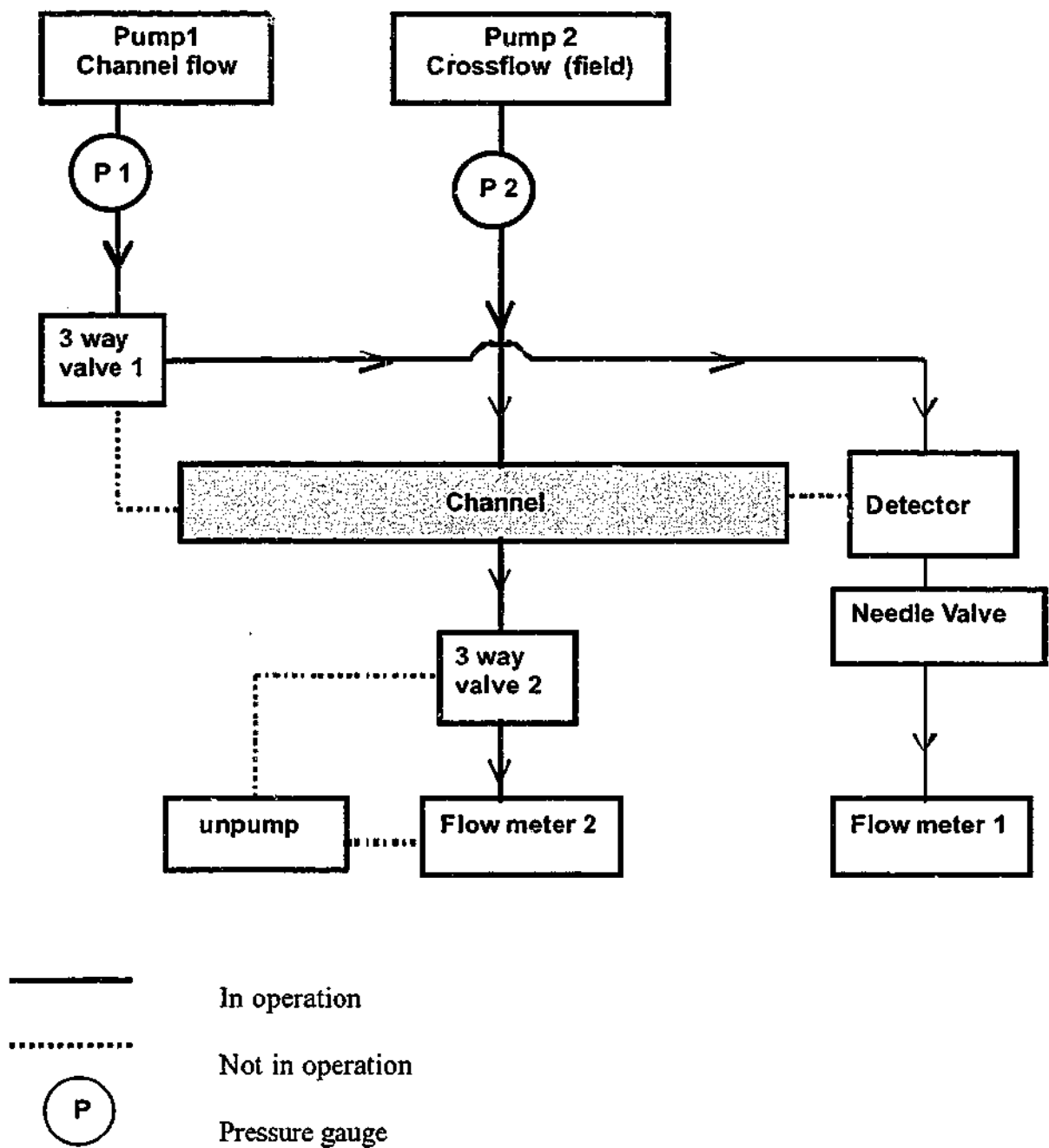


Figure 3.7: Schematic diagram of a FIFFF system illustrating how the back pressures and flow rates are balanced. (a) Channel flow is by passed and the crossflow is going through the channel. Unpump is off.

(b)

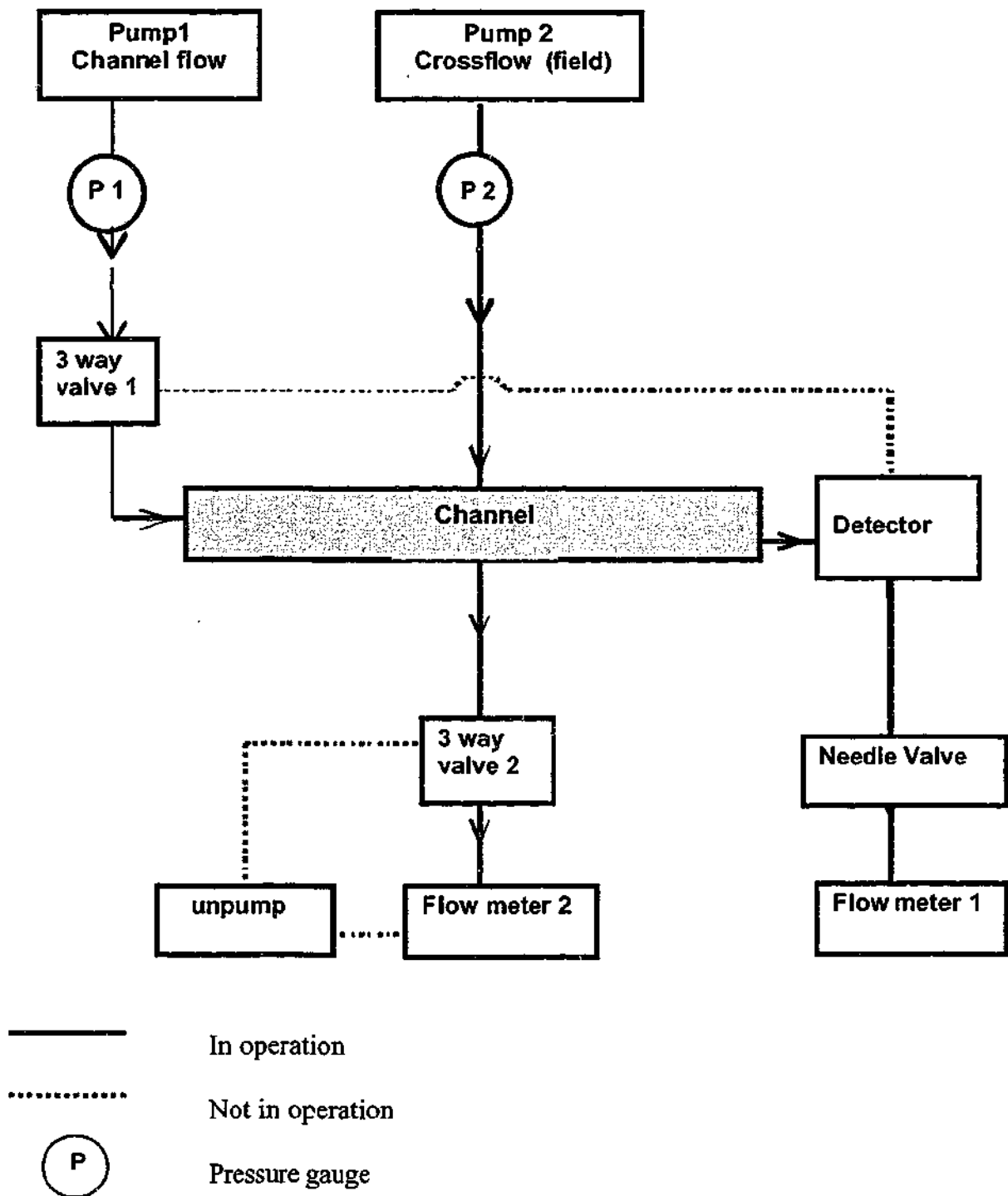


Figure 3.7: Schematic diagram of a FIFFF system illustrating how the back pressures and flow rates are balanced. (b) Channel flow and crossflow are going through the channel. Unpump is off.

(c)

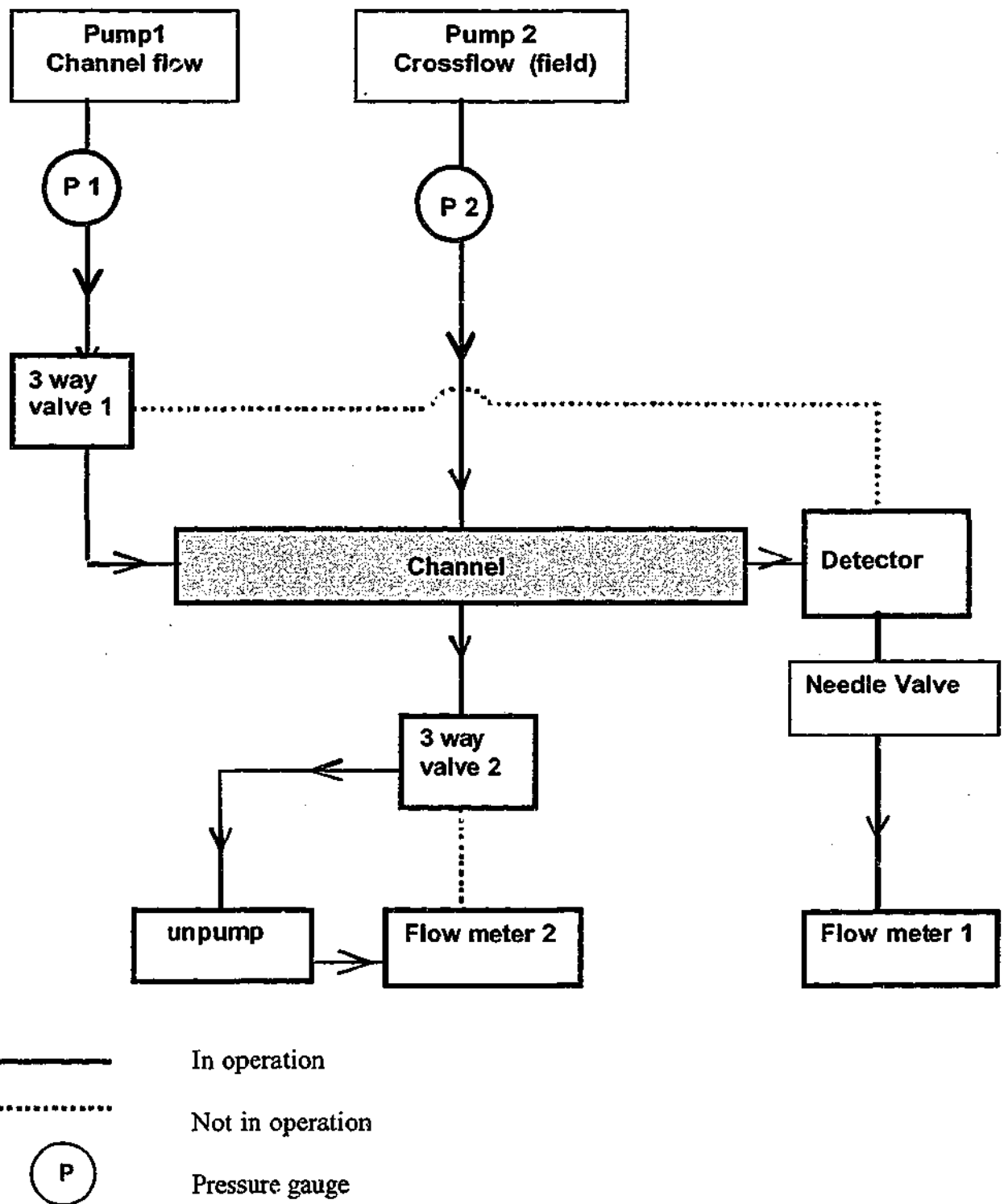


Figure 3.7: Schematic diagram of a FIFFF system illustrating how the back pressures and flow rates are balanced. (c) Channel flow and crossflow are going through the channel.

Unpump is on.

3.4.3 MEMBRANE SYNTHESIS:

A cellulose acetate membrane was used to cover the accumulation wall to prevent loss of sample during the run. The membrane was manufactured using the method of Manjikian *et al.* [11]. A solution of 25% (by weight) cellulose acetate, 45% acetone, and 30% formamide was mixed for 2-3 days on a rolling bottle mixer. Care was taken not to introduce bubbles into the mixture. The viscous liquid was poured into the reservoir of a casting knife fitted with a blade that could be adjusted to a set distance above the glass plate. A thin coating of the cellulose acetate solution (approximately 0.08 mm) was cast on a glass plate. The glass plate was immersed in an ice-water bath for about 30 minutes. The membrane was then peeled off from the glass plate, rolled and stored in deionized water containing 0.05% NaN_3 as bactericide.

3.4.4 VOID VOLUME MEASUREMENT

The void volume V^0 is the volume of the empty space inside the channel. The geometric void volume can be calculated from the channel area and the thickness of the spacer. In principle, the experimental void volume V^0 , can be equated to the experimental retention volume of a component that is unaffected by the applied external fields. Such a component will be distributed evenly over the channel cross-section and its observed average velocity will equal the mean velocity of the carrier fluid in the channel. Therefore the component should be detected after a volume of the carrier approximately equal to the volume of the empty space, or void volume is displaced through the channel [12].

Although the geometric void volume can be estimated from the channel dimensions, it should be determined experimentally due to the small uncertainties that can occur in these dimensions of FFF channels particularly in channel thickness (w). In FIFFF a

compressible membrane is clamped under a spacer. The uncompressed part of the membrane can protrude into the channel space and occupy some of the volume that would normally be part of the void volume. This protrusion reduces the channel thickness and thus the void volume [12]. The void volume is an important parameter and its value should be determined accurately in order to derive molecular size or mass information from FFF measurements.

In this work the void volume was measured using the "rapid breakthrough method" [12]. In this method, a high molecular mass probe is injected into the FFFF channel with no field and the elution peak profile is measured using a UV detector. Using a high mass probe ensures minimal diffusion across the channel. The following procedure was used to measure the void volume:

A suspension of 0.33 μm latex bead (Polysciences Inc., U.S.A) was prepared by adding 2 drops of the 10% stock to 1 mL of deionized water and mixing thoroughly using a Vortex mixer. Two drops of this suspension were added to a 10 mL solution of TRIS buffer (Section 3.3.5) and mixed by Vortex mixer. The field outlet of the channel was blocked. A high channel flow rate (5-6 mL/min) was applied. A chart recorder was used to record the runs, using a speed of 300 mm/min. The channel flow rate was recorded every 10 seconds and 5 flow rates were recorded before each run. The polystyrene beads were injected about 15 times.

The breakthrough time (t_b) was calculated using the elution time when the detector signal has reached 0.86 of the maximum peak height ($0.86 h_{\text{max}}$) [12]. The breakthrough time was converted to the breakthrough volume using the channel flow rate.

In a flat FFF channel the fastest probe molecules, situated at the central plane between the channel walls, travel at a velocity 1.5 times greater than the average flow velocity [12]. The time of first appearance of sample which corresponds to the breakthrough time (t_b) will precede the void time t^0 , which corresponds to the elution time of probe molecules that sample all streamlines. The relationship between the measured t_b and t^0 is:

$$t_b = \frac{2}{3} t^0 \quad (3.24)$$

thus:

$$V^0 = 1.5 V_b \quad (3.25)$$

Pre channel and post channel dead volumes were deducted from V_b , prior to the calculation of the void volume.

3.4.5 CARRIER

Two carrier liquids were used in the studies presented in this thesis:

- Dionised water (Millipore, Milli Q) with the pH and ionic strength adjusted accordingly by addition of HCl, NaOH and NaCl.
- Deionized water containing 0.05 M TRIS buffer tris(hydroxymethyl)aminomethane, 0.0268 M HNO₃ and 0.0012 M NaN₃. This preparation resulted in a solution pH of 7.9 and an ionic strength of 0.08 M.

3.5 CONCLUSIONS

In this chapter the general theory of flow field-flow fractionation (FIFFF) has been explained. It is shown that separation in FIFFF is based on the physical interactions of the sample with the field and the sample diffusivity. The theory of FIFFF enables calculation of the diffusion coefficient of the sample from first principles. This is a great advantage for FIFFF compared to the other available methods. The diffusion coefficient can then be related to the hydrodynamic size using the Stokes-Einstein equation. The need for calibration arises when the molecular weight needs to be calculated.

FIFFF can give the distribution of a measured parameter. The peak maximum does not always give a good representation of the whole data, especially in case of highly polydisperse samples. Therefore it is often better to report the number or weight average parameters. This process should be done carefully. When converting the x -axis of a distribution the relevant change in the y -axis must also be computed. Calculation schemes to obtain number and weight average molecular weight, diffusion coefficient and molecular diameter parameters using the UV signal of the fractogram have been given in this chapter.

3.6 REFERENCES

1. Giddings, J.C., Field-Flow Fractionation, *C & E News*, 66 (1988) 34-45.
2. Giddings, J.C., and Caldwell, K.D., Field-Flow Fractionation, in B.W. Rossiter, and Hamilton, J.F., (Eds.), *Physical methods of chemistry*, John Wiley & Sons, New York, 1989, 867-938.

3. Beckett, R., and Hart, B.T., Use of field-flow fractionation techniques to characterize aquatic particles and macromolecules, in Buffle, J., and van Leeuwen, H.P., (Eds.), *Environmental Particles*, Lewis Publishers. 1993, 165-205.
4. Beckett, R., Zhang J., and Giddings C., Determination of molecular weight distributions of fulvic and humic acids, using flow field-flow fractionation, *Environmental Science and Technology*, 21 (1987) 289-295.
5. Dycus, P.J.M., Healy, K., Stearman, G.K., and Wells, M., Diffusion coefficients and molecular weight distributions of humic and fulvic acids determined by flow field-flow fractionation, *Separation Science and Technology*, 30 (1995) 1435-1453.
6. Schimpf, M.E., and Petteys, M.P., Characterisation of humic materials by flow field-flow fractionation, *Colloids and Surfaces, A*, 120 (1997) 87-100.
7. Schimpf, M., Caldwell, K and Giddings, J.C, (Ed.), *Field-Flow Fractionation Handbook*, John Wiley & Sons, New York, 2000.
8. Aiken, G.R., and Gilham, A.H, Determination of molecular weight of humic substances by colligative property measurement, in Hayes, M.H.B., MacCarthy, P., Malcolm, R.L., and Swift, R.S., (Eds.), *Humic Substances II, In Search of Structure.*, John Wiley & Sons, Chichester, 1989, 516-544 .
9. Chin, Y.P., and Gschwend, P.M., The abundance, distribution and configuration of porewater organic colloids in recent sediments, *Geochimica et Cosmochimica Acta*, 55 (1991) 1309-1317.
10. Assemi, S., Newcombe, G., Heplewhite, C., and Beckett R., Characterisation of natural organic matter fractions separated by ultrafiltration using flow field-flow fractionation, *Water Research* (submitted).

11. Minjikian S., L.S., and McCutcham J.W., Improvement in fabrication techniques for reverse osmosis desalination membrane. in: The first international symposium on water desalination. 1965. Washington D.C, United States Government Printing Office.
12. Giddings, J.C., Benincasa, A.M., Williams P.S., Rapid Breakthrough Measurement of Void Volume for Flow Field-Flow Fractionation channels, *Journal of Chromatography*, 627 (1992) 23-35.
13. Specht, C.H., Kumke, M.U., and Frimmel, F.H, Characterization of NOM adsorption to clay minerals by size exclusion chromatography, *Water Research*, 34(16) (2000) 4063-4069.
14. Ranville J., Benedetti, M., Ulmann, L., Kellen, C., Amy, G., Hendry, J. and Frimmel, F.H., Characterization of aquatic natural organic matter using flow field-flow fractionation with on-line element specific detectors, Ninth International Symposium on Field-Flow Fractionation, Golden, U.S.A., June 2001.

CHAPTER 4

DETERMINATION OF DIFFUSION COEFFICIENTS OF SUWANNEE RIVER FULVIC ACID: COMPARISON OF FLOW FIELD-FLOW FRACTIONATION WITH SOME OTHER NEW TECHNIQUES

4.1 INTRODUCTION

In Chapter two it was demonstrated that the literature on the size and molecular weight of humic substances contains a wide range of data. This is partly because the measurements have been performed under different conditions and using different techniques. Each technique measures a different parameter and hence may yield a different average. This fact needs to be taken into account when comparing and interpreting such data from various sources.

This chapter presents the results of collaborative work between three laboratories to estimate the size and diffusion coefficients of a humic standard (Suwannee River fulvic acid) at different solution pH and ionic strength. Measurements have been carried out under similar experimental conditions using flow field-flow fractionation (FIFFF), fluorescence correlation spectroscopy (FCS) and pulse-field gradient (PFG) NMR. In addition, the size obtained from atomic force microscopy (AFM) has been compared with these results. One reason for undertaking this study was to obtain some validation of the FIFFF results.

The FCS and PFG-NMR experiments were performed at the Centre for Analytical and Environmental Research (CABE), University of Geneva, Switzerland, by Dr Jamie Lead. The PFG-NMR experiments were performed in the Department of Chemistry, University of Kansas, USA, by Professor Cynthia Larive and Ben Cutak.

The above mentioned techniques carry out the measurements in solution (except for AFM) and disturb the humic samples minimally. FCS can measure sizes in the nanometer range where light scattering and photon correlation spectroscopy cannot provide reliable results. AFM is a promising technique, which has a sub-nanometer vertical resolution. Under the right experimental conditions (correct sample preparation, comparable solution conditions) the images obtained by AFM can be used directly to validate the size data obtained by other techniques.

Each of these techniques has been used previously for measurement of average diffusion coefficients of natural organic macromolecules [1-5]. However, the differences in solution conditions and the nature of the organic matter used do not permit an absolute

comparison. Suwannee River fulvic acid was chosen for this experiment because it is a well characterised standard humic substance with little tendency to aggregate at high concentrations [6].

Among the techniques used in this chapter only FIFFF can provide distribution of the diffusion coefficient from first principles. In FCS and PFG-NMR the data is obtained as an average diffusion coefficient. This data can then be converted to a distribution of diffusion coefficients by using certain assumptions and mathematical approximations.

4.2 THEORY

Theories of FIFFF and AFM are explained in Chapters 3 and 7, respectively. An overview of FCS and PFG-NMR techniques will be presented here. A more comprehensive explanation can be found elsewhere [5, 7, 8].

4.2.1 FLUORESCENCE CORRELATION SPECTROSCOPY (FCS)

In FCS laser light is focused into the sample of interest using confocal optics. In this manner a small, illuminated volume element (approximately $0.5\text{-}1.0\ \mu\text{m}^3$) called the confocal volume is created. The size of the confocal volume is usually calibrated with a standard. In order to optimise the signal-to-noise ratio, the confocal volume should be occupied by a small number of fluorescent molecules at any given point in time. Temporal fluctuations in the measured fluorescence intensity are used to derive an autocorrelation curve. In the absence of any other processes, which affect sample fluorescence, such as chemical reactions, the autocorrelation curve will be related to the translational diffusion of the fluorophore across the confocal volume. Therefore, diffusion

times of the fluorescent molecules through the confocal volume (ω) can be determined using the following equation:

$$D = \frac{\omega_1^2}{4\tau_2} \quad (4.3)$$

where ω_1 is the width of the confocal volume and τ_1 is the characteristic diffusion time of the particle through the confocal volume.

The value of ω_1^2 was calculated by calibrating the system with rhodamine (R6G), which has a known diffusion coefficient of $2.8 \times 10^{-10} \text{ m}^2\text{s}^{-1}$ [9]. To determine distributions of diffusion times from the FCS autocorrelation function the FCS diffusion time scale is divided into a finite number n of intervals i denoted. The corresponding fraction of particles c_i in each interval is represented by a bar height and the corresponding FCS autocorrelation function is given by:

$$G(t) = \sum_{i=1}^n c_i \left(1 + \frac{t}{\tau_i}\right)^{-1} \left(1 + \frac{t}{p^2\tau_i}\right)^{-1/2} \quad (4.4)$$

where t is the delay time and p is the structural parameter or the ratio between the transverse and longitudinal dimensions of the confocal volume ($p = \omega_1/\omega_2$). The normalising condition is given by:

$$\sum_{i=1}^n c_i = G(0) \quad (4.5)$$

The bar heights are varied in order to minimise the differences between the calculated and experimental correlation function. This approach is an ill-posed problem, which is overcome by introducing a regularisation condition [7].

4.2.2 PULSED-FIELD GRADIENT NMR (PFG-NMR)

In PFG-NMR magnetic pulse gradients are incorporated into the NMR pulse sequence to vary the magnetic field linearly over the entire sample. The first gradient pulse results in dividing the bipolar pulse BPLED experiment, the intensity of a resonance, I , is related to the diffusion coefficient of the molecule, D , by the equation:

$$I = I_0 \exp \left[-D \left(\Delta - \frac{\delta}{3} - \frac{\tau}{2} \right) G^2 \gamma^2 \delta^2 \right] \quad (4.6)$$

where I_0 is the resonance intensity in the absence of a gradient pulse, Δ is the time during which diffusion occurs, δ and G are the duration and amplitude of the bipolar pulse pair, respectively, τ is the delay following each gradient pulse and γ is the gyromagnetic ratio. The PFG-NMR spectral data were analysed to determine diffusion coefficients using the computer program CONTIN, which approximates a solution to the ill-posed problem of an inverse Laplace transformation applied to the intensity decay by using assumed prior knowledge of the possible diffusion coefficients [5].

4.3 EXPERIMENTAL

SRFA was obtained from the International Humic Substances Society as freeze dried solids. Samples with a concentration of 50 mg L⁻¹ were prepared by dissolving the freeze

dried sample in the carrier solution and mixing using a vortex mixer one day prior to the experiments. The samples were mixed again for 30 seconds immediately before injection into the FIFFF channel.

Deionized water (Milli Q, Millipore) was used as carrier and the pH and ionic strength were adjusted by addition of NaOH, HCl and NaCl. All the materials used were analytical grade. The ionic strengths were kept constant for solutions with different pH values. Experiments were carried out in three different pH solutions (5.5, 6.8 and 8.5) and three ionic strengths (0.005, 0.05 and 0.5 M).

4.3.1 FLOW FIELD-FLOW FRACTIONATION

The FIFFF channel had a void volume of 1.14 mL and a channel thickness of 0.02 cm. The crossflow and channel flow rates were maintained at approximately 3.90 and 0.80 mL min⁻¹ respectively. A sample injection loop of 20 μ L was used, corresponding to an injected sample mass of 1 μ g.

4.3.2 ATOMIC FORCE MICROSCOPY

Atomic force microscope measurements were performed on a Digital Instruments Nanoscope III AFM (Santa Barbara, CA). In order to image the SRFA on mica, a piece of mica was immersed in 100 ppm SRFA (pH=6, I=0.0007 M), then removed and rapidly blown dried with an N₂ gun. Imaging was performed in Tapping mode™ in air.

4.3.3 FCS AND PFG-NMR

The experimental procedures for FCS and PFG-NMR are described in Lead *et al.* [8].

4.4 RESULTS AND DISCUSSION

4.4.1 FIFFF RESULTS

COMPARISON OF THE DIFFUSION COEFFICIENT DISTRIBUTIONS

The distributions of diffusion coefficients (Figure 4.1) were obtained from the fractograms. The x -axis was converted to the diffusion coefficient using equation 3.2 and the y -axis was converted to the relative mass using equation 3.7 as discussed in Chapter 3.

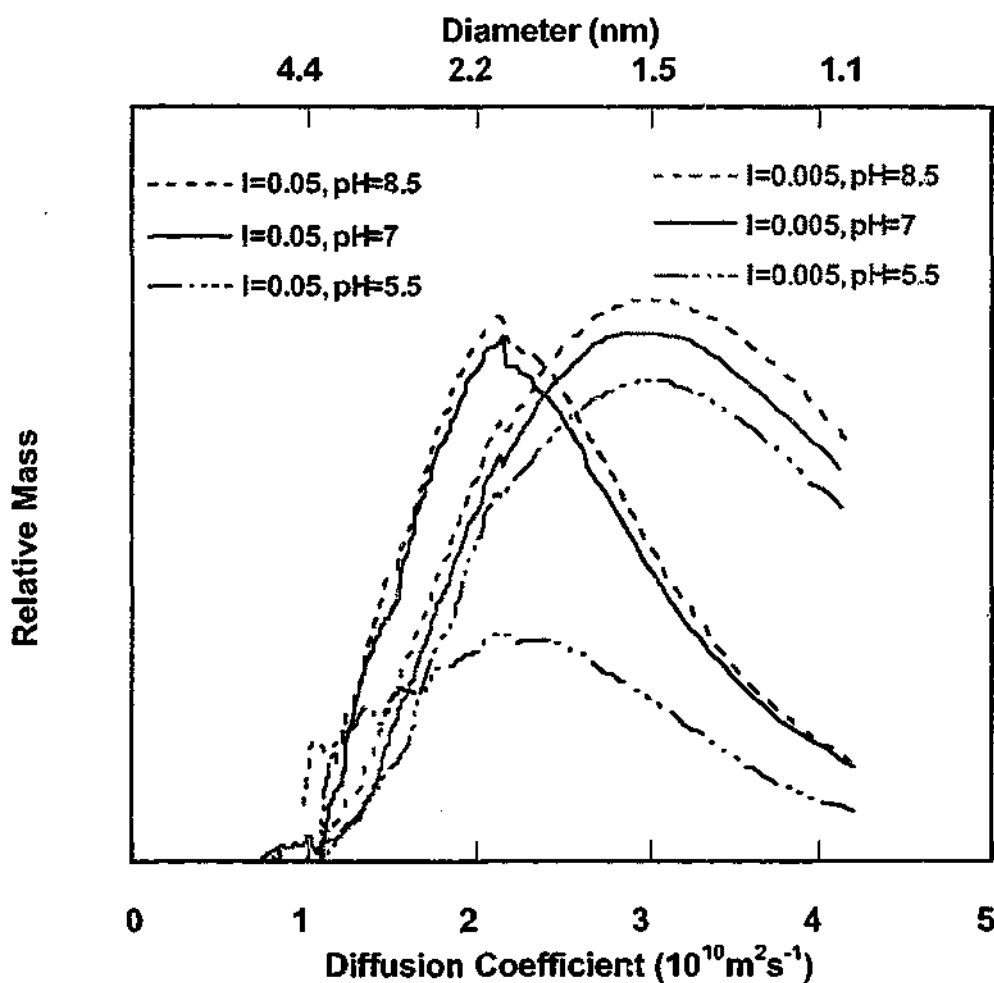


Figure 4.1: Distribution of diffusion coefficients of SRFA at different pH (5.5, 7, 8.5) and ionic strengths (0.005 and 0.05 M) in deionized water. Hydrodynamic diameters corresponding to the diffusion coefficients are given on the upper x -axis.

Comparison of the two sets of data at ionic strengths of 0.005 M and 0.05 (Figure 4.1) shows a clear shift in the diffusion coefficient distribution curves. (from $\sim 3 \times 10^{-10} \text{ m}^2\text{s}^{-1}$ to $\sim 2.2 \times 10^{-10} \text{ m}^2\text{s}^{-1}$). This suggests that under the conditions of this experiment a ten-fold increase in the ionic strength resulted in limited aggregation of SRFA at pH value 7-8.5.

At higher pH values (7-8.5), some free carboxylic acid groups convert to carboxylate anions and increase hydrogen bonding interactions with unionized weak acid groups, such as phenols. The negative charge created by high pH may also tend to disrupt molecular interactions because of electrostatic repulsion [10] However, the charge on SRFA does not change significantly between pH 7-8.5 [11] Therefore, a change in pH between 7-8.5 did not affect the interaction between SRFA molecules. Even at lower pH values no significant difference between the distribution of diffusion coefficients was observed.

At the lower pH value of 5.5 and higher ionic strength of 0.05 M, the peak area decreased significantly compared to the other conditions studied. This could be explained in terms of molecules adsorbing onto the membrane. At the higher ionic strength of 0.5 M, no peak was observed even at a pH of 8.5.

This effect can be explained in terms of aggregation induced by higher ionic strength. The applied field would concentrate these aggregates near the membrane surface. This can result in adsorption of the aggregates onto the membrane surface. Emergence of large peaks after termination of the field at the end of the FIFFF run provides evidence for this explanation.

COMPARISON OF THE HYDRODYNAMIC DIAMETERS

Comparison of the distributions of the diffusion coefficients and the calculated equivalent spherical hydrodynamic diameters of the SRFA at peak maxima suggests a slight increase in size from 1.5 to 2.1 nm by increasing the ionic strength from 0.005 M to 0.05 M. This corresponds to a 2.7 fold increase in mass, which can be interpreted as the aggregation of some of the components of SRFA by formation of dimers and trimers. However, one cannot disregard the possibility of membrane repulsion at low ionic strengths, which might result in a lower calculated hydrodynamic diameter. Nonetheless, previous studies using sedimentation FFF suggest that a 5 mM ionic strength is high enough to effectively eliminate significant perturbations due to particle-wall and particle-particle repulsion [12].

The distribution of diffusion coefficients obtained from FIFFF makes it possible to calculate weight average and number average diffusion coefficients (Table 4.1). An index of polydispersity might be deduced by comparing the D_n and D_w values.

Table 4.1: Comparison of the diffusion coefficients of SRFA obtained by FIFFF at different solution pH and ionic strength (I). D_p is the diffusion coefficient at the peak maximum, D_n is the number average diffusion coefficient and D_w is the weight average diffusion coefficient. The unit for all the D values is $10^{-10} \text{ m}^2 \text{ s}^{-1}$

I(M)	pH=5.5				pH=7				pH=8.5			
	D_p	D_n	D_w	$\frac{D_n}{D_w}$	D_p	D_n	D_w	$\frac{D_n}{D_w}$	D_p	D_n	D_w	$\frac{D_n}{D_w}$
0.005	3.0 (0.01)	3.3 (0.01)	2.9 (0.04)	1.1	2.9 (0.03)	3.3 (0.01)	2.9 (0.05)	1.1	3.0 (0.08)	3.3 (0.05)	3.0 (0.05)	1.1
0.05	1.9 (0.08)	2.8 (0.01)	2.4 (0.06)	1.2	2.2 (0.04)	2.9 (0.02)	2.5 (0.04)	1.2	2.2 (0.03)	2.9 (0.01)	2.5 (0.02)	1.2
0.5	ND				ND				No peak			

The FIFFF results indicate that, under the conditions examined here, the SRFA consists mainly of relatively small macromolecules rather than molecular aggregates. The hydrodynamic diameter at the peak maxima can be estimated as 1.5-2.1 nm. The results obtained from FIFFF will be compared to those obtained from FCS and PFG-NMR in the following sections.

4.4.2 COMPARISON OF THE FLFFF RESULTS WITH THOSE OBTAINED FROM FCS

The diffusion coefficients at the peak maxima, obtained from FIFFF and FCS are compared in Figure 4.2.

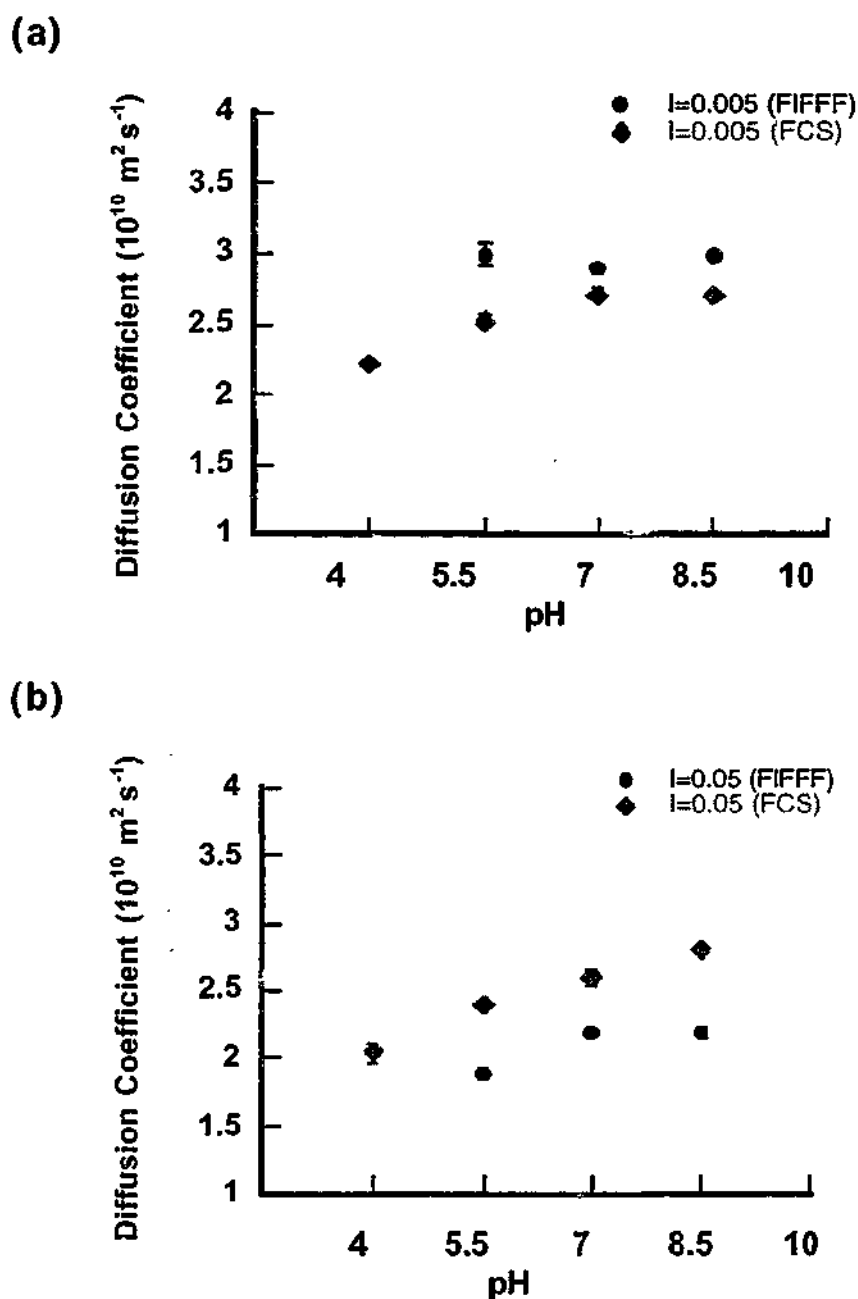


Figure 4.2: Comparison of the diffusion coefficient at the peak maximum obtained by FIFFF with the most probable diffusion coefficient obtained from FCS at similar conditions.

Figure 4.2 shows that the data obtained by FIFFF and FCS fall within the same range. It appears that the FCS data show a slight increase in the diffusion coefficient with increasing pH. More points are needed to be able to be conclusive about the trends in the FIFFF data.

4.4.3 COMPARISON OF THE FLFFF RESULTS WITH THOSE OBTAINED FROM PFG-NMR

PFG-NMR gives diffusion coefficient data for molecules in the sample. Several different estimates were obtained depending on the functional groups using ^1H NMR spectrum [5]. The diffusion coefficients were fitted to a distribution using the CONTIN computer program [8]. The diffusion coefficients at the peak maxima for four different spectral regions at an ionic strength of 0.03 M are compared with FIFFF results at 0.05 M (Figure 4.3). Table 4.2 gives the functional groups corresponding to each region of the PFG-NMR spectrum.

Table 4.2: Functional groups corresponding to each region in the PFG-NMR results[8].

Region	Functional Group
1 (0.8-1.9 ppm)	protons on terminal methyl groups of methylene chains, protons on aliphatic carbons bonded to other carbons protons on methyl groups of branched aliphatic structures
2 (1.9-3.5 ppm)	protons on aliphatic carbons which are two or more carbons from an aromatic ring or polar functional groups
3 (3.5-4.3 ppm)	protons on carbons adjacent to aromatic rings or electronegative functional groups
4 (6.3-8.1 ppm)	aromatic protons

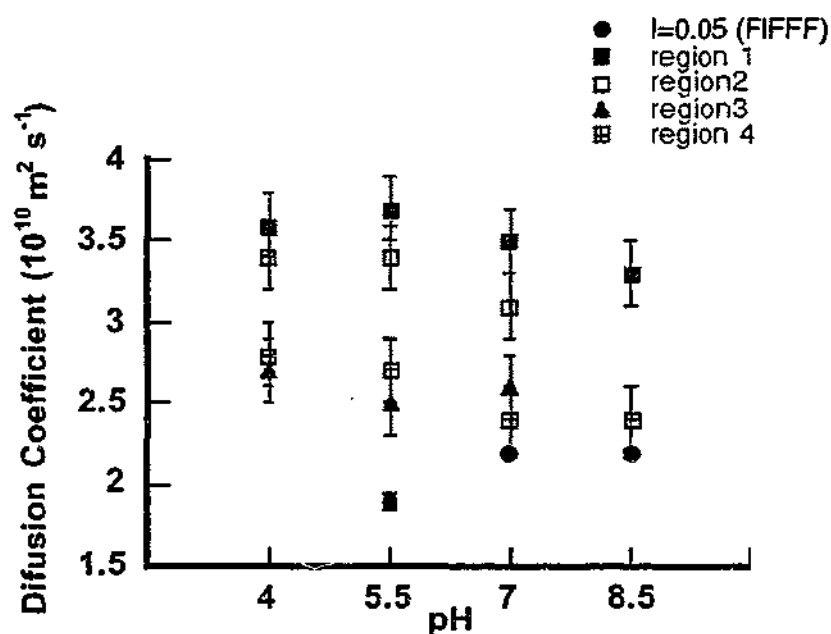


Figure 4.3: Comparison of the diffusion coefficients at the peak maxima obtained from FIFFF with the diffusion coefficients at the peak maxima obtained from PFG-NMR for SRFA solutions at different pH values. The ionic strength was 0.03 M for the NMR experiments and 0.05 M for the FIFFF runs. (see Table 4.2 for description of the NMR regions)

For PFG-NMR, the increase in pH resulted in a slight decrease in the diffusion coefficient. No significant change was reported as a result of changing the ionic strength from 0.03 M to 0.5 M [8]. An interesting point is that the diffusion coefficients of region 3 (protons on carbons adjacent to aromatic rings or electronegative functional groups) and region 4 (aromatic protons) are more comparable to the FIFFF results at similar ionic strengths (0.03M and 0.05 M). This may be because the FIFFF fractograms are collected using a UV detector, which gives a signal only for molecules containing chromophores. These chromophores are likely to be regions of the molecules containing aromatic rings.

4.4.4 COMPARISON OF THE FLFFF RESULTS WITH THE SIZE OBTAINED FROM AFM

The AFM image of SRFA in pH 6 and ionic strength of 0.0007 M is given in Figure 4.4. In AFM, the size of the molecules are often measured vertically. The vertical size is determined by the tip-sample separation and is more precise than the lateral size which is determined by the resolution of the computer screen (pixels). The vertical size can be determined by subtracting the height of the molecule from that of the background for a given molecule. This can be done by using the section analysis facility of the AFM software (Nanometer III). The section analysis of two points for the SRFA sample on mica is given in Figure 4.4.(b). The vertical size of the SRFA molecules can be estimated as 0.3 nm and 0.6 nm at those two points.

The AFM measurements might give values smaller than measurements of hydrodynamic diameters. The reason could be due to tip-sample and sample-substrate interactions and the fact that the samples are not in solution. The ionic strength of the solution was 0.0007 M. At this ionic strength molecular repulsion can prevent the association of molecules.

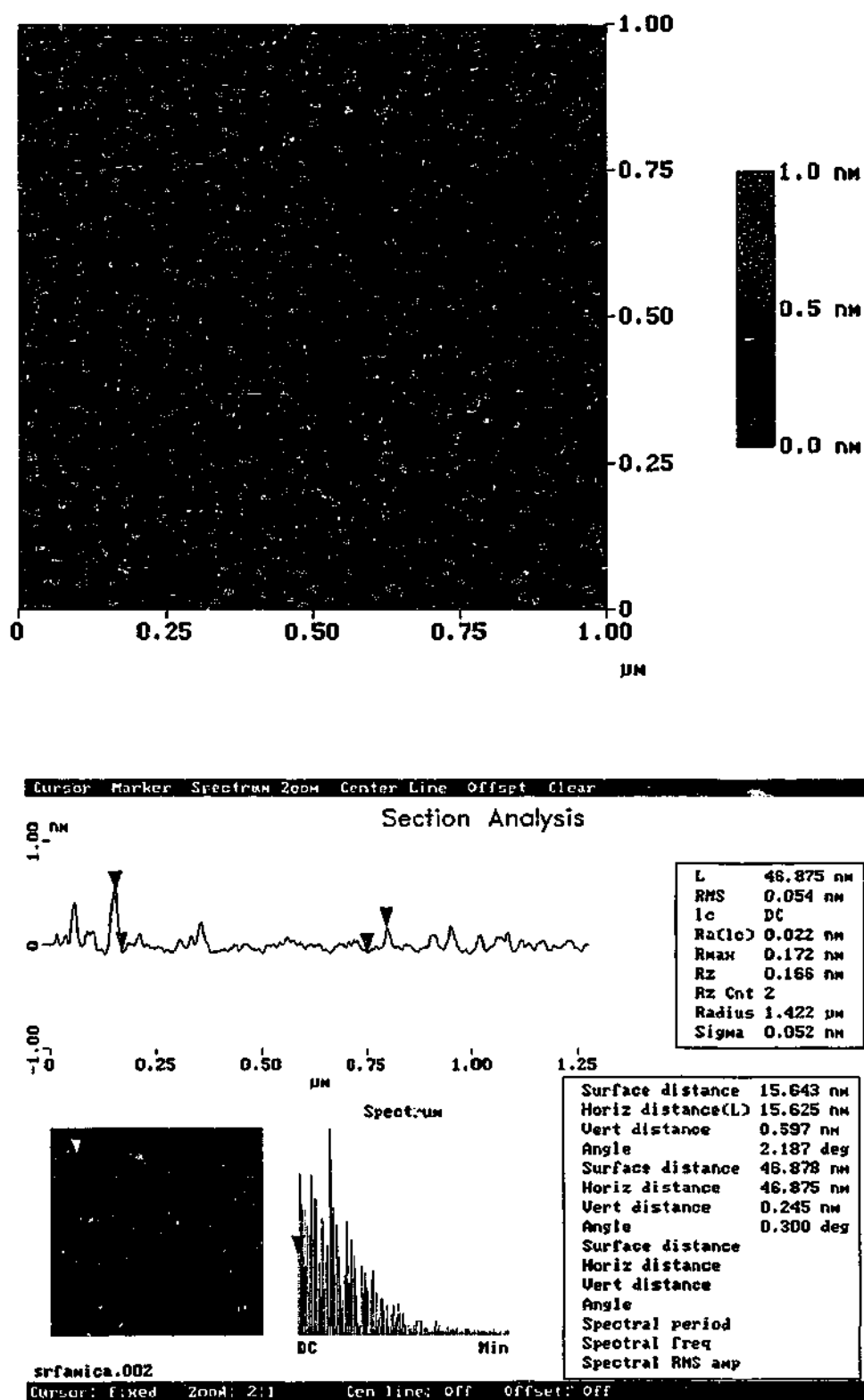


Figure 4.4: (a) Tapping modeTM AFM image of the SRFA on mica in air. pH=6, I=0.0007 M, (b) Section analysis of two points on the image for measurement of the vertical size of the SRFA molecules.

4.5 COMPARISON OF THE TECHNIQUES

In general the diffusion coefficients obtained by the three techniques are in the range of $1.9-3.5 \times 10^{-10} \text{ m}^2 \text{ s}^{-1}$. Assuming a compact sphere and using Stokes equation these values correspond to a diameter of 1.2 nm to 2.3 nm. This is in the range obtained by other FIFFF, HPSEC and small-angle X-ray studies (see Chapter 2).

FIFFF provides a distribution of diffusion coefficient from first principles. No calibration or fit to a pre-assumed distribution is required. The data can be collected using a fairly low initial concentration of sample (in this case 50 mg L^{-1}) and the runs are completed in a relatively short time (minutes). On the other hand, the use of a membrane to prevent sample loss through the accumulation wall limits the analysis to moderate conditions of pH and ionic strength. This range could be increased by using other membranes with different properties. Most of the membranes have an iso-electric point (IEP) of around pH 3-4. This limits the FIFFF runs to carrier solutions having pH values above that point in order that the humic molecules and the accumulation wall both have a negative charge. Table 4.3 compares the diffusion coefficients obtained from FIFFF with some other data collected from the literature.

Table 4.3: comparison of the diffusion coefficients obtained by FIFFF with some other data collected from the literature.

Technique	Sample	D ($\times 10^{10} \text{ m}^2\text{s}^{-1}$)	Reference
FIFFF	SRFA	1.9-3.0	This work
	SRFA/SRHA	3.0-4.1	[1]
	SRHA	2.8(D_p)	[2]
FCS	SRHA	2.05-2.8	[8]
	Aquatic NOM	2.1-2.9	[4]
PFG-NMR	SRFA	2.4-3.7	[8]
	SRFA	3.5-5.0	[5]
PCS	Aquatic HA	0.03-0.04	[13]
Voltametry	Aquatic HA/FA	1-4.7	[14]
	Aquatic FA	0.6-1.2	[15]

In general the values of the diffusion coefficients obtained by FIFFF are comparable to the values obtained by other techniques. Small differences within the values in the table can be explained in terms of variable solution conditions, and the use of different types of NOM and different analytical techniques. One exception is photon correlation spectroscopy (PCS), which gives a much lower diffusion coefficient. The reason might be that the measurements are performed at higher concentrations. Also PCS is biased

towards larger molecules and the nature of the humic acids which were analysed. Although the PFG-NMR data were collected at comparable concentrations with those in reference [13]. PFG-NMR values of diffusion coefficients are higher than the PCS values, most likely because PFG-NMR is less biased towards the larger fraction.

4.6 CONCLUSIONS

This chapter has compared the FIFFF data with those obtained from several quite different techniques and performed in different laboratories under similar conditions. The results presented indicate that the diffusion coefficients of SRFA obtained by FIFFF are in close agreement with FCS and PFG-NMR spectroscopy under similar experimental conditions. The results obtained are also in the same range as other data available in the literature. The minor differences in the results can be explained in terms of the different techniques, which are based on entirely different principles, detection methods and data processing.

4.7 REFERENCES

1. Beckett, R., Zhang J., and Giddings C., Determination of molecular weight distributions of fulvic and humic acids, using flow field-flow fractionation, *Environmental Science and Technology*, 21 (1987) 289-295.
2. Dycus, P.J.M., Healy, K., Stearman, G.K., and Wells, M., Diffusion coefficients and molecular weight distributions of humic and fulvic acids determined by flow field-flow fractionation, *Separation Science and Technology*, 30 (1995) 1435-1453.
3. Schimpf, M.E., and Petteys, M.P., Characterisation of humic materials by flow field-flow fractionation, *Colloids and Surfaces, A*, 120 (1997) 87-100.

4. Lead, J.R., Balnois, M., Hosse, M., Menghetti, R., and Wilkinson, K.J., Characterisation of Norwegian natural organic matter: size, diffusion coefficients, and electrophoretic mobilities, *Environment International*, 25 (1999) 245-258.
5. Dixon, A., and Larive, C., Modified pulsed-field gradient NMR experiments for improved selectivity in the measurements of diffusion coefficients in complex mixtures: Application to the analysis of the Suwannee river fulvic acid, *Analytical Chemistry*, 69 (1997) 2122-2128.
6. Leenheer, J.A., McKnight, D.M., Thurman, E.M., MacCarthy, P., *Humic Substances in the Suwannee River, Georgia: Interactions, Properties and Proposed Structures*, US Geological Survey, Denver, 1995.
7. Starchev, K., Buffle, J., and Perez, E., Applications of fluorescence correlation spectroscopy: polydispersity measurements, *Journal of Colloid and Interface Science*, 213 (1999) 479-489.
8. Lead, J. R., Wilkinson, K. J., Balnois, E., Cutak, B. J., Larive, C. K., Assemi, S. and Beckett, R. Diffusion Coefficients and Polydispersities of the Suwannee River Fulvic Acid: Comparison of Fluorescence Correlation Spectroscopy, Pulsed-Field Gradient Nuclear Magnetic Resonance, and Flow Field-Flow Fractionation, *Environmental Science and Technology*, 34 (2000) 3508-3513.
9. Magde, D., Elson, E.L., and Webb, W.W., Fluorescent correlation spectroscopy. II. An experimental realization, *Biopolymers*, 13 (1974) 28-62 .
10. Leenheer, J.A., Brown, P.A., and Noyes, T.I, Implications of mixture characteristics of humic-substance chemistry, in H.I. Suffer, and MacCarthy, P., (Eds.), *Aquatic Humic Substances*, American Chemical Society: Washington DC. 1989, 26-39 .

11. Bowles, E.C., Antweiler, R.C., and MacCarthy, P., Acid-Base Titration and Hydrolysis of Fulvic Acid from the Suwannee River, in R.C. Averett, R.C., Leenheer, J.A., McKnight, D.M., and Thorn, K.A., (Eds.), Humic Substances in the Suwannee River, Georgia: Interactions, Properties, and Proposed Structures, U.S. Geological Survey, Denver, 1995, 115-127 .
12. Hansen, M.E., Giddings, C.J., and Beckett, R., Colloid characterisation by sedimentation field-flow fractionation VI. Perturbations due to overloading and electrostatic repulsion, *Journal of Colloid and Interface Science*, 132 (1988) 300-312.
13. Reid, P. M., Wilkinson, A. E., Tipping, E., and Jones, M. N., Aggregation of humic substances in aqueous media as determined by light-scattering methods, *Journal of Soil Science*, 42 (1991) 259-70.
14. Greter, F.L., J. Buffle, and W. Haerdi, Voltammetric study of humic and fulvic substances. Part I. Study of the factors influencing the measurement of their complexing properties with lead, *Journal of Electroanalytical Chemistry. Interfacial Electrochemistry*, 101 (1979) 211-29.
15. Pinheiro, J. P., Mota, A. M., d'Oliveira, J. M. R., and Martinho, J. M. G., Dynamic properties of humic matter by dynamic light scattering and voltammetry, *Analytica Chimica Acta*, 329 (1996) 15-24.

CHAPTER 5

USE OF FLOW FIELD-FLOW FRACTIONATION TO CHARACTERISE NATURAL ORGANIC MATTER SEPARATED BY ULTRAFILTRATION

5.1 INTRODUCTION

Ultrafiltration (UF) has been widely used for isolation and fractionation of humic substances since the 1970s [1]. UF has several advantages that makes it attractive to use. It is simple to operate, can handle large volumes, does not require chemical reagents and does not change the nature of the sample.

Among the applications of UF are: estimation of the diffusion coefficient of humic substances [2], preparation of fractions for further analysis [3, 4], concentration of humic substances [2, 5]. It has also been used to study the interactions between humic acids and metals [6-10], organic contaminants [11] and radionuclides [12-14].

In addition UF has also been used to estimate the apparent molecular weight distribution of humic substances. However, the results reported for the average molecular weight have varied from 0.5-10 k daltons for aquatic fulvic acids or as high as 40-300 k daltons for humic acids. These results are far greater than the values obtained recently by other methods (typically 0.5-2 k daltons for aquatic fulvic acids and 1.5-5 k daltons for aquatic humic acids) [15-18]. The main assumption used in all these studies is that the measured size and molecular weight of the humic fractions obtained are the same as the nominal molecular weight cut off (NMWCO) of the membrane, but it is not uncommon to find species with larger sizes passing through membranes with a smaller NMWCO or vice versa [19, 20].

The nominal cutoff of UF membranes is defined as the molecular weight at which at least 90% of a globular solute of that MW is retained by the membrane [21]. Different cut off values to those claimed by the membrane manufacturers have been determined using other standards such as inorganic ions and dyestuff [22], organic compounds (e.g., organic acids, sugar compounds, etc.) [23] and poly(styrenesulfonate) MW standards [24].

Experimental conditions such as the mode of filtration, initial concentration of the organic matter, solution characteristics such as the pH and the ionic strength have proven to be important in determining the extent of rejection of humic substances by the membranes [25-29]. Many of these factors would be expected to influence solute-membrane interactions. Adsorption of the sample onto the membrane is another important phenomenon, which has been shown to occur for cellulosic [25, 26], polysulfone and acrylic [30] membranes.

Separation in ultrafiltration can be improved by the use of high sample ionic strength, low initial concentration of the sample and pre calibration with materials as close to the nature of the retentate as possible. It is also recommended that the volume in the filtration cell is kept constant by compensating for the volume of filtrate by addition of solvent (diafiltration).

Methods like size exclusion chromatography have been used to assess the performance of UF membranes. Some studies confirmed the UF results [27, 31], but it is likely that SEC results could also be subject to some of the same artifacts as UF. The performance of SEC can be affected by composition, pH and ionic strength of the mobile phase and also the type of packing material [32]. Chin and Gschwend [18] showed that the MW of humic samples were strongly dependent on the calibration material and the ionic strength of the solution (see Table 2.1).

In this chapter FIFFF has been used to determine the size and MW of the nominal natural organic matter (NOM) fractions obtained by a series of commonly used UF membranes (Amicon YM and YC series). The YCO5, YMI and YM3 membranes were calibrated with low molecular weight sugars as well as globular proteins according to the information provided by the manufacturer [21]. Solid state ^{13}C NMR was used to obtain some structural information on the humic fractions in order to help in interpretation of the UF results. These fractions were analysed by HPSEC for molecular weight distributions [33]. This provides an opportunity to compare the results obtained by the two different techniques.

5.2 EXPERIMENTAL

5.2.1 NOM PREPARATION AND ULTRAFILTRATION

The ultrafiltration and solid-state ^{13}C NMR of the fractions have been performed by Dr Gayle Newcombe and Chris Hepplewhite of South Australia Water. A brief procedure is outlined in this section. A more comprehensive description of NOM isolation and the ultrafiltration process is given in Newcombe *et al.* [32].

NOM was concentrated from two natural water sources (Myponga Reservoir and Hope Valley) in South Australia. The Myponga Reservoir is located 60 km south of Adelaide in the Fleurieu Peninsula (an agricultural region) and the Hope Valley reservoir is located 15 km northeast of Adelaide in the Adelaide Hills. Samples were taken during the Australian winter (July 1996).

The NOM was concentrated using an anion exchange resin column [32]. This method concentrated approximately 80% of the NOM. The unrecovered remaining 20% part presumably consists of non-ionic, non-humic material [32]. The concentrated sample (2000 mg L⁻¹) was fractionated using Amicon YC05, YM3, YM10 and YM30 UF membranes in stirred 600 mL ultrafiltration cells. Sequential filtration was then applied.

Starting with the 30 k daltons membrane, 400 mL of the sample was placed in the cell and N₂ at a pressure of 55 kPa was applied. When the volume of the isolate was reduced to approximately 100 mL, either 0.01 M NaCl (Hope Valley samples) or deionized water (Myponga Reservoir samples) was added to the cell to increase the volume back to 400 mL. This process continued until the permeate had no colour. Five fractions with nominal

molecular weight cutoff (NMWCO) of <0.5, 0.5-3, 3-10, 10-30 and >30 k daltons, respectively were produced with pH values falling within the range of 7-8. The concentration of total organic carbon (TOC) in each fraction are given in Table 5.1.

Table 5.1: Concentration of the NOM in UF fractions as determined by total organic carbon (TOC) and UV absorbance measurements.

Sample	Fraction	Concentration(mg/L)	Concentration(mg/L)
		TOC	from UV @254 nm
Myponga Reservoir	<500	2402	1800
	500-3K	10752	9000
	3K-10K	3096	2600
	10K-30K	1848	2000
	>30K	5220	4200
Hope Valley	<500	167*	125
	500-3K	1100*	920
	3K-10K	844*	709
	10K-30K	648*	701
	>30K	813*	654

*Calculated from TOC/UV ratio of Myponga Reservoir Samples.

5.2.2 MATERIALS

Deionized water (Milli-Q, Millipore) was used for the preparation of samples and the carrier solution in FIFFF experiments. All chemicals were of analytical grade. Glassware was soaked in 5% EXTRAN® (Merck) solution overnight and rinsed with deionized water several times prior to use. Sodium poly(styrenesulfonate) molecular weight standards were obtained from Polyscience, Inc.

5.2.3 FLOW FIELD-FLOW FRACTIONATION EXPERIMENTS

The channel void volume was determined as 1.16 mL and the channel thickness as 0.02 cm using the Breakthrough method [34]. The samples were injected using a 20 μL Rheodyne® injection loop. The channel flow rate and the field (crossflow) rate were maintained at about 4 mL min⁻¹. The channel pressure was 40 psi. TRIS buffer was used as the carrier. In order to obtain the optimum injection mass, the total organic carbon (TOC) of each fraction from Myponga Reservoir NOM was measured using a SHIMADZU 5000® TOC analyser. The TOC of the Hope Valley NOM was calculated using the UV absorbance of each fraction and the TOC/UV ratio of the Myponga Reservoir NOM fractions. The samples were then diluted to obtain sub samples of 1 ppm concentration. Three different injection masses of the Myponga Reservoir fractions (0.625, 1.25 and 2.5 μg) were used to optimise the concentration of samples to be injected. An injection mass of 1.25 μg was used thereafter.

5.2.4 MOBILITY MEASUREMENTS

The method used by Beckett and Le [35] was applied in order to measure the relative charge density of the NOM fractions. Synthetic goethite ($\alpha\text{-FeOOH}$) particles were coated with the humic fractions and the electrophoretic mobility of the suspended particles was measured. Each suspension contained 20 mg L⁻¹ of goethite, 0.5 mg L⁻¹ of the NOM fraction and 10⁻³ M of KNO₃. Three minutes of probe ultrasonic treatment was used to fully disperse the particles. The pH values of the samples were maintained at 6.0±0.1 immediately before the measurements were made. The measurements were carried out by Doppler shift light scattering, using a ZETAPLUS® instrument (Brookhaven

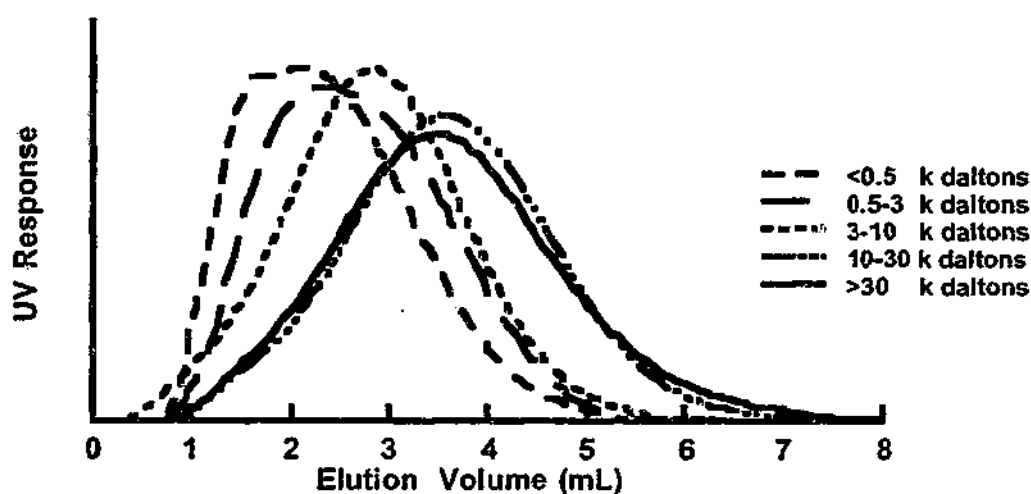
Instruments Corporation). Approximately 1 mL of each sample was used for three cycles of measurements, with the voltage being reversed after each 10 to 15 cycles. Each measurement cycle consisted of 3 readings.

5.3 RESULTS AND DISCUSSION

5.3.1. FIFFF FRACTOGRAMS

The FIFFF data was obtained as a fractogram, which is a plot of UV response at a wavelength of 254 nm versus the retention volume or retention time. As explained in Chapter 3 the smaller particles with larger diffusion coefficients, elute faster from the channel. Thus in a fractogram an increase in retention volume means a decrease in diffusion coefficient which corresponds to an increase in hydrodynamic diameter. Fractograms of the Myponga Reservoir and Hope Valley NOM fractions are given in Figure 5.1.

(a)



(b)

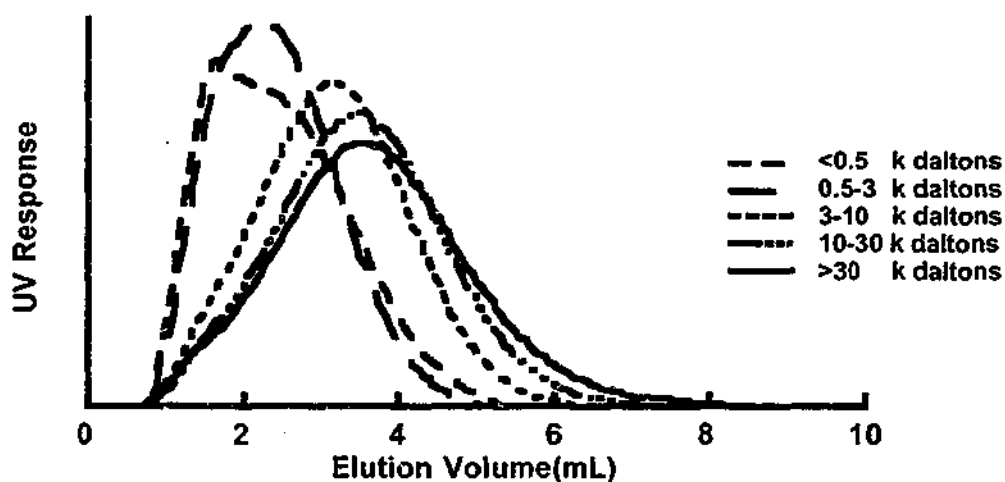


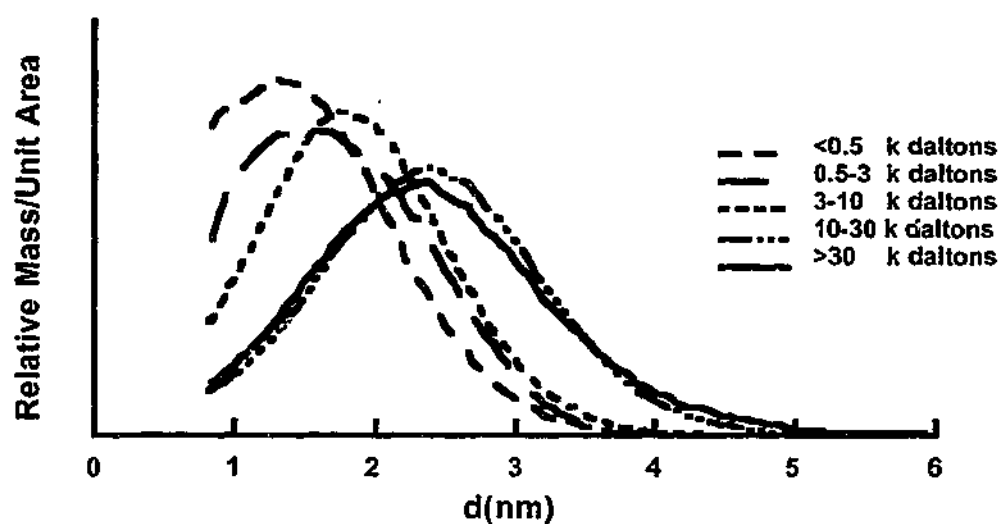
Figure 5.1: FIFFF fractograms of (a) Myponga Reservoir and (b) Hope Valley NOM samples

The fractograms of fractions <0.5 k daltons and 0.5-3 k daltons in Hope Valley samples, also 10-30 k daltons and >30 k daltons in both samples nearly overlap despite the differences in nominal MW. This suggests that separation into discrete size ranges has not been achieved. In fact plots of the first and last two fractions overlap, suggesting that no size base separation has been achieved for these fractions in both samples.

5.3.2. SIZE DISTRIBUTIONS

Size distributions for Myponga Reservoir and Hope Valley samples are given in Figure 5.2. Table 5.2 shows the calculated size parameters for each fraction.

(a)



(b)

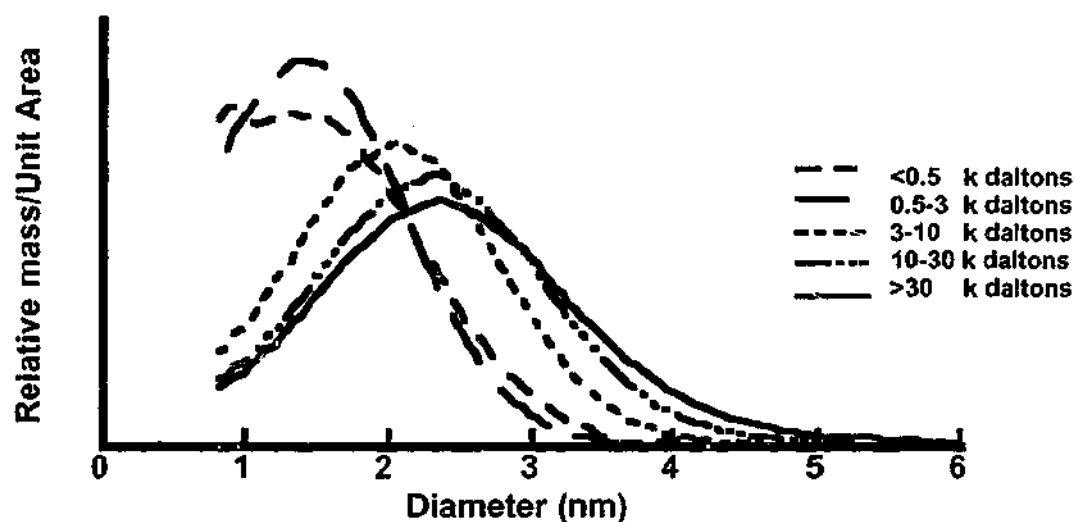


Figure 5.2: FIFFF Size distributions of (a) Myponga Reservoir and (b) Hope Valley NOM samples

Table 5.2: Comparison of the hydrodynamic diameter ranges and averages for the UF fractions obtained by FIFFF. d_p , d_n and d_w , are calculated using equations 3.3 and 3.4 and correspond to the M_p , M_n and M_w values for the samples and obtained from the MW distributions as explained in the text.

NMWCO of Fraction (kDa)	Diameter (nm)								
	Filter Range	Myponga Reservoir				Hope Valley			
		FIFFF Range	d_p	d_n	d_w	FIFFF Range	d_p	d_n	d_w
<0.5	< 1.04	0.99-2.50	1.24	1.47	1.83	0.99-2.56	1.00	1.47	1.83
0.5-3	1.04-2.4	1.10-2.65	1.52	1.57	1.96	0.99-2.36	1.30	1.44	1.73
3-10	2.4 -4.4	1.15-2.75	1.86	1.71	2.14	1.25-3.03	2.07	1.81	2.29
10-30	4.4 - 7.4	1.45-3.45	2.37	2.07	2.62	1.35-3.57	2.39	2.02	2.64
>30	> 7.4	1.40-3.60	2.34	2.08	2.73	1.40-3.69	2.39	2.08	2.76

The FFF ranges have been calculated by excluding 10% of the material from each end of the distribution. Species smaller than 1 nm may not have been recorded by FIFFF as they may not be fully resolved from the void peak. Since there is not enough information about the pore sizes of UF membranes in the literature, the nominal filter diameters were calculated using a pore radius of 0.52 nm for a cellulosic membrane of a NMWCO of 500 (Amicon UMO5). This pore radius has been measured using the flow rate of the pure water through the membrane [36]. Combining equations (3.3) and (3.4), pore sizes of the filters can be estimated using the following equation:

$$\frac{d_2}{d_1} = \left(\frac{M_1}{M_2} \right)^b \quad (5.1)$$

where for the humic substances $b \cong 0.5$. Thus for a given NMWCO the corresponding pore diameter can be estimated.

5.3.3. MOLECULAR WEIGHT DISTRIBUTIONS

MW distributions of the samples were obtained as explained in Chapter 3 (section 3.2.1) and by using sodium poly (styrene sulfonate) samples (PSS) as MW standards. The calibration line is given in Figure 5.3.

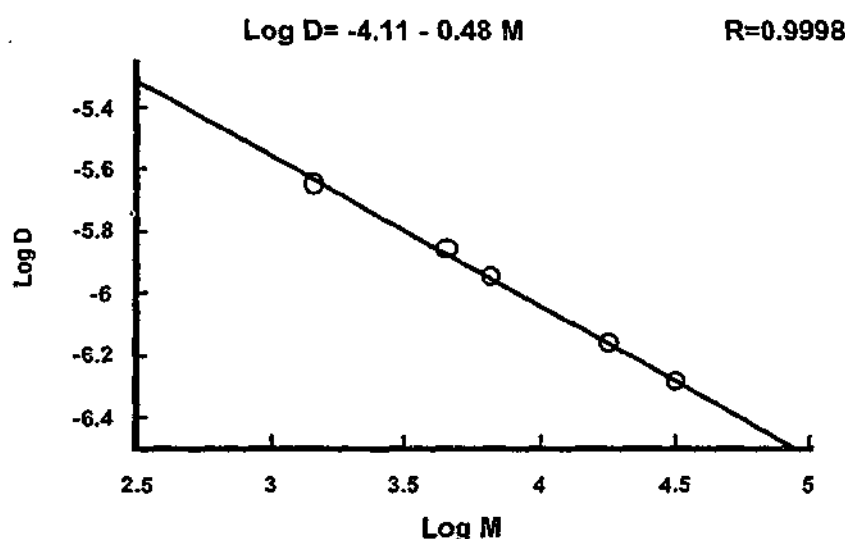


Figure 5.3: Calibration line with sodium poly (styrenesulphonate) MW standards used to calculate MW distributions of the NOM fractions.

The plot of log D versus log M is used to calculate the peak MW and MW distributions of the humic. The constants found together with some other values from the literature are given in Table 5.3. .

Table 5.3: FIFFF calibration constants found in this study, together with some literature values.

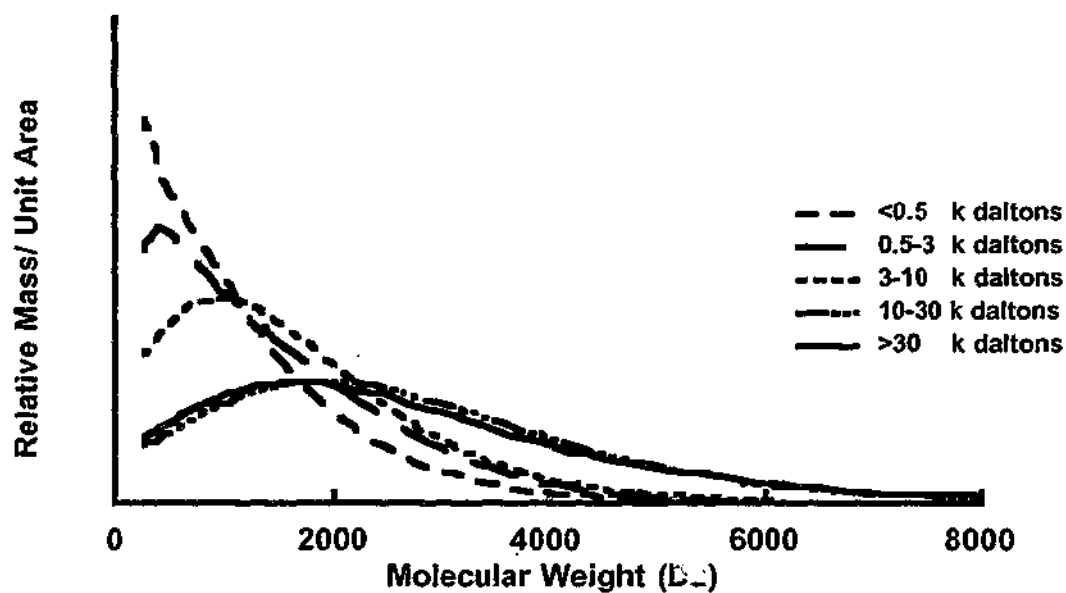
Reference	A (intercept)	b (slope)
This work	7.6×10^{-5}	-0.481
Beckett <i>et al.</i> [16]	6.00×10^{-5}	-0.422
Dycus <i>et al.</i> [37]	7.7×10^{-5}	-0.400

MW distributions of the fractions are given in Figure 5.4 for both samples and the data are summarized in Table 5.4.

Table 5.4: Comparison of the nominal molecular weight ranges of the fractions with the MW ranges and averages obtained from FIFFF. Mp, Mn and Mw are the fractogram peak maximum, number average and weight average MW values obtained by FIFFF.

NMWCO (k daltons)	Molecular Weight (daltons)							
	Myponga Reservoir				Hope Valley			
Filter Range	FIFFF Range	Mp	Mn	Mw	FIFFF Range	Mp	Mn	Mw
< 0.5	400-2770	620	890	1390	400-2880	390	880	1390
0.5-3	350-3100	950	1010	2370	400-2460	690	850	1240
3-10	550-3340	1440	1210	1920	660-4090	1790	1385	2215
10-30	890-5360	2370	1810	2920	770-5060	2420	1730	2970
>30	830-5820	230	1820	3190	830-6140	2420	1814	3260

(a)



(b)

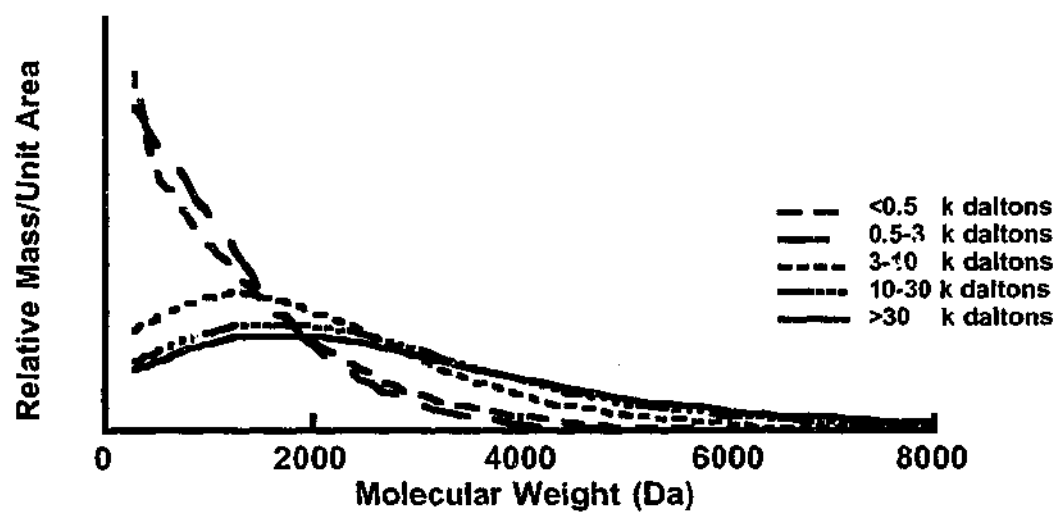


Figure 5.4: FIFFF molecular weight distributions of (a) Myponga Reservoir and (b) Hope Valley NOM fractions obtained by ultrafiltration.

5.3.4. MOBILITY MEASUREMENTS

It has been demonstrated that organic matter can adsorb on mineral surfaces and alter their electrophoretic mobility [35, 40, 41]. The electrophoretic mobility of the coated particles can be measured by particle microelectrophoresis. This method has been used by Beckett and Le, to study the surface charge behaviour of natural and model colloidal particles [35].

In this study, the experimental conditions were chosen so that the goethite particles were completely coated with the natural organic matter [35]. Under similar solution conditions, the measured mobility should reflect the surface charge behaviour of the NOM fractions. The magnitude of the charge of the <0.5 k daltons MW fraction was slightly higher than the other fractions but the charges on the other fractions were about the same. The charge of the molecules measured in solution by potentiometric titration show a slight difference between some fractions and no difference between others [32]. De Nobili *et al.* [42] used gel electrophoresis to compare the charge on different UF fractions and also found no significant difference between the charges of the fractions from the same source. Thus it would seem that charge density of the molecules is not a significant factor in determining the selective filterability of these NOM fractions.

The electrophoretic mobilities of the NOM fractions from Myponga Reservoir, adsorbed to goethite are given in Table 5.5. No significant difference is observed between the mobilities of the adsorbed fractions.

Table 5.5: Electrophoretic mobility of goethite and goethite coated with NOM fractions from Myponga Reservoir. All measurements conducted at pH 6 and 10^{-3} M KNO_3 . The mobility has been converted to zeta potential by the instrument, using the Smoluchowski approximation [43].

Sample (goethite + NOM coating)	Mobility $\times 10^8$ ($\text{m}^2 \text{V}^{-1} \text{s}^{-1}$)	Zeta Potential (mV)
No coating	0.41 – 0.02	5.31–0.28
< 0.5 k daltons Fraction	- 0.34 – 0.01	-4.42 – 0.08
0.5-3 k daltons Fraction	-0.48 – 0.01	-6.17– 0.11
3-10 k daltons Fraction	-0.49 – 0.12	-6.30– 0.16
10-30 k daltons Fraction	-0.47– 0.01	-5.96– 0.08
>30 k daltons Fraction	-0.42 – 0.01	-5.45– 0.07

5.3.5 SOLID STATE ^{13}C NMR OF THE NOM FRACTIONS

Solid state ^{13}C NMR data were obtained for the fractions of both samples. The ^{13}C NMR spectra of Hope Valley NOM is given in Figure 5.6. The ^{13}C NMR spectra of nominal fractions of Myponga Reservoir NOM have been reproduced from an earlier publication [32] and is shown in Figure 5.7

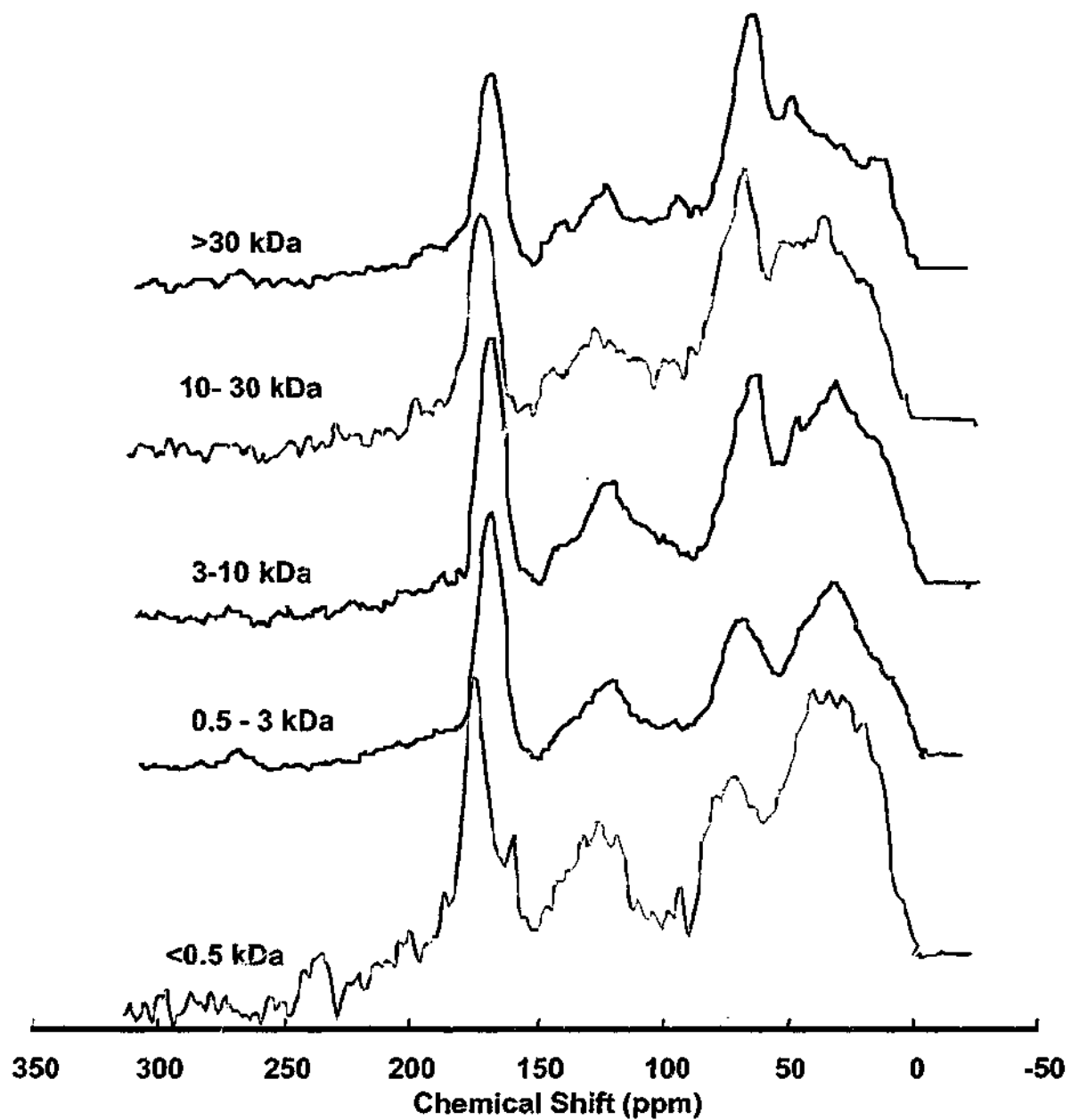


Figure 5.5: Solid state ^{13}C NMR spectra of ultrafiltration fractions of Hope Valley NOM.

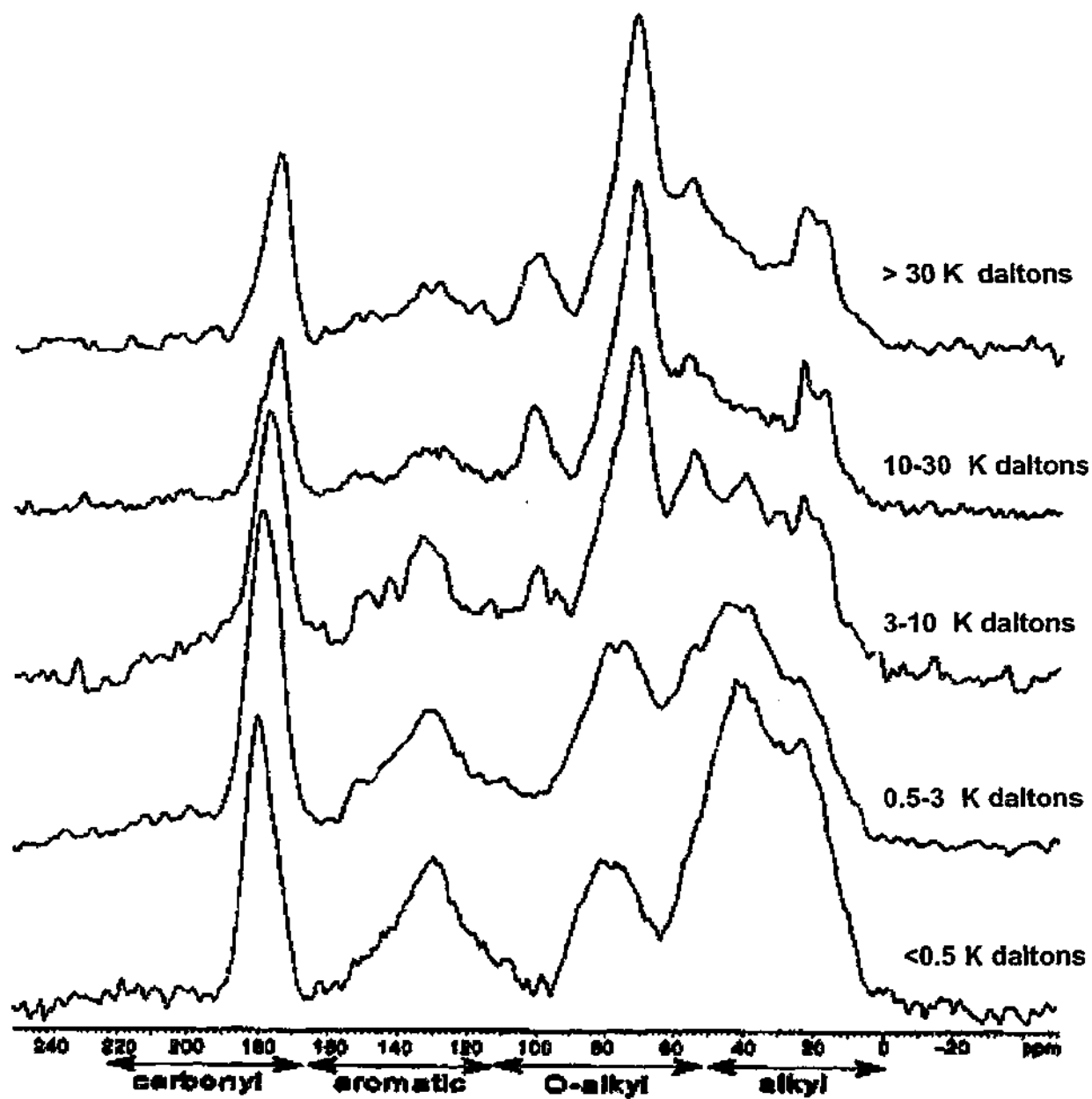


Figure 5.6 : ^{13}C NMR spectra of ultrafiltration fractions of Myponga Reservoir NOM. (Figure from Ref.[32]).

In general, for fractions from >30 k daltons to <0.5 k daltons, the percentage of alkyl groups (0-50 ppm) increased, the percentage of O-alkyl groups (60-110 ppm) decreased and the percentage of aromatic groups (110-165 ppm) increased. In a similar study by Rao and Choppin [14], sediment and Aldrich humic acids were fractionated by UF into three nominal fractions of 1-10, 50-100 and >300 k daltons. Solid state ^{13}C NMR spectra of the fractions showed that the area of the aromatic and alkyl groups decrease with an increase in nominal size of the molecules. These spectra suggest that separation by membrane ultrafiltration involves a dependence on structure as well as size. The same effect has been recently reported by Tombacz [44].

The shape of the spectrum for the first two (<0.5, 0.5-3 k daltons) and last two fractions (10-30, >30 k daltons) are very similar especially for the Myponga Reservoir fractions. Thus in terms of structure the sample can be divided into three distinct fractions instead of five. The same trend is seen in the results obtained by FIFFF, in which the first two and last three fractions show similarity in their fractograms and hence size and MW distribution plots. This means that some fractions with similar structure and size distributions have been both retained and passed through a membrane regardless of the nominal pore size. For example the membrane filter with NMWCO of 30 k daltons has retained fractions with the same size distribution as the fraction that has passed through it and the NMR spectra of both fractions show only minor differences in structure. If there are any differences between the size distribution, structure or charge of these fractions, they are too subtle to be picked up by the measurements made in this research.

5.3.6 COMPARISON OF THE MOLECULAR WEIGHT DATA WITH THOSE OBTAINED FROM HPSEC

Pelekani *et al* [33], have measured the size distribution of the same NOM fractions (from Hope Valley and Myponga Reservoir), using high performance size exclusion chromatography. (HPSEC). A glycol functionalised silica gel column was used for separation. The carrier was 0.02 M phosphate buffer adjusted to an ionic strength of 0.1 M with NaCl, with a pH of 6.8. The column was calibrated using polystyrene-sulphonate molecular weight standards. The polydispersity values and the molecular weight range obtained from HPSEC are given in Table 5.6:

Table 5.6: Polydispersity and molecular weight ranges of Myponga Reservoir and Hope Valley NOM fractions, obtained by HPSEC.

NOM Fraction (k daltons)	M_w/M_n		HPSEC Range	
	Myponga Reservoir	Hope Valley	Myponga Reservoir	Hope Valley
<0.5	1.35	1.32	467-1960	356-1170
0.5-3	1.16	1.14	1010-2450	631-1470
3 -10	1.22	1.24	1370-3420	851-2310
10 -30	ND*	1.32	ND	837-2970
>30	1.36	1.56	1375-5410	851-3750

*ND: Not determined.

The molecular weight ranges obtained by the two techniques are compared in Figure 5.7. These results suggest that within the technical limitations of each method for characterization of molecular weight, there is a good agreement between the overall range. The difference between FIFFF and HPSEC ranges are more significant for Hope Valley

The diameters d_p , d_n and d_w displayed in Table 5.2 are obtained using the MW distribution plots. They correspond to the peak maximum (M_p) number average (M_n) and weight average (M_w) molecular weights. In general the size and molecular weights obtained by FIFFF are smaller than the nominal filter ranges, especially for the last three fractions. FIFFF gives a total size range for all size fractions, of 1-5.7 nm and a MW range of 400-6200. The diameters found by FIFFF are comparable with the values reported in the literature for humic substances. The average diameter of Suwannee River fulvic acid has been determined by Aiken *et al.* as 1.76 nm using small angle X-ray scattering [38] and 1.64 nm by Thurman *et al.* [39] (see also Chapter 2).

In the lower size fractions (<0.5, 0.5-3 k daltons), species with molecular weight higher than the nominal cut-off have passed through the filters. This may indicate a change in molecular conformation of some NOM species. Leppard *et al.* [3] suggested that loose aggregates can pass the filters even when the aggregate size is much larger than the pore size. Perhaps the aggregates dissociate and reform in the filtrate solution. Shaw *et al.* also observed humic substances larger than the nominal filter cutoff in their filtrates [20]. In all fractions species smaller than the nominal filter size were observed in the retentates. This could be due to adsorption of smaller size species to the filters or charge repulsion that would be particularly apparent within pores in the membrane. Non-uniformity of pores may be another reason.

The following paragraph should be read before viewing Figure 5.7.

This can be explained by the higher alkyl content of the hope Valley water in all fractions except for the <500 fraction (Figure 5.5) and the possibility of the humic samples adsorbing onto the silicagel. Solid-state ^{13}C NMR of the fractions show that Myponga Reservoir and Hope Valley samples have similar percentages of carboxyl and aromatic groups. But Hope Valley samples have a slightly higher alkyl content. This difference in chemical structure might have resulted in the different behavior of the two samples in the silicagel column or the FIFFF channel. Any more speculation on the nature of the interactions would require more specific experiments to be performed.

Reservoir samples. This has been explained by the higher alkyl content of Hope Valley water, except for the <500 fraction (Figure 5.5) and adsorbing on the silica gel surface in HPSEC [32,33].

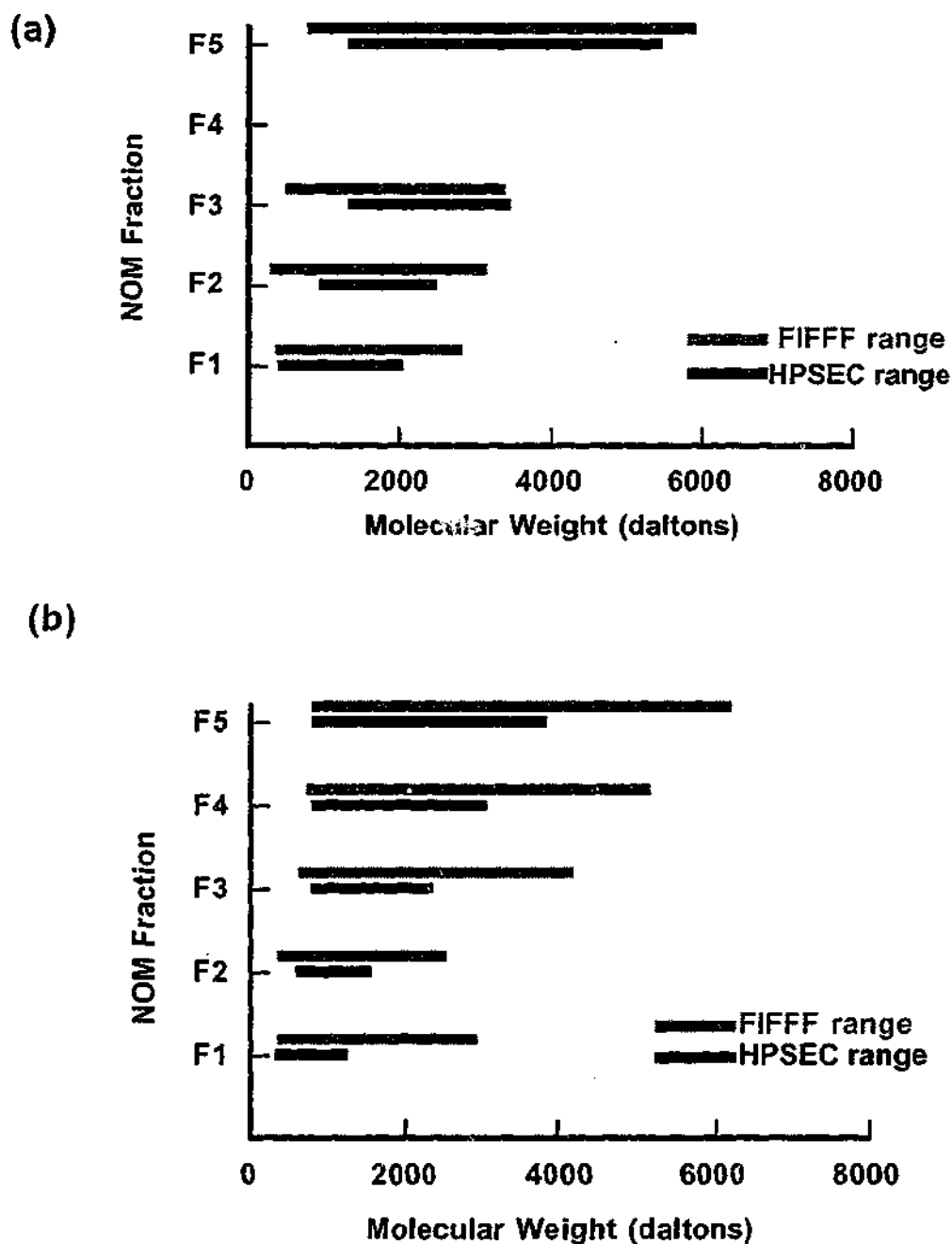


Figure 5.7: Comparison of the molecular weight ranges calculated from molecular weight distributions obtained by FIFFF and HPSEC (a) Myponga Reservoir and (b) Hope Valley NOM,. The range was calculated by excluding 10% of the data from each side of the MW distribution.

5.4 CONCLUSIONS

UF is commonly used for isolation and fractionation of humic substances. Many factors can affect the quality of fractionation of humic substances, including the method of filtration, pH and ionic strength of the solution, initial concentration of the sample, material used for calibration of the membrane filters and the type of the membrane used.

In this study NOM from two sites in South Australia were isolated and fractionated using cellulosic membranes and the fractions were characterised for size and MW by FIFFF. The results obtained, show that only a small degree of size fractionation has been achieved. Although five fractions were collected, only three distinct size fractions were identified and these three differ only slightly from each other in size (less than 1 nm).

^{13}C NMR indicated that the separation was influenced by structural differences as well as size. The size and MW values of the fractions do not agree at all well with the nominal filter ranges. Molecules much smaller than the nominal MWCO are rejected by the 30 kDa and 10 k daltons membranes. For example the M_w value for the >30 k daltons fractions is only about 3200 for the two samples studied. This corresponds to a hydrodynamic diameter of about 2.7 nm whereas the estimated pore diameter is 7.4 nm. In contrast the smallest NMWCO membranes appear to be permeable to molecules larger than the pore size. Comparison of the molecular weight data obtained from FIFFF with those obtained from HPSEC, shows that molecular weight range and the polydispersities obtained from the two techniques are in good agreement with each other and are smaller than the UF range for all fractions except fraction <0.5 k daltons.

These results cast considerable doubt on the worth of membrane filtration as a size selective separation method for humic substances. In view of this, the findings of a large number of studies, which have reported substantial conclusions on the effect of MW and molecular size on various properties should be handled with caution.

5.5 REFERENCES:

1. Gjessing, E.T., Ultrafiltration of aquatic humus, *Environmental Science and Technology*, 4 (1970) 437-438.
2. Cornel, P.K., Summers R.S., and Roberts, P.V., Diffusion of Humic Acid in Dilute Aqueous Solution, *Journal of Colloid and Interface Science*, 110 (1985) 149-164.
3. Leppard, G.G., Buffle, J., and Baudat, R., A Description of the aggregation properties of aquatic pedogenic fulvic acids, *Water Research*, 20 (1986) 185-196.
4. Ephraim, J., H, Pettersson, C., and Allard, B., Correlations between acidity and molecular size distributions of an aquatic fulvic acid, *Environment International*, 22 (1996) 475-583.
5. Crum, R.H., Murphy E.M. and Keller, C.K., A non-adsorptive method for the isolation and fractionation of natural dissolved organic carbon, *Water Research*, 30 (1996) 1304-1311 .
6. De Mora, S.J., and Harrison, R.M., The Use of physical separation techniques in trace metal speciation studies, *Water Research*, 17 (1983) 723-733 .
7. Ephraim, J.H., and Marinsky, J., Ultrafiltration as a technique for studying metal-humate interactions: Studies with iron and copper, *Analytica Chimica Acta*, 232 (1990) 171-180.

8. Lakshman, S., Mills, R. and Patterson, H., Apparent differences in binding site distributions and aluminum(III) complexation for three molecular weight fractions of a coniferous soil fulvic acid, *Analytica Chimica Acta*, 282 (1993) 101-108 .
9. Langford, C.H., and Cook, R.L., Kinetic versus equilibrium studies for the speciation of metal complexes with ligands from soil and water, *Analyst*, 120 (1995) 591-596.
10. Martin, J.M., Dai, M.H., and Cauwet, G., Significance of colloids in the biogeochemical cycling of organic carbon and trace metals in the Venice lagoon (Italy), *Limnology and Oceanography*, 40 (1995) 119-131.
11. Burgess, R.M., McKinney R.A., Brown W.A. and Quinn, J.G., Isolation of marine sediment colloids and associated polychlorinated biphenyls- An evaluation of ultrafiltration and reverse-phase chromatography, *Environmental Science and Technology*, 30 (1996) 1923-1932.
12. Kim, J.I., Rhee, D.S., Wimmer, H., Buckau, G., and Klenze, R., Complexation of trivalent actinide ions (Am^{3+} , Cm^{3+}) with humic acid, a comparison of different experimental methods, *Radiochimica Acta*, 62 (1993) 35-43 .
13. Czerwinski, K.R., Buckau G., Scherbaum, F. and Kim , J.I., Complexation of the uranyl ion with aquatic humic acid, *Radiochimica Acta*, 65 (1994) 111-119 .
14. Rao, L., and Choppin, G.R., Thermodynamic study of the complexation of Neptunium (V) with humic acids, *Radiochimica Acta*, 69 (1995) 87-95 .
15. Aiken, G.R., and Malcolm, R.L., Molecular weights of aquatic fulvic acids by vapor pressure osmometry, *Geochimica et Cosmochimica Acta*, 51 (1987) 2177-2184 .

16. Beckett, R., Zhang J., and Giddings C., Determination of molecular weight distributions of fulvic and humic acids, using flow field-flow fractionation, *Environmental Science and Technology*, 21 (1987) 289-295 .
17. Reid, P.M., Wilkinson, A.E., Tipping, E. and Jones, M.N., Determination of molecular weights of humic substances by analytical (UV scanning) ultracentrifugation, *Geochimica et Cosmochimica Acta*, 54 (1990) 131-138.
18. Chin, Y.P., and Gschwend, P.M., The abundance, distribution and configuration of porewater organic colloids in recent sediments, *Geochimica et Cosmochimica Acta*, 55 (1991) 1309-1317.
19. Ogura, N., Molecular weight fractionation of dissolved organic matter in coastal seawater by ultrafiltration, *Marine Biology*, 24 (1974) 305-312.
20. Shaw, P.J., Jones, R.I., and De Haan, H., Separation of molecular size classes of aquatic humic substances using ultrafiltration and dialysis, *Environmental Technology*, 15 (1994) 765-774 .
21. Amicon Co., *Membrane Filtration Chromatography Catalogue*, (1993).
22. Wilander, A., A study on the fractionation of organic matter in natural water by ultrafiltration techniques ,*Schweizerische Zeitschrift fur Hydrologie*, 34 (1972) 190-200 .
23. Buffle, J., Deladoey P. and Haerdi W., The use of ultrafiltration for the separation and fractionation of organic ligands in frash waters, *Analytica Chimica Acta*, 101 (1978) 339-357.
24. Kilduff, J., and Weber W.J. Jr., Transport and separation of organic macromolecules in ultrafiltration processes, *Environmental Science and Technology*, 26 (1992) 569-577.

25. Zeman, L.J., Adsorption effects in rejection of macromolecules by ultrafiltration membranes, *Journal of Membrane Science*, 15 (1983) 213-230.
26. Aiken, G.R., Evaluation of ultrafiltration for determining molecular weight of fulvic acid., *Environmental Science and Technology*, 18 (1984) 978-981.
27. Aster, B., Burba, P., and Broekaert, J.A.C., Analytical fractionation of aquatic humic substances and their metal species by means of multistage ultrafiltration, *Fresenius Journal of Analytical Chemistry*, 354 (1996) 722-728.
28. Bedrock, C.N., Cheshire M.V., Chudeck J.A., Fraser A.R., Goodman B.A., Shand C.A., Effect of pH on precipitation of humic acid from peat and mineral soils on the distribution of phosphorus forms in humic and fulvic acid fractions, *Communications in Soil Science and Plant Analysis*, 26 (1995) 1411-1425.
29. Giddings, J.C., Field-Flow Fractionation, *C & E News*, 66 (1988) 34-45.
30. Jucker, C., and Clark, M.M., Adsorption of aquatic humic substances on hydrophobic ultrafiltration membranes, *Journal of Membrane Science*, 97 (1994) 37-52.
31. Bedrock, C.N., Cheshire, M.V., Chudek, J.A., Goodman, B.A. and Shand, C.A., ^{31}P NMR studies of humic acid from a blanket soil, in N. Senesi, and Miano, T.M., (Ed.), *Humic Substances in the Global Environment and Implications on Human Health*, Elsevier Science, 1994, 227-232 .
32. Newcombe, G., Drikas, M., Assemi, S., and Beckett, R., The influence of the characterized natural organic material on activated carbon adsorption:1. Characterisation of concentrated reservoir NOM., *Water Research*, 31 (1997) 965-972.

33. Pelekani, C., Newcombe, G., Snoeyink, V.L., Hepplewhite, C., Assemi, S., and Beckett, R., Characterisation of natural organic matter using size exclusion chromatography, *Environmental Science and Technology*, 33 (1999) 2807-2813 .
34. Giddings, J.C., Benincasa A.M., Williams P.S., Rapid breakthrough measurement of void volume for flow field-flow fractionation channels, *Journal of Chromatography*, 627 (1992) 23-35.
35. Beckett, R., and Le, N.P., The role of organic matter and ionic composition in determining the surface charge of suspended particles in natural waters, *Colloids and Surfaces*, 44 (1990) 35-49.
36. Buffle, J., Perret, D., and Newman, M., The use of filtration and ultrafiltration for size fractionation of aquatic particles, colloids and macromolecules, in Buffle J., and van Leeuwen H.P., (Eds.), *Environmental Particles*, Lewis Publishers, Michigan. 1984, 171-230.
37. Dycus, P.J.M., Healy, K., Stearman, G.K., and Wells, M., Diffusion coefficients and molecular weight distributions of humic and fulvic acids determined by flow field-flow fractionation, *Separation Science and Technology*, 30 (1995) 1435-1453.
38. Aiken, G.R., Brown, P.A., Noyes, T.I., and Pinckney, D.J., Molecular size and weight of fulvic and humic acids from the Suwannee River, in Averett, R.C., Leenheer, J.A., McKnight, D.M., and Thorn, K.A., (Eds.), *Humic Substances in the Suwannee River, Georgia: Interactions, Properties, and Proposed Structures*, U.S. Geological Survey, Denver, 1995, 89-97.
39. Thurman, E.M., Wershaw, R.L., Malcolm, R.L and Pinckney, D.J., Molecular size of aquatic humic substances, *Organic Geochemistry*, 4 (1982) 27-35.
40. Tipping, E., The adsorption of aquatic humic substances by iron oxides, *Geochimica et Cosmochimica Acta*, 45 (1981) 191-199.

41. Tipping, E., Adsorption by goethite ($\alpha\text{-FeOOH}$) of humic substances from three different lakes, *Chemical Geology*, 33 (1981) 81-89.
42. De Nobili, M., and Fornasier, F., Assessment of the effect of molecular size on the electrophoretic mobility of humic substances, *European Journal of Soil Science*, 47 (1996) 223-229 .
43. Hunter, R.J., *Foundations of Colloid Science*. Vol. 1. Oxford University Press, New York, 1987.
44. Tombacz, E., Colloidal properties of humic acids and spontaneous changes of their colloidal state under variable solution conditions, *Soil Science*, 164 (1999) 814-824.

CHAPTER 6

EFFECT OF SOLUTION PH AND IONIC STRENGTH ON SIZE AND DIFFUSION COEFFICIENT OF HUMIC SUBSTANCES

6.1 INTRODUCTION

The aggregation of humic substances has been widely studied in relation to their physico-chemical nature and behaviour in soils [1-3], water [3] and coal [4]. The coagulation of aquatic natural organic matter and its affinity for surfaces may strongly affect the roles and behaviour of organic and organometallic associations in aquatic ecosystems. Hydrophobic pollutants can interact with mobile humic containing colloids and be transported through soil or groundwater. The properties that influence the aggregation and stability of such colloids are crucial in the study of contaminant transport in aquatic and terrestrial systems.

Some important factors in the aggregation of humic substances include the origin and concentration of humic material, pH and ionic strength of the medium, as well as the type of the salts present. It is reported that the addition of divalent and trivalent salts enhances the aggregation process of humic substances [3].

Cations can induce aggregation by shrinking the electrical double layer thickness and thus decreasing the charge density on the macromolecules [5]. Divalent and trivalent cations such as Ca^{2+} and Al^{3+} may also enhance aggregation by bridging the molecules of the humic substances. Alum precipitation is a major process in water treatment for removal of organic matter. Solution chemistry is known to be important in the extent of binding of polycyclic aromatic carbons and metals by humic substances [3, 6, 7].

6.1.1 CHEMICAL PROCESSES INVOLVED IN THE AGGREGATION OF HS

Aggregation occurs when the various processes involved result in a negative Gibbs free energy. The major interactions involved in these processes are [8]:

- Hydrogen bonding, which can occur between acid, phenol and similar groups.
- π - bonding (stacking of planar π -donor-planar π^* -acceptor to form a complex)
- Coulombic attractions between oppositely charged sites on the polyelectrolyte molecules or between shared counter ions and polyelectrolyte molecules.
- Charge transfer interactions between aromatic groups.
- Hydrophobic interactions, which occur due to rearrangement of water molecules around a hydrophobic moiety.

6.1.2 METHODS USED IN THE STUDY OF HS AGGREGATION

Different methods have been used to study the aggregation of humic substances, among them being Viscometry [9, 10], Transmission Electron Microscopy (TEM) [2, 11, 12], Scanning Electron Microscopy (SEM), Ultracentrifugation (UC), Dynamic Light Scattering (DLS), Small Angle X-ray Spectroscopy (SAXS), atomic force microscopy [13, 14] and FIFFF [15].

Much controversy exists in the literature on the effect of solution conditions on the size and conformation of humic substances. The coiling or uncoiling, association or dissociation of the humic substance molecules as a result of a change in solution pH and salt concentration is disputed. The focus of this chapter is to study the effect of solution pH and a 1:1 electrolyte concentration on the hydrodynamic diameter of several humic substance samples.

6.2 MATERIALS AND METHODS

6.2.1 SAMPLE PREPARATION

Three humic acids and two fulvic acids from aquatic, sediment and coal origins have been used in this study. Chaffey Reservoir humic and fulvic acids have been extracted and characterised as explained in Appendix 2. Suwannee River humic and fulvic acids and Leonardite coal humic acid were purchased from the International Humic Substances Society (IHSS, Colorado, U.S.A).

Tris (hydroxymethyl)aminomethane (TRIS) was used as the carrier medium in these experiments to ensure that the pH of the solutions would not change during the experiments. The composition of this carrier has been explained in Chapter 3.

The samples were prepared by dissolving the freeze-dried sample in TRIS buffer solution, having a specific pH and ionic strength. The ionic strength of the sample was changed by either addition of NaNO_3 or reduction of the amount of NaN_3 . The solution pH was adjusted by addition of HNO_3 and any change in the ionic strength induced by addition of acid, was compensated for, by reducing the amount of NaN_3 .

6.2.2 FIFFF RUN CONDITIONS

The channel void volume was measured as 1.16 mL using the breakthrough method [16]. The channel and crossflow rates were maintained at about 0.90 and 3.90 mL min^{-1} respectively. Following a series of trial injections an injection mass of 2.5 μg was used in all runs.

6.3 RESULTS AND DISCUSSION

6.3.1 EFFECT OF THE PH ON AGGREGATION OF HUMIC SAMPLES

The effects of solution pH on the size of humic samples were studied in three different solution pH values (6.8, 7.9 and 9.3) at constant ionic strength (0.004 M). Figure 6.1 illustrates the size distribution of the samples. The diameter at the peak maximum (d_p), weight average and number average diameters (d_w and d_n) are given in Table 6.1. As the pH was decreased from 9.2 to 6.8 the peak maxima for all samples were shifted to a higher hydrodynamic diameter. The shift is about 0.5 nm for the fulvic acid samples and

Paragraph "1" should be read instead of the paragraph starting with "*Titration curves of humic substances...*" in line 5 paragraph 1, page 118.

Paragraph marked "2" should be read instead of the sentence starting with: "*The initial size...*" in line 5 of paragraph 3, page 118.

1)

Titration curves of humic substances show that within the pH range used in this study (6.8-9.2) the charge can decrease up to about 20% by reducing the pH [17,34,35]. The reduced columbic repulsion could mean that attractive forces such as hydrogen bonding and Van der Waals forces could contribute to aggregation.

2)

The nature of the molecules can also be a parameter in determining the aggregate size. Aquatic humic and fulvic acid molecules are more soluble than humic substances isolated from soil, sediment or coal. The terrestrial humic substances are apparently less soluble because they are solid forms left after leaching by water in the environment. Thus they have a comparatively higher tendency to aggregate.

0.8-1 nm for the humic acid samples. A decrease in pH results in the neutralisation of the ionised COOH and phenolic OH groups in the humic molecules. This will reduce the columbic repulsion between the molecules, which in turn will increase the probability of association of the humic molecules. However, some of the functional groups will be protonated by a decrease in pH. Titration curves of humic substances show that the charge does not vary considerably within the pH range used in this study (6.8-9.2) [17]. This suggests that a reduction in coulombic repulsion may not be the major driving force for aggregation, but instead hydrogen bonding could be the dominant force. Van der Waals forces and hydrophobic interactions might also have contributory aggregative effects [8, 18].

The weight average diameter (d_w) and number average diameter (d_n) were plotted against the solution pH (Figure 6.2). The trend of increasing d_w is the same for the sediment and coal humic acids. The d_w of the sediment and coal humic samples were higher compared to the SRHA and SRFA and CHFA.

Figure 6.2 shows that the hydrodynamic diameters of Chaffey HA and Leonardite exhibit a sharper decrease in size with increasing pH, compared to the SRHA and FA samples. One possibility is that they have a higher charge density compared to the aquatic samples. The initial size of the molecule can also be a parameter in determining the aggregate size. The method used in the original isolation of the humic acid samples can have an effect on aggregation. SRFA, SRFA and ChFA have been separated or purified using XAD-8 resins. It is possible that some of the high molecular weight molecules have been lost due to irreversible adsorption onto the XAD-8 resin.

Table 6.1: Size parameters of the humic substances as determined by FIFFF. Diameter at the peak maximum (d_p), number and weight average diameters (d_n and d_w), and the diffusion coefficient at the peak maximum (D_p), number and weight average diffusion coefficients (D_n and D_w), are given

Sample Solution Condition	Suwanne River FA			Chafley FA			Suwanne River HA			Chafley HA			Leonardite HA		
	d_p (nm)	d_n (nm)	d_w (nm)	d_p (nm)	d_n (nm)	d_w (nm)	d_p (nm)	d_n (nm)	d_w (nm)	d_p (nm)	d_n (nm)	d_w (nm)	d_p (nm)	d_n (nm)	d_w (nm)
PH=7.9 I=0.02 M	<1	1.4	1.6	ND	ND	ND	1.1	1.6	2.1	1.2	1.8	2.8	1.7	1.9	2.9
PH=7.9 I=0.04 M	1.2	1.5	1.8	1.1	1.5	1.7	1.6	1.7	2.3	2.2	2.1	3.4	2.6	2.2	3.4
PH=7.9 I=0.08 M	1.3	1.6	1.9	1.4	1.7	2.1	1.9	1.8	2.4	2.6	2.4	4.2	2.8	2.4	3.6
PH=7.9 I=0.1 M	1.6	1.7	2.0	1.5	1.7	2.2	1.9	1.8	2.3	2.6	2.3	3.5	2.7	2.5	3.6
PH=6.8 I=0.04 M	1.5	1.8	2.7	1.5	1.6	2.1	1.9	1.9	2.8	2.6	2.5	4.3	2.7	2.6	4.4
PH=9.2 I=0.04 M	1	1.4	1.7	1.1	1.5	1.8	1.4	1.7	2.3	1.6	1.9	2.8	1.9	1.9	3.0

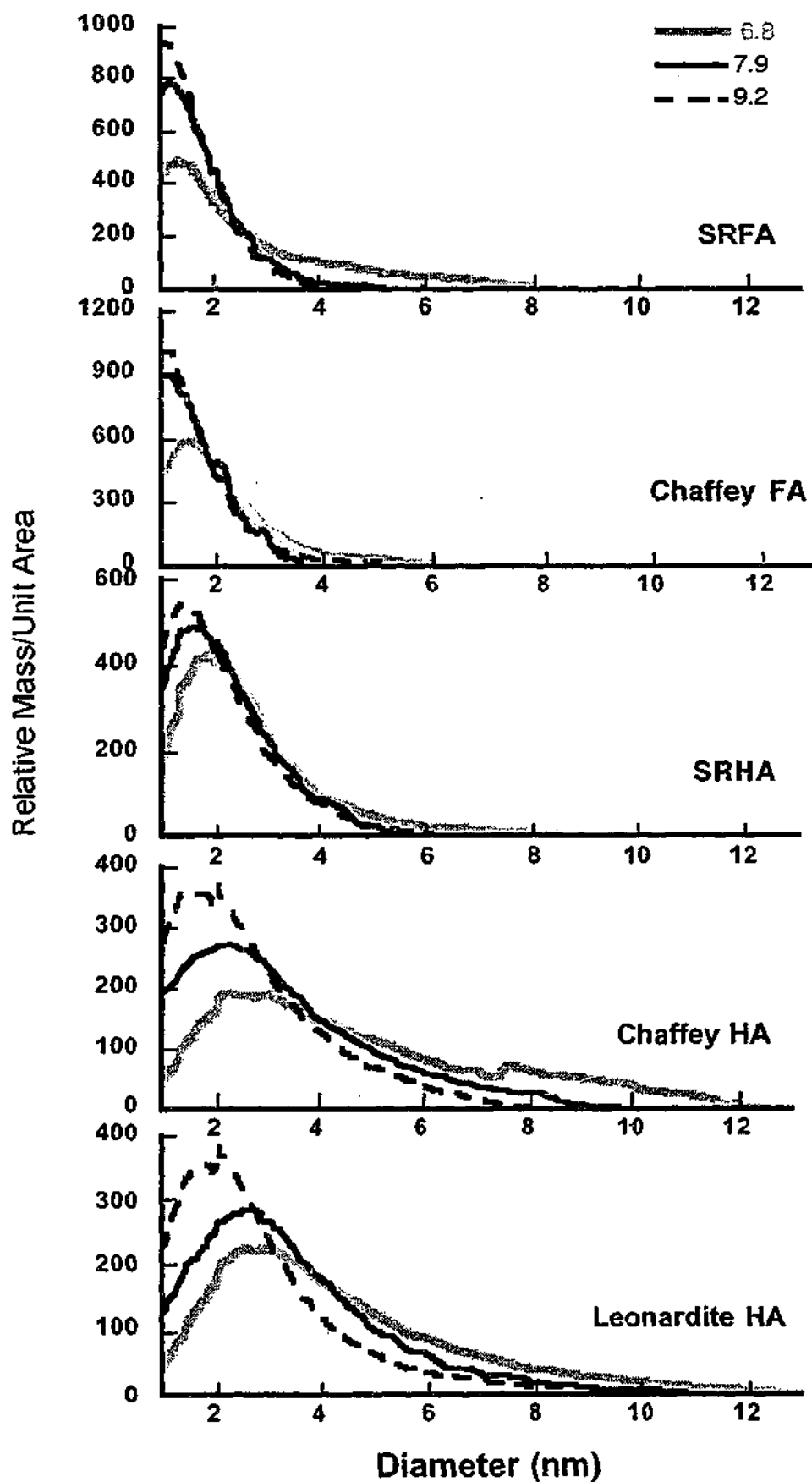
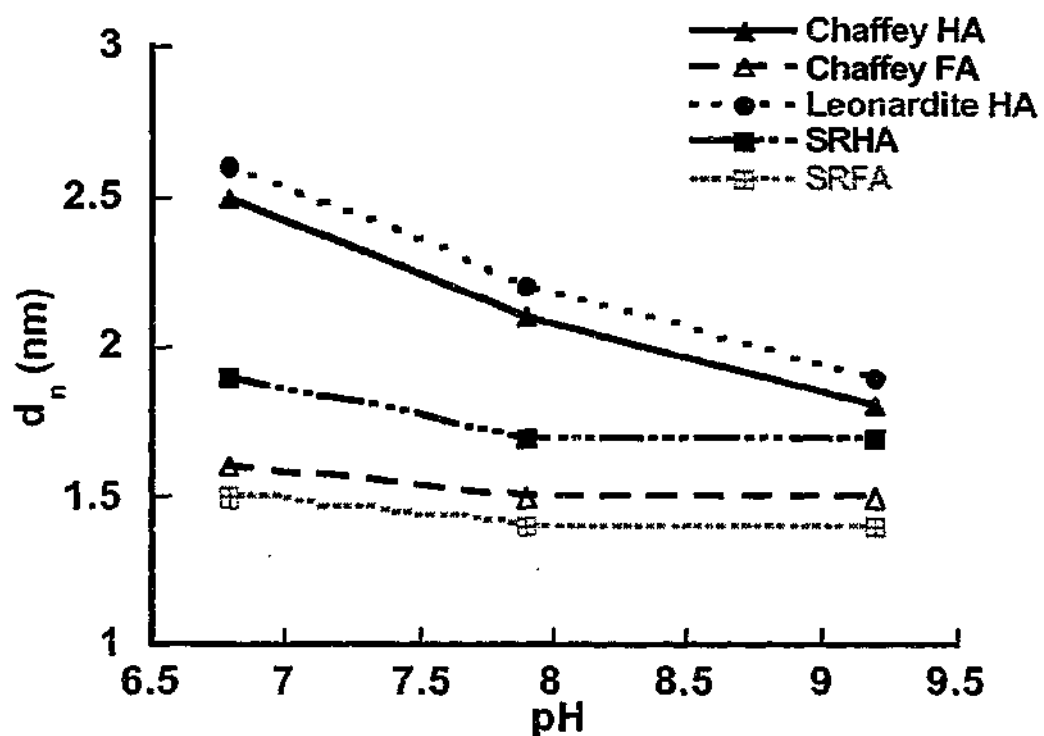


Figure 6.1: Effect of the solution pH on size distribution of humic samples in 0.04 M TRIS buffer.

(a)



(b)

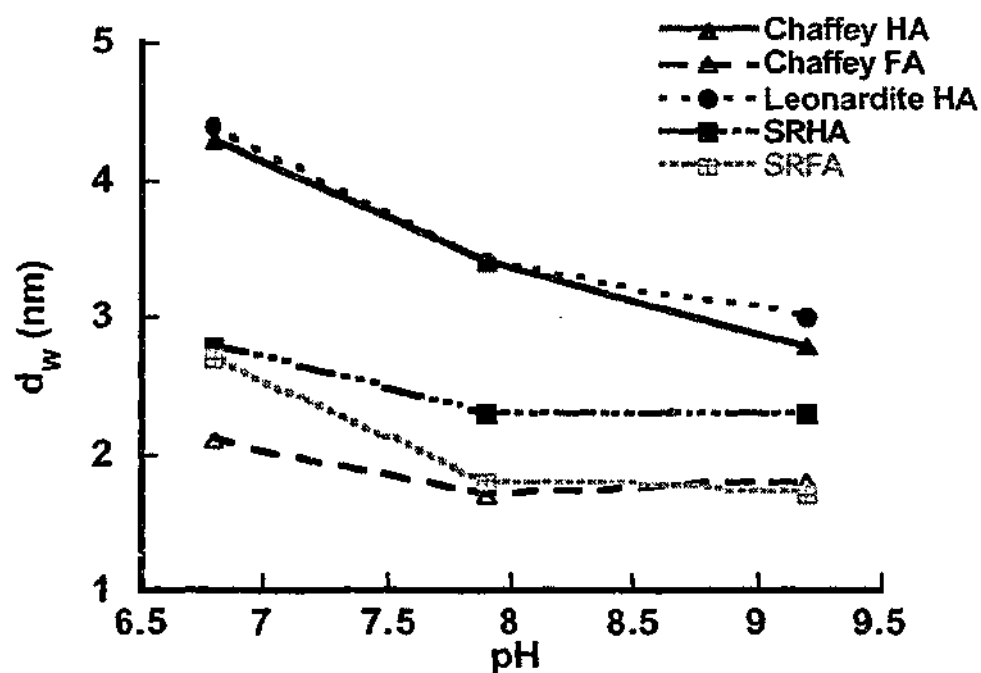


Figure 6.2 : Effect of pH on the (a) number average and (b) weight average diameters of humic samples in 0.04 M TRIS buffer .

6.3.2 EFFECT OF IONIC STRENGTH ON AGGREGATION OF HUMIC SAMPLES:

The effect of the solution ionic strength on d_n and d_w of the samples is illustrated in Figure 6.3. Increasing the ionic strength has resulted in broadening the size distribution and a shift to larger size in all samples. Comparison of the d_p values indicates an increase in the peak maximum as the ionic strength increases. The d_p for SRFA has increased about 0.6 nm when the ionic strength is increased from 0.02 M to 0.1 M, whereas the humic acid samples show an increase of about 1.5 nm in d_p within the same range. Figure 6.3 shows that except for the lowest ionic strength, the size distributions show a major change in the peak maxima. The tailings almost overlap (except for Chaffey humic acid). It can be speculated that the aggregation is more pronounced in the lower size regions, similar to the effect observed when the pH is increased (Figure 5.2). Increasing the ionic strength will result in the contraction of the diffuse parts of the double layers around the humic molecules.

A decrease is noted for the d_n and d_w of the Chaffey HA and d_w of SRHA. This is probably because the larger molecules have stuck to the channel under the high field, so only the smaller ones could emerge from the channel. Evidence for this is the emergence of large peaks after termination of the field and the decrease in area noted for all samples on increasing the ionic strength and decreasing the pH.

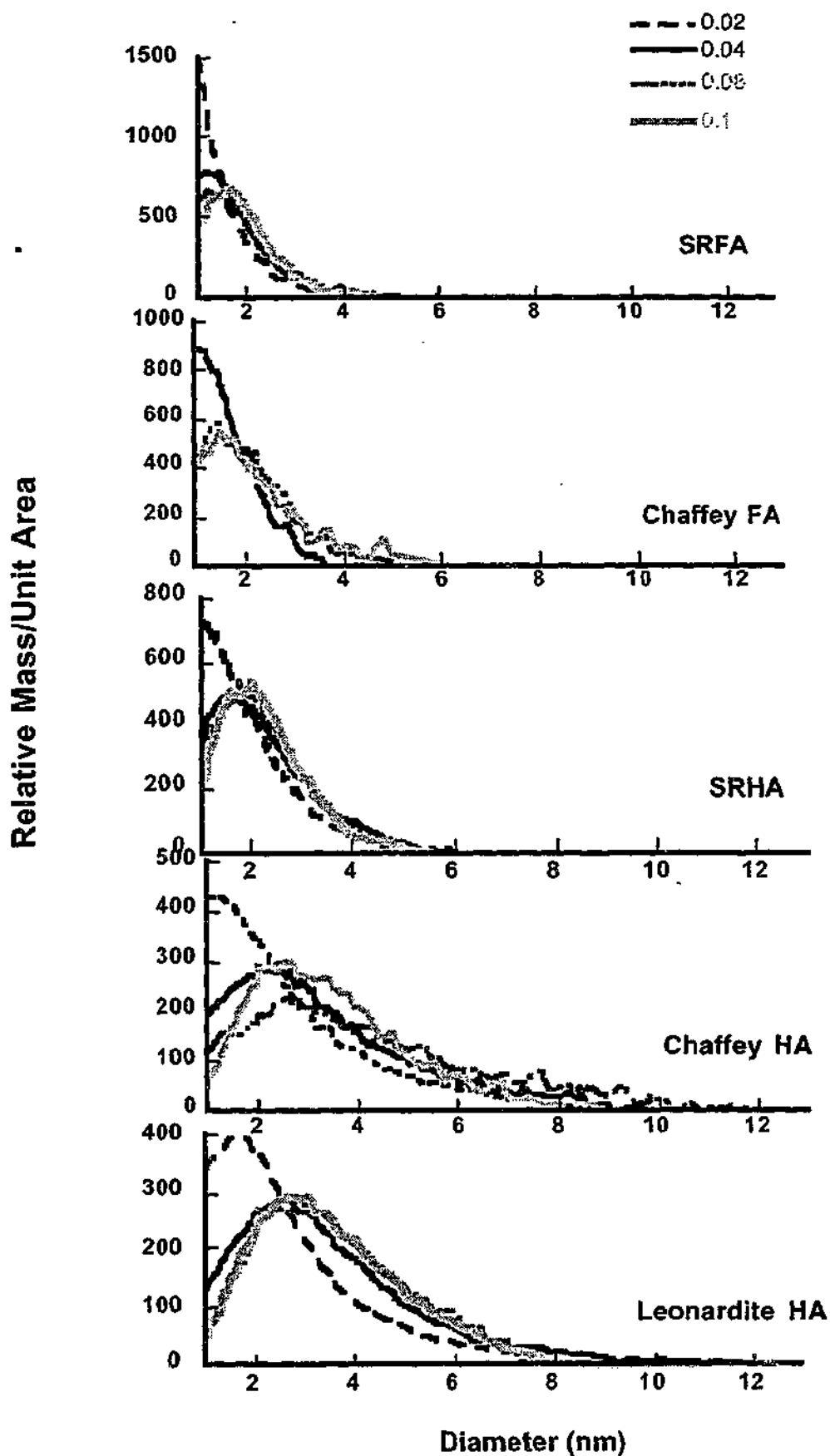
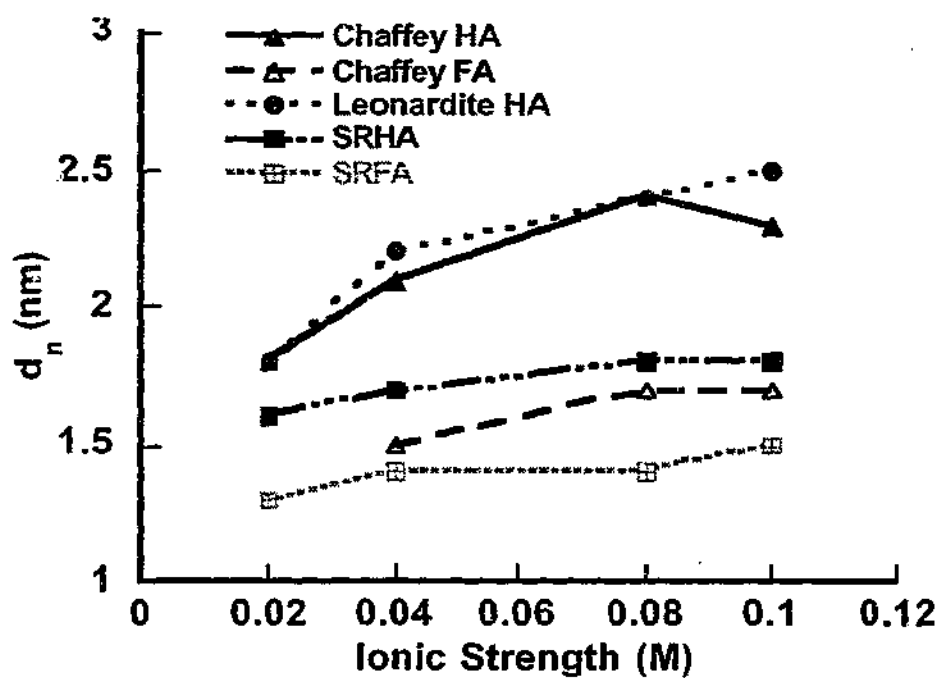


Figure 6.3: Effect of the ionic strength on the size distribution of humic samples in TRIS buffer.

(a)



(b)

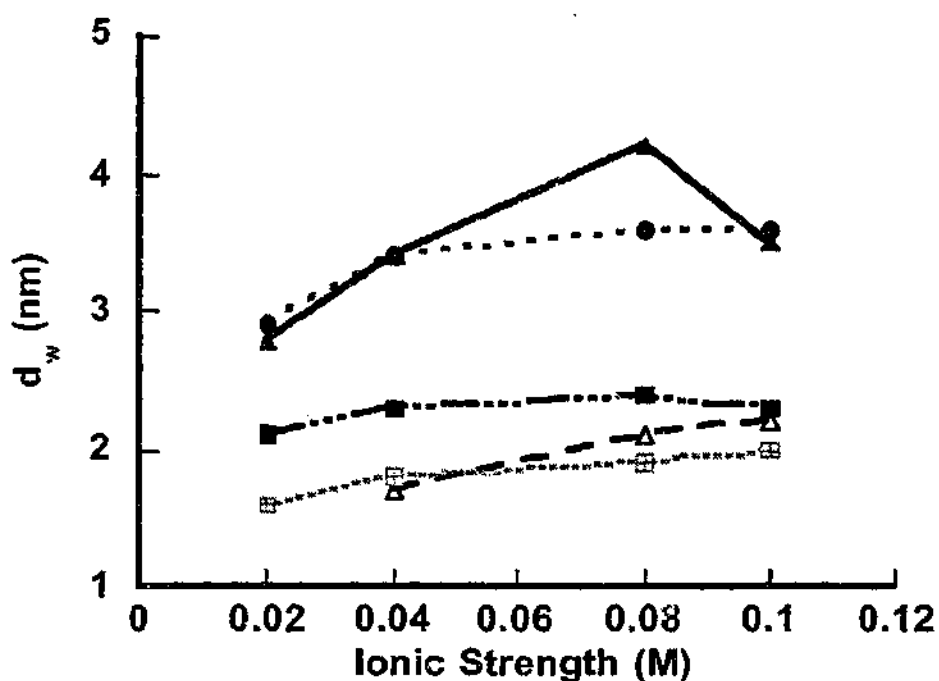


Figure 6.4: Effect of the ionic strength on (a) d_n and (b) d_w of the humic samples (carrier TRIS buffer), pH = 7.9.

Schimpf *et al.* [15] have used FIFFF previously to study humic substances under different solution pH and salt concentrations (NaCl and CaCl₂). They observed a shift of the peak maxima towards the smaller size range, reduction in the peak area and bimodal peaks by decreasing the pH further to pH~3. The same effect was observed by addition of CaCl₂. However, addition of NaCl resulted in a slight increase in the hydrodynamic diameter of the samples.

Shimpf *et al.* [15] explained the reduction in the peak area and shift towards the lower size range by coiling of the humic substances and their penetration through the membrane. However, if large aggregates were formed, there is a strong possibility that they could have been adsorbed irreversibly onto the membrane under the applied field. Thus the residual peak observed could be due to the smaller, unadsorbed fraction. Schimpf *et al.* [15] reported observation of peaks after termination of the field, which is due to the release of material sticking to the membrane. They stated that since the peak observed after the termination of the field did not compensate for the sample loss, some of the molecules had been coiled and passed through the membrane. It should be noted that in the case of irreversible adsorption, the humic material may not be desorbed by the same carrier. A solution with higher pH (~9) and moderate salt concentrations may be required to recover all the sample.

Adsorption onto the membrane would be expected to be even more severe at pH ~3. Cellulose acetate membranes have an IEP of about 4 [19]. In solutions of lower pH the membrane would acquire a positive charge, resulting in adsorption of the negatively charged humic molecules. Therefore it is vital to set the pH of the solution to values well above the IEP of the membrane to eliminate this effect.

6.4 SIMULATION OF THE EFFECT OF PH ON CONFORMATION OF A MODEL FULVIC ACID

The subject of coiling and uncoiling of the humic substances as a result of the change in solution conditions is an important issue that has often led to confusion in the interpretation of experimental results. Different models have been proposed for shapes and conformations of humic substances.

Wershaw [20] has proposed that humic molecules consist of separate hydrophobic and hydrophilic parts. This amphiphilic structure results in the formation of membrane-like aggregates on mineral surfaces and micelle-like aggregates in the solution. Tombacz [21] suggests that humic substances are associations of relatively small molecules, which are held together by weak interaction forces. In this model the aggregation is explained by intramolecular coiling or shrinkage of the sponge-like expanded hydrodynamic units, followed by interparticle interactions.

The concept of contraction and expansion of humic substances in different solution conditions was suggested by Gosh and Schnitzer [22]. In their classic work a macromolecular conformation was suggested for humic substances based on surface pressure and viscosity measurements. Humic molecules were considered to be flexible linear colloids at low sample concentration, low pH and neutral salt concentrations. A spherocolloidal structure was proposed for high sample concentrations, very low solution pH values and high salt concentrations.

Another macromolecular model was proposed by Cameron, Swift and Hayes [23-25], where the humic molecules were modelled as long strands with charge distributed along

their lengths (Figure 6.5). In this model the humic molecule assumes a loose spheroidal shape, but cannot not fully open up. The molecule coils randomly with respect to time and space. This results in a molecule with a density, which is greatest at the centre and approaches zero at the outer limits of the sphere. Thus the molecule has a roughly spherical shape which its density and diameter change with change in solution conditions and pH. This model was used to explain the reduction in size of large humic molecules (in the μm range) by increasing the ionic strength or reducing the pH. The increase in the concentration of cations and the decrease in pH both can result in a reduction of the electrostatic charge (Figure 6.5).

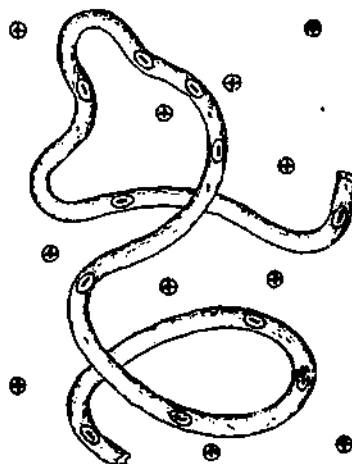


Figure 6.5: A model polyelectrolyte structure proposed for humic substance (Figure from Ref. [25])

The structures proposed for humic substances are usually different to the model given in Figure 6.5. (see Appendix 1). Humic structures appear to be more rigid and sometimes cross-linked rather than a long flexible backbone with attached functional groups.

Whenever it is possible to measure the size or MW of the humic samples in low concentrations (FCS, recent SEC results and FIFFF), it is usually found that humic

substances consist of small molecules. The sizes measured for humic substances in conditions of moderate pH and ionic strength, are mainly about 1-4 nm in hydrodynamic diameter [26-28]. The diameter of the humic substances obtained from potentiometric titrations of the humic substances are in the same range. (0.5-2.2 nm) [29].

deWit *et al.*[30] have indicated that a random coil structure is not very likely for the low MW humic substances and that the statistics for the formation of a random coil only apply to linear polyelectrolytes with at least one hundred statistical segments. A statistical segment itself contains several ordinary segments (Figure 6.6). As a result, the low MW humic substances will only consist of a very limited number of statistical segments.

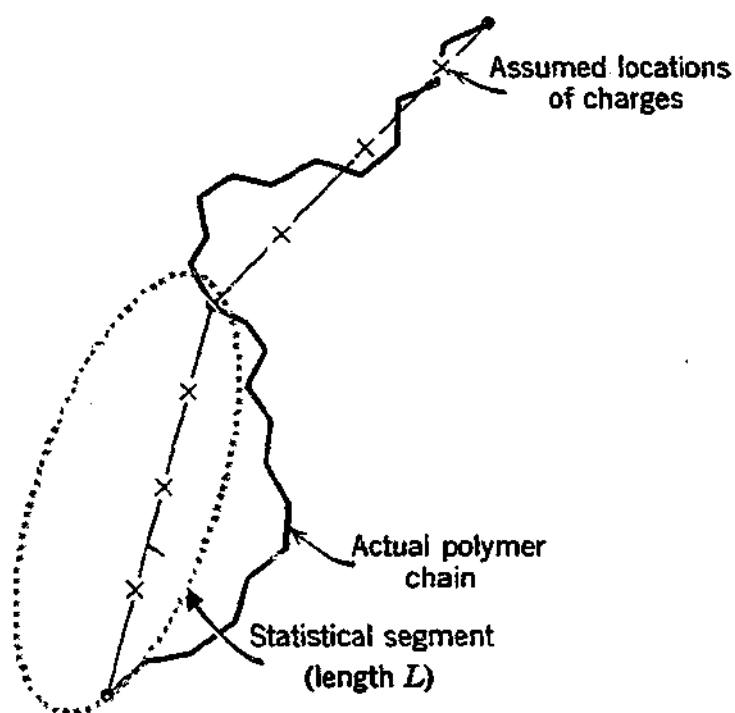


Figure 6.6: Two adjacent statistical segments of a chain with three charges per segment (Figure from Ref.[33])

Computer simulation was used to study the effect of solution pH on the conformation of humic substances. For this purpose a model humic acid was chosen (Steelink model,

Figure 6.7). The proposed structure has seven chiral centres, which compute to 64 different isomers. All the 64 isomers have been generated by Sein *et al* [31], and the isomer RSSRSSR, illustrated in Figure 6.7, was identified as the one with the minimum energy.

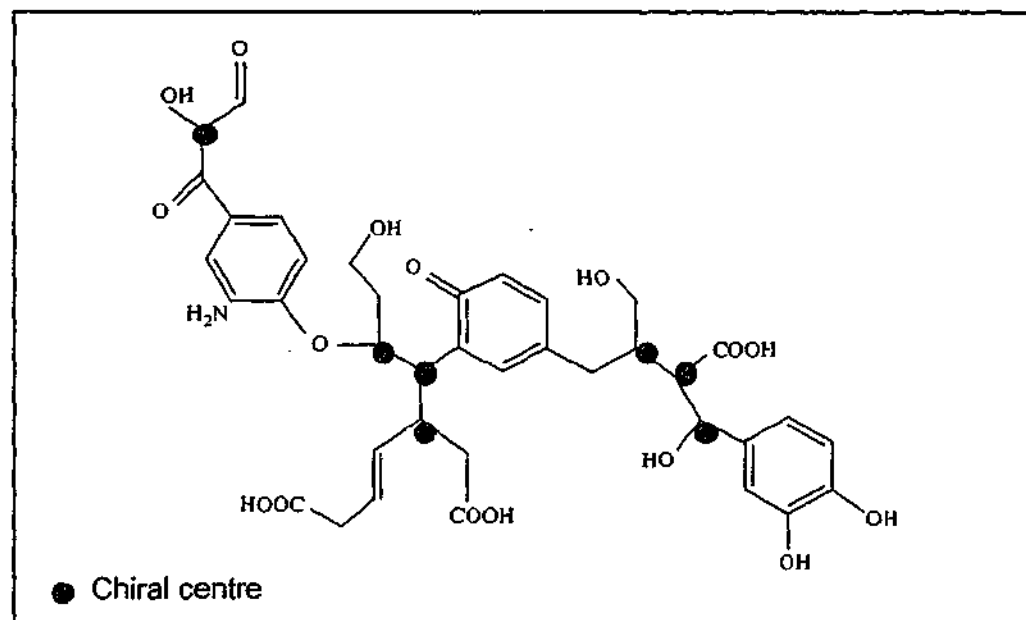


Figure 6.7: Steelink humic acid structure (Figure adapted from Ref.[31]).

The program INSIGHTII (MS1 ([32])) was used to generate the minimised energy structure for isomer RSSRSSR in a vacuum. The generated model is presented in Figure 6.8. This model represents the molecule where all the functional groups maintain their charges and can therefore be regarded to exist in the neutral state. The maximum end to end distance for this molecule is measured as 1.5 nm.

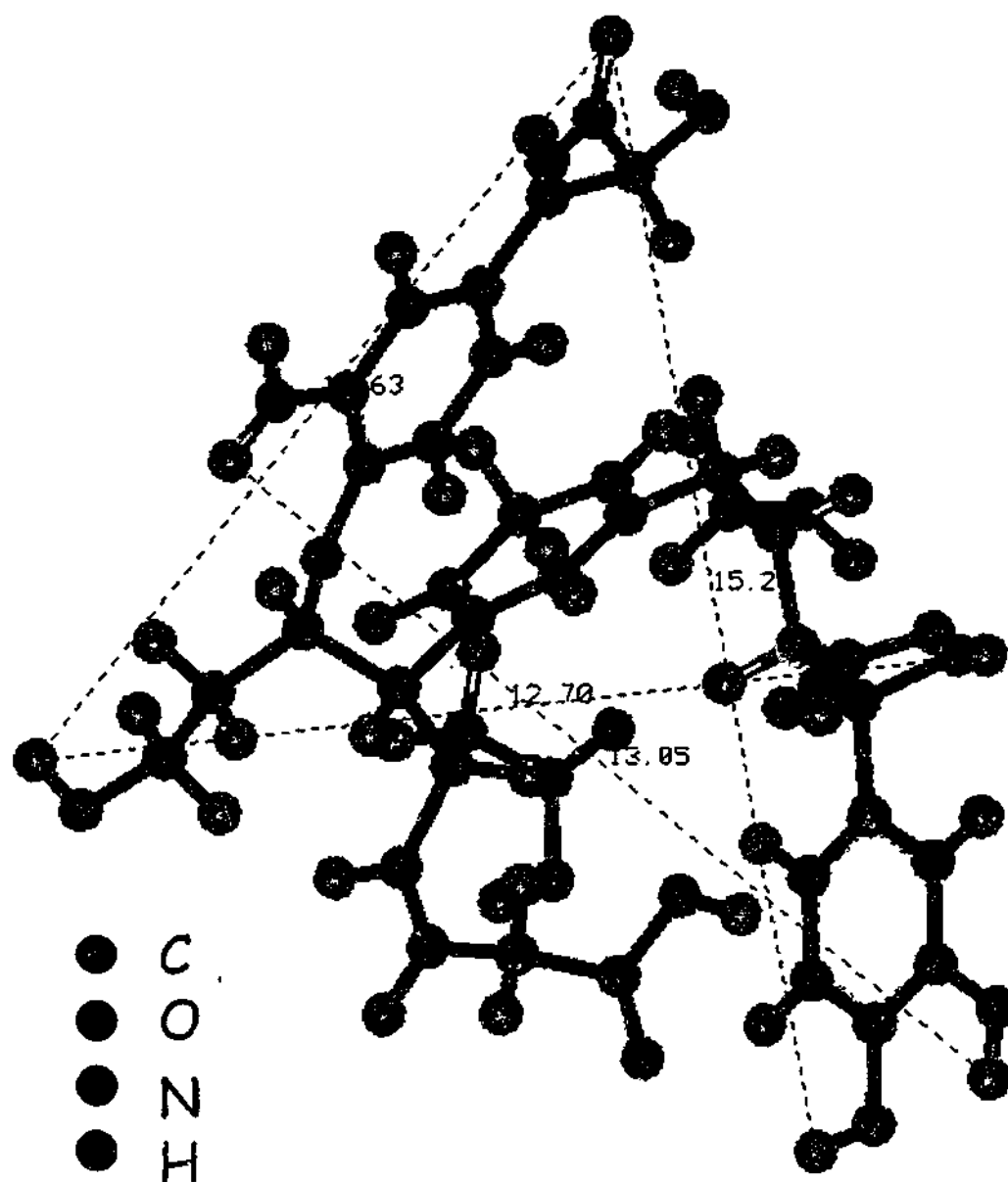


Figure 6:8: Simulation of Stealink structure in a vacuum. No charge effects are considered. Maximum end to end distance: 1.5 nm (end to end distances on the figure are given in Å°).

In order to simulate the basic solution conditions the hydrogen atoms on the carboxylic groups were removed, which corresponds to a pH range of ~8. This resulted in a maximum end to end distance of about 1.4 nm for this molecule (Figure 6.9), which shows a minor reduction when compared to the neutral molecule (Figure 6.8).

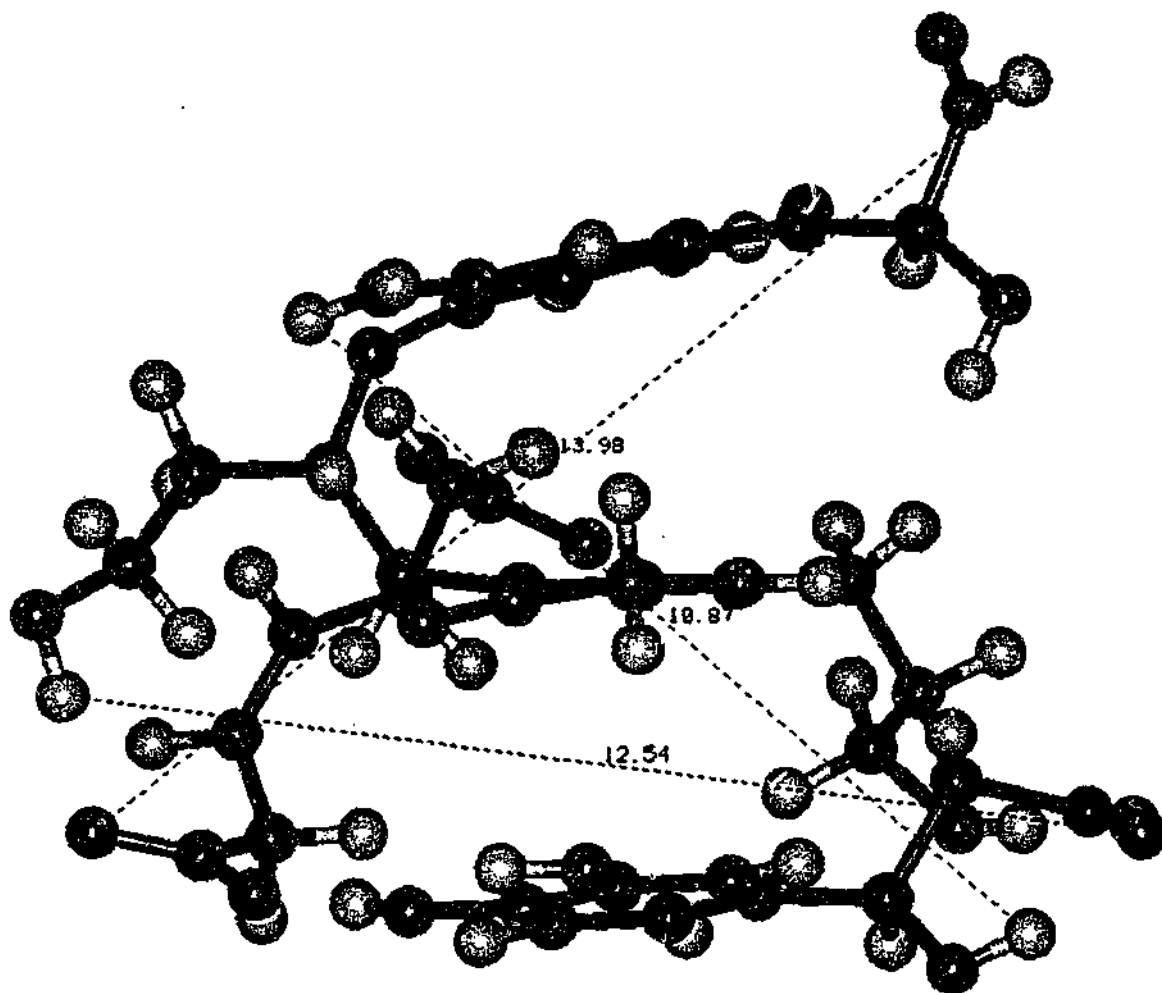


Figure 6.9: Simulation of Steelink structure in a vacuum with a hydrogen removed from each carboxyl groups. Maximum end to end distance: 1.4 nm (end to end distances in the figure are given in Å°).

When all the OH and COOH groups are charged, corresponding to a pH of about 10, the molecule opens up as a result of charge repulsion and the maximum end to end distance increases to 2.2 nm (Figure 6.10).

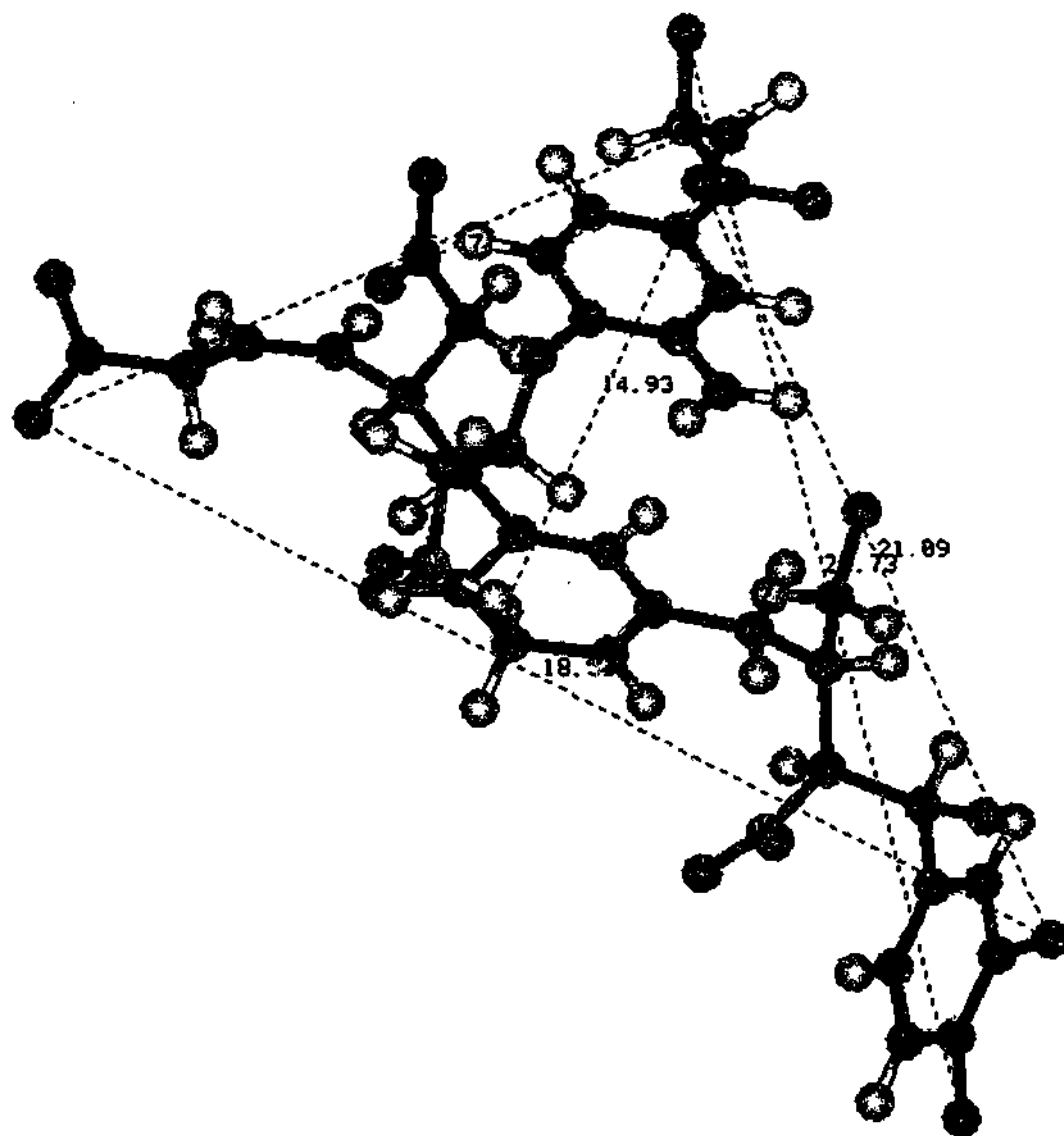


Figure 6.10: Simulation of Steelink structure in a vacuum. Hydrogen atoms on all the phenolic and carboxyl groups are removed. Maximum end to end distance: 2.2 nm (end to end distances on the figure are given in Å).

When a hydrogen atom from the amine group is also removed, corresponding to a pH of 13 and over, the molecule fully opens up and the maximum end to end distance increases to 2.4 nm (Figure 6.11).

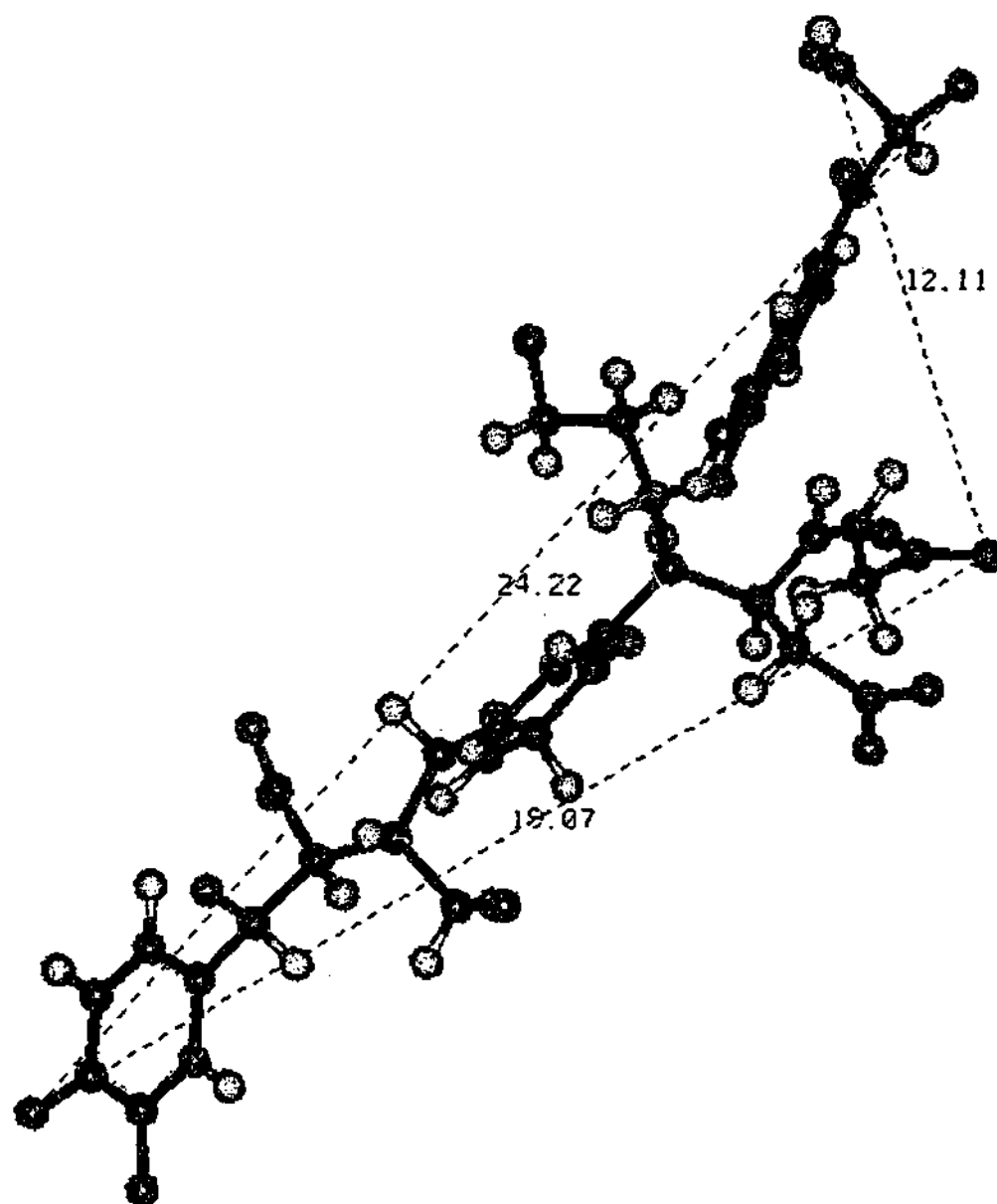


Figure 6.11: Simulation of Steelink structure in a vacuum. All the carboxyl, phenolic and amine groups are charged. Maximum end to end distance: 2.4 nm. (end to end distances on the figure are given in Å°)

In order to simulate the acidic situation the amine group was protonated, corresponding to a pH less than 4. The maximum end to end distance was found to be about 1.5 nm (Figure 6.12).

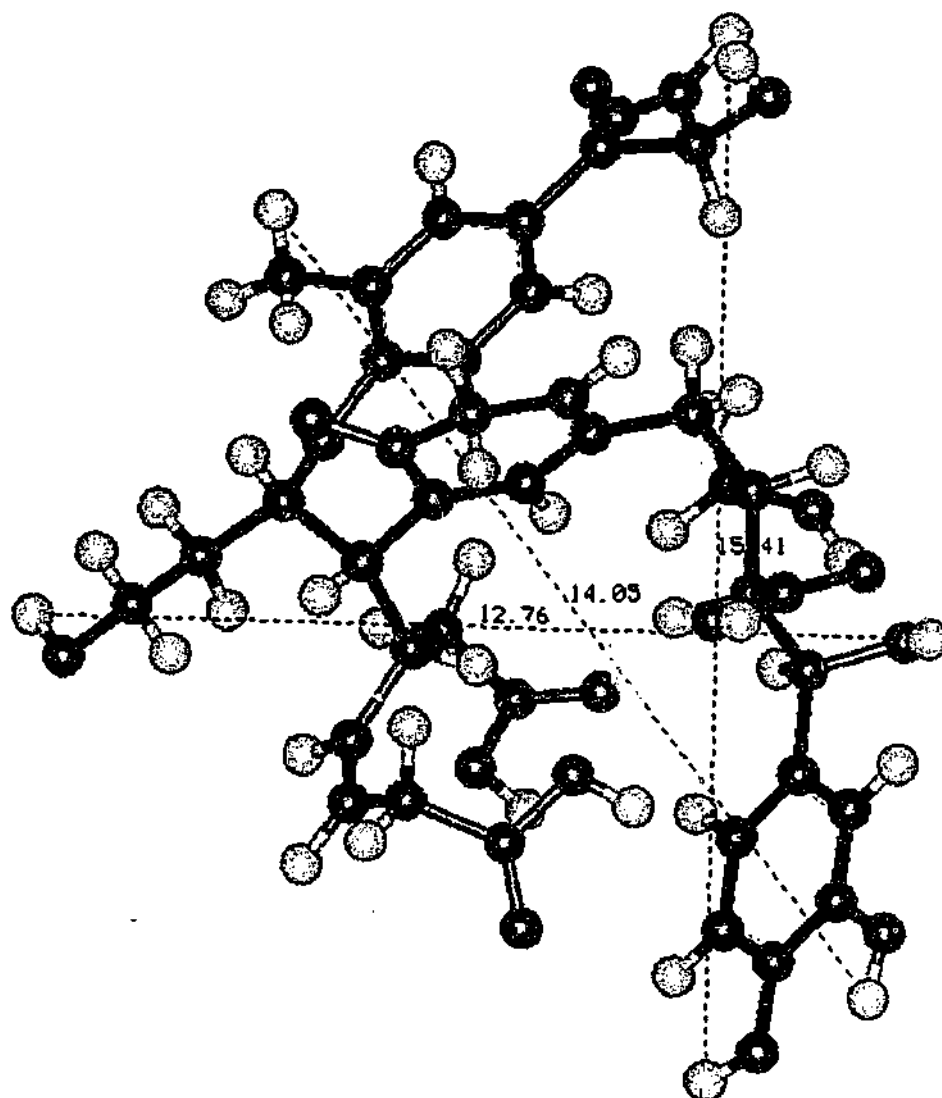


Figure 6.12: Simulation of Steelink structure in a vacuum with the amine group protonated. Maximum end to end distance: 1.5 nm (end to end distances on the figure are given in Å°).

The situation could be different in water because of the interactions that may occur between the humic molecule and the water molecules as well as the influence of the counter ions in the solution. However Sein *et al.* [31] reported that solvation of this structure did not result in a significant difference in the conformation. Only a slight rotation of the H-bonding functional groups towards the nearby water molecules was observed. The gross overall folding remained largely unaffected and there was no re-

The following should be read after the first paragraph in the conclusion section.

In conclusion it could be stated that the results obtained from FIFFF in this chapter are in contrast with predictions of the random coil model for the humic substances (page 127). A random coil model usually assumes a macromolecular state for humic substances and predicts coiling and reduction in size by increasing the ionic strength and decreasing the pH of the solution analogous to the behavior of a linear polyelectrolyte.

However, the results of this study demonstrate that under the experimental conditions used, the humic substances are rather small molecules and in fact associate and increase in size by increasing the ionic strength and decreasing the pH of the solution. The modeling exercise also shows that coiling is improbable in the pH range used. A linear polyelectrolyte, however, could undergo significant change in size by changing the solution conditions. For example data in the literature suggest that the size of sodium poly(styrenesulphonate) can change significantly (e.g. 1.5–3.5 times) by changing the ionic strength of the solution (2.5–10 times) [36,37].

The random coil model discussed in page 127 is based on a series of experiments performed by Cameron et al. [8] using GPC, UF and ultracentrifuge (UC) to produce fractions with low polydispersity and determine the radius of gyration of the fractions using UC.

When the f/f_{\min} (ratio of the frictional coefficient of the humic molecule to the frictional coefficient of a molecule with the same volume but having a condensed spherical conformation) for each fraction was plotted against the molecular weight, the slope of the line corresponded to " $0.3M^{0.167}$ ". For polyelectrolytes this slope could be an indication of conformation of either a random coil ($M^{0.167}$) or an oblate ellipsoid ($M^{0.165}$) [23].

Cameron et al. chose the former conformation. However within the experimental errors, it is very difficult to confirm either of the constants. Considering that the last three results have been excluded from the data fitting [23].

There is not enough experimental evidence to support the random coil model for now. Because of the complex nature of the humic substances, the experimental conditions can bias the results towards any judgement. Ultrafiltration has been commonly used to obtain fractions of humic substances and assign size or molecular weight to the fractions. These results should be handled with caution. It has been demonstrated in Chapter 5 that fractionation of the humic substances by ultrafiltration membranes results in fractions, which do not reflect the nominal size or MW of the membranes. TEM or SEM images of concentrated or precipitated humic substances show strands of fibers with sizes in the micron range, whereas experiments performed with FIFFF, High Pressure Size Exclusion Chromatography (HPSEC), Fluorescence Correlation Spectroscopy (FCS) and some titration experiments indicate a much lower size for humic substances in the range of a few nanometers (see Chapters 2 and 4).

Most of the models proposed for humic substances based on NMR and mass spectroscopy data show some degree of cross linking and are more likely to have an oblate shape rather than a long strand (see Appendix 1). However, to obtain a better understanding of the conformation of the humic substances it would be necessary to extend the range of experiments carried out in this chapter. In addition the effect of the concentration of humic substances and salt type on molecular conformation should also be examined. It would be useful if the membrane type and run conditions could be optimized to allow experiments to be performed at extreme values of solution pH and salt concentration.

ordering of the isomers in terms of energy. The solvation and re-ordering effects might be slightly different for other models (see Appendix 1).

This simulation on a model humic acid demonstrates that within the pH range of natural waters (6-8) and the pH range used in FIFFF experiments (6-9.2) there is minimal change in the conformation of the humic substances. Therefore, in the experimental conditions presented in this chapter the primary effect of decreasing pH could be the association and aggregation of the humic substances, which leads to an increase in size.

6.5 CONCLUSIONS

In this chapter FIFFF has been used to study the effect of solution pH and ionic strength on the hydrodynamic diameter of a range of humic samples. It was observed that increasing the ionic strength and decreasing the pH resulted in association of the humic molecules and an increase in the average hydrodynamic diameters (d_n and d_w) of the samples. Aggregation behaviour was different for humic substances from different origin (aquatic and terrestrial). This could be related to the isolation procedure, which involved treatment with a hydrophobic resin for Suwannee river humic and fulvic acid and Chaffey Reservoir fulvic acid. A computer simulation using a model humic acid was used to demonstrate that coiling is improbable because of the relative rigidity and small size of the humic molecules.

FIFFF has an advantage over other humic characterisation methods in that it can produce a distribution of size rather than an average value. However, it has limitations when high concentrations need to be used. Also, the experiments should be conducted in moderate

34. Newcombe, G., Drikas, M., Assemi, S., and Beckett, R., Influence of characterised natural organic material on activated carbon adsorption: 1. Characterisation of concentrated reservoir water, *Water Research*, 31(5) (1997) 965-972.
35. Ephraim, J.H., Pettersson, C., and Allard, B., Correlations between acidity and molecular size distributions of an aquatic fulvic acid, *Environment International*, 22(5) (1996) 475-483.
36. Mandel, M., Some properties of polyelectrolyte solutions and the scaling approach, in Masanori Hara (Ed.) *Polyelectrolytes: Science and Technology*, Marcel Dekker, Inc. New York. 1993, pp 1-75.
37. Cornel, P.K., Summers, R.S., and Roberts, P.V., Diffusion of humic acid in dilute aqueous solution, *Journal of Colloid and Interface Science*, 110 (1) (1986) 149-164.

conditions of ionic strength and pH. The use of a membrane to cover the accumulation wall introduces some charge into the channel, which may result in retention or repulsion of the samples.

6.6 REFERENCES

1. Schnitzer, M., and Khan, S.U., *Humic Substances in the Environment.*, Dekker, New York, 1972 .
2. Leppard, G.G., Buffle, J., and Baudat, R., A description of the aggregation properties of aquatic pedogenic fulvic acids, *Water Research*, 20 (1986) 185-196.
3. Tipping, E., and Ohnstad, M., Aggregation of aquatic humic substances, *Chemical Geology*, 44 (1984) 349-357.
4. Tombacz, E., and Meleg, E., A Theoretical explanation of the aggregation of humic Substances as a function of pH and electrolyte concentration, *Organic Geochemistry*, 15 (1990) 375-381.
5. Beckett, R., The composition and surface properties of suspended particulate matter, in B.T. Hart, (Ed.), *Water Quality Management: The role of particulate matter in the transport and fate of contaminants*, Chisholm Institute of Technology, Melbourne. 1986,. 113-142.
6. Schlautman, M.A., and Morgan, J.J., Effects of aqueous chemistry on the binding of polycyclic aromatic hydrocarbons by dissolved humic materials, *Environmental Science and Technology*, 27 (1993) 961-969.
7. Benedetti, M.F., Van Riemsdijk W. H. and Koopal L.K., Humic substances considered as a heterogenous Donnan gel phase, *Environmental Science and Technology*, 30 (1996) 1805-1813.

8. Wershaw, R.L., and Pinckney, D.J., Determination of the association and dissociation of humic acid fractions by small angle X-ray scattering, *Journal of Research U.S Geological Survey*, 1 (1973) 701-707.
9. Chen, Y., and M. Schnitzer., Viscosity measurements on soil humic substances, *Soil Science Society of America Journal*, 40 (1976) 866-872 .
10. Ghosh, K., and Schnitzer, M., Macromolecular structures of humic substances, *Soil Science*, 129 (1980) 266-276.
11. Chen, Y., and Schnitzer, M., Sizes and shapes of humic substances by electron microscopy, in M.H.B Hayes, MacCarthy, P., Malcolm, R.L., and Swift, R.S., (Eds.), *Humic Substances II, In Search of Structure*, John Wiley & Sons, Chichester, 1989, 621-638.
12. Chen, Y., Electron microscopy of soil structure and soil components, in P.M. Huang, Senesi, N., and Buffle, J., (Eds.), *Structure and surface reactions of soil particles*, John Wiley & Sons , Baffins Lane, 1998, 155-181.
13. Plashke, M., Romer, J., Klenze, R., and Kim, I.J., In situ AFM study of sorbed humic acid colloids at different pH, *Colloids and Surfaces A.*, 160 (1999) 269-279.
14. Balnois, E., Wilkinson, K. J., Lead, J.R., and Buffle, J., Atomic force microscopy of humic substances: effect of pH and ionic strength, *Environmental Science and Technology*, 33 (1999) 3911-3917.
15. Schimpf, M.E., and Petteys, M.P., Characterisation of humic materials by flow field-flow fractionation, *Colloids and Surfaces, A*, 120 (1997) 87-100.
16. Giddings, J.C., Benincasa A.M., Williams P.S., Rapid breakthrough measurement of void volume for flow field-flow fractionation channels, *Journal of Chromatography*, 627 (1992) 23-35.

17. Bowles, E.C., Antweiler, R.C., and MacCarthy, P., Acid-base titration and hydrolysis of fulvic acid from the Suwannee River, in Averett, R.C., Leenheer, J.A., McKnight, D.M., and Thorn, K.A., (Eds.), *Humic Substances in the Suwannee River, Georgia: Interactions, Properties, and Proposed Structures*, U.S. Geological Survey, Denver, 1995, 115-127.
18. Chen, Y., and M. Schnitzer., Scanning electron microscopy of a humic acid and of a fulvic acid and its metal and clay complexes., *Soil Science Society America Journal*, 40 (1976) 682-686 .
19. Childress, A.E., Elimelech, M., Effect of solution chemistry on the surface charge of polymeric reverse osmosis and nanofiltration membranes, *Journal of Membrane Science*, 119 (1996) 253-268.
20. Wershaw, R.L., Model for humus in soils and sediments, *Environmental Science and Technology*, 27 (1993) 814-816.
21. Tombacz, E., Colloidal properties of humic acids and spontaneous changes of their colloidal state under variable solution conditions, *Soil Science*, 164 (1999) 814-824.
22. Ghosh, K. and M. Schnitzer, Effects of pH and neutral electrolyte concentration on free radicals in humic substances, in *Soil Science Society of America Journal*, 44 (1980) 975-978.
23. Cameron, R., Thornton, B.K., Swift, R.S., and Posner, A.M., Molecular weight and shape of humic acids from sedimentation and diffusion measurements on fractionated extracts, *Journal of Soil Science*, 23 (1972) 394-408.
24. Hayes, M.H.B., and Swift, R.S., The chemistry of soil organic colloids, in D.J. Greenland, and Hayes, M.H.B., (Eds.), *The Chemistry of Soil Constituents*, Wiley and Sons, New York, 1978, 179-320.

25. Swift, R.S., Molecular weight, size, shape, and charge characteristics of humic substances: some basic considerations, in M.H.B. Hayes, MacCarthy, P., Malcolm, R.L., and Swift, R.S., (Eds), *Humic Substances II: In Search of Structure*, John Wiley&Sons, Chichester, 1989, 449-465 .
26. Beckett, R., Zhang J., and Giddings C., Determination of molecular weight distributions of fulvic and humic acids, using flow field-flow fractionation, *Environmental Science and Technology*, 21 (1987) 289-295 .
27. Dycus, P.J.M., Healy, K., Stearman, G.K., and Wells, M., Diffusion coefficients and molecular weight distributions of humic and fulvic acids determined by flow field-flow fractionation, *Separation Science and Technology*, 30 (1995) 1435-1453.
28. Chin, Y.P., and Gschwend, P.M., The abundance, distribution and configuration of porewater organic colloids in recent sediments, *Geochimica et Cosmochimica Acta*, 55 (1991) 1309-1317.
29. Barak, P., and Chen, Y., Equivalent radii of humic macromolecules from acid-base titrations, *Soil Science*, 154 (1992) 184-195.
30. de Wit, J.C.M., van Riemsdijk W.H., and Koopal L.K., Proton binding to humic substances 1. Electrostatic effects, *Environmental Science and Technology*, 27 (1993) 2005-2022.
31. Sein, L.T., Varnum, J.M., and Jansen, S.A, Conformational modelling of a new building block of humic acid: Approaches to the lowest energy conformer, *Environmental Science and Technology*, 33 (1999) 546-552.
32. MS1, InsightII (Discover minimisation module using CUFF forcefield), San Diego CA, USA.
33. Tanford, C, *Physical Chemistry of Macromolecules*. John Wiley & Sons, New York, 1967.

CHAPTER 7

ADSORPTION OF SUWANNEE RIVER FULVIC ACID ON GOETHITE, STUDIED BY DIRECT FORCE MEASUREMENT IN ATOMIC FORCE MICROSCOPY

7.1 INTRODUCTION

One of the major roles of humic substances in aquatic systems is the modification of surface charge of suspended particulate matter by imparting a negative charge to their surfaces [1-4]. This modification of the surface properties of minerals influences important phenomena, such as colloidal stability and contaminant adsorption. For this reason, humic coated model particles, such as goethite, have been used as surrogates for natural particles in laboratory studies [1, 2, 5].

Atomic force microscopy (AFM) is a relatively new technique [6] that can provide information on the structure of the interfaces and on intermolecular forces. It has a sub-

nanometer vertical resolution and can provide three dimensional images. The experiments can be carried out in solution, air or vacuum. AFM has been applied in imaging humic substances since 1996 [7-12].

One major feature of AFM that has not yet been used in the study of humic substances is its ability to measure the forces between the AFM tip and the sample surface. The force versus distance curves can provide valuable information on the interactive forces of humic substances.

Muscovite mica is often used as substrate in AFM experiments because of its exceptional smoothness. However, the surface of mica acquires a significant negative charge in aqueous solution, which means that the similarly charged humic substances adsorb only weakly to the surface. This weak affinity results in imaging artifacts due to the AFM tip dragging sample material across the surface [11]. A solution to this problem is the modification of the substrate surface so that it can retain humic substances in aqueous environments. Such a modified substrate would make it possible to image the humic substances in different solution conditions more representative of natural aquatic systems.

This chapter has focused on the development of a goethite surface which can retain humic substances, especially at pH values below the IEP (pH~7), and which represents a suitable model for the surface of certain aquatic colloids. Surface force measurements between a spherical silica colloid probe and the goethite surface, with and without the presence of Suwannee River fulvic acid (SRFA), have been used to characterize the surface chemical properties of both the coated and uncoated goethite surface. This data can provide an estimate of the thickness of the adsorbed fulvic acid layer.

7.2 ATOMIC FORCE MICROSCOPY (AFM)

Atomic Force microscopy (AFM), also known as scanning force microscopy (SFM), is a powerful technique for imaging mineral surfaces in air or in solution, at sub-nanometer resolution. The technique was developed in 1985 by Binnings, Gerber and Quate [6]. The basic principle of AFM is that a flexible cantilever with a very low spring constant induces forces smaller than inter-atomic forces to the sample, so that its topography could be measured without displacing the sample atoms (Figure 7.1).

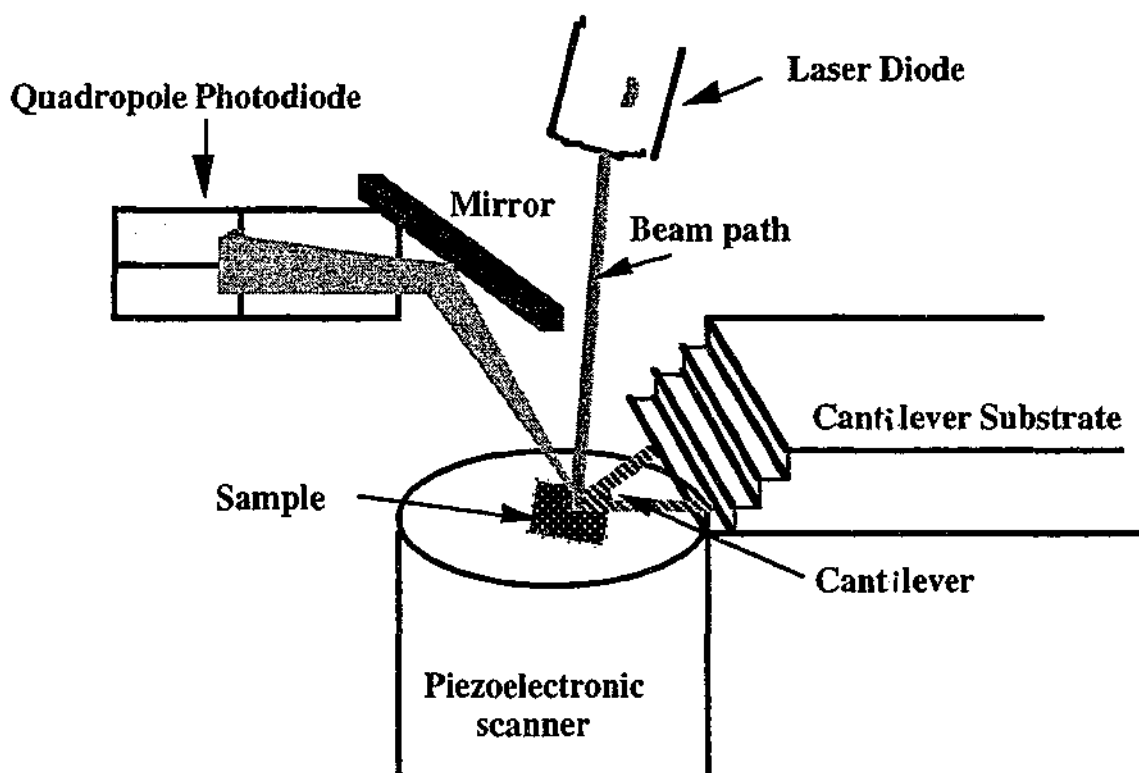


Figure 7.1: Schematic diagram of the optical scanning system in AFM (Adapted from Nanoscope III manual -Digital Instruments, Santa Barbara, CA).

In practice the sample surface is raster scanned under a sharp tip attached to a cantilever and the deflection of the cantilever is monitored, usually by laser deflection. A topography of the surface can be reproduced in this way. Both electrically conducting and

non-conducting samples can be imaged by AFM. The imaging can be performed in three different modes: Contact mode, Non-contact mode and Tapping mode™.

7.2.1 CONTACT MODE

In this mode the tip contacts the sample that is raster scanned underneath the cantilever tip. The path of the laser beam monitors any change in the deflection of the cantilever resulting from the undulations in the surface topography. This is recorded by a change in output from the photodiode. A feedback loop is used to keep the deflection of the cantilever constant by moving the sample vertically.

7.2.2 NON-CONTACT MODE (CONSTANT HEIGHT MODE)

In the non-contact mode, the tip does not contact the sample. The tip is scanned over the sample surface while the Van der Waals forces between the sample and the tip are sensed. The cantilever is vibrated and brought near the sample surface. The force gradient due to the interaction between the tip and the sample surface then modifies the spring constant of the cantilever and changes its resonant frequency. The shift in the cantilever's resonant frequency changes the cantilever's response to the vibration source. The control system maps the sample surface by adjusting the piezo height to maintain a constant vibration amplitude. Some problems are associated with the non-contact mode. The most important of which are the very low resolution because the lateral resolution is determined by sample-tip distance and the trapping of the tip in the adsorbed water layer.

7.2.3 TAPPING MODE™

In Tapping mode™ (Digital Instruments), also known as Intermittent Contact mode (IC-AFM), the scanning tip lightly taps the surface. A feedback loop maintains the oscillatory amplitude and the vertical displacement is recorded. The tips are stiffer than the contact mode and result in larger resonant frequencies and force constants. As a result the tip can overcome the "trapping" in the adsorbed water layer. The lateral resolution is defined by the tip shape and is comparable to that of the contact mode. The three modes of AFM are illustrated in Figure 7.2:

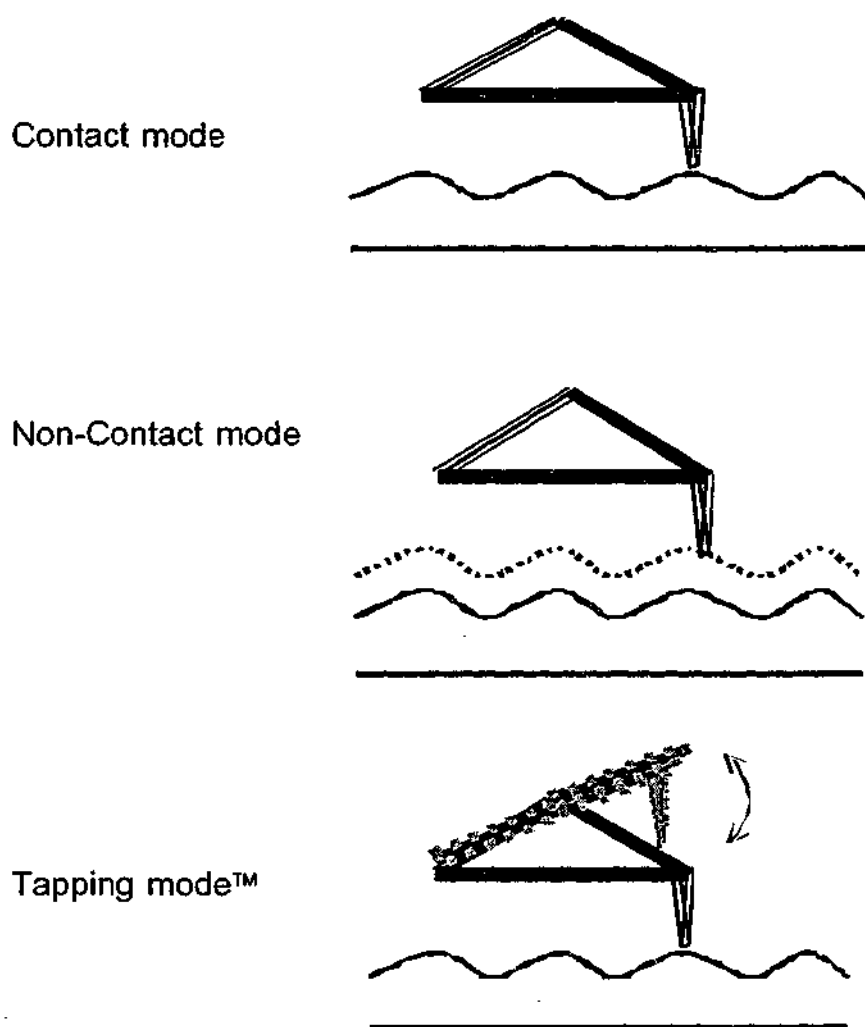


Figure 7.2: Illustration of the operating modes of AFM.

7.2.4 FORCE MEASUREMENT

AFM can be used to measure the forces between the tip and the sample surface from the cantilever deflection in contact mode AFM. A force versus distance curve is a plot of the deflection of the cantilever versus relative tip-surface separation. The cantilever has a spring constant k , and moves in accordance with the forces acting on its tip. A detector measures the cantilever's position, which can then be used to determine the force (F) on the tip by using Hooke's law:

$$F = kz \quad (7.1)$$

where z is the cantilever displacement.

MODIFICATION OF THE TIP FOR FORCE MEASUREMENTS:

In 1991 Ducker *et al.* [13, 14] were able to measure the forces in solution between planar mica and a silica sphere attached to the AFM tip. The same approach has been used in this study to measure the forces between a silica probe and a fulvic acid sample.

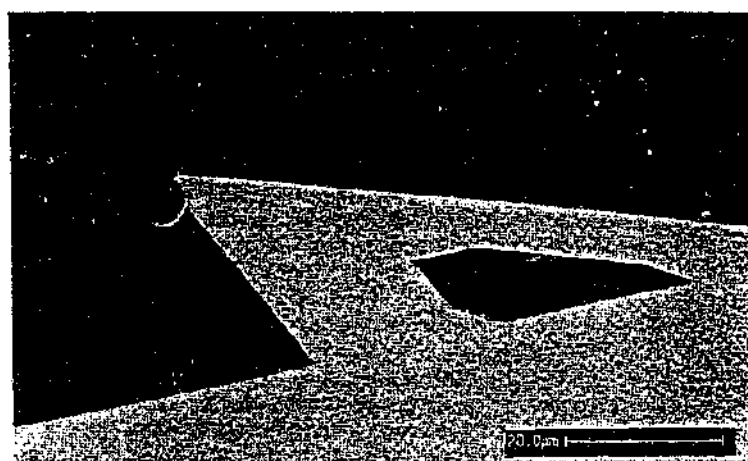


Figure 7.3: A silica sphere glued to an AFM cantilever tip (Figure from Ref. [13])

JUMP INTO CONTACT

At sufficiently small separations between the colloid probe and the sample, van der Waals attractive forces overcome electrostatic repulsive forces. In such a condition the two surfaces can jump together [15]. At this point the gradient of the attractive force between the probe and the surface exceeds the spring constant of the cantilever. In a force versus separation curve the jump can be observed by a sudden change in the force direction, from repulsion into attraction, and then repulsion as the tip is withdrawn from the surface (Figure 7.4).

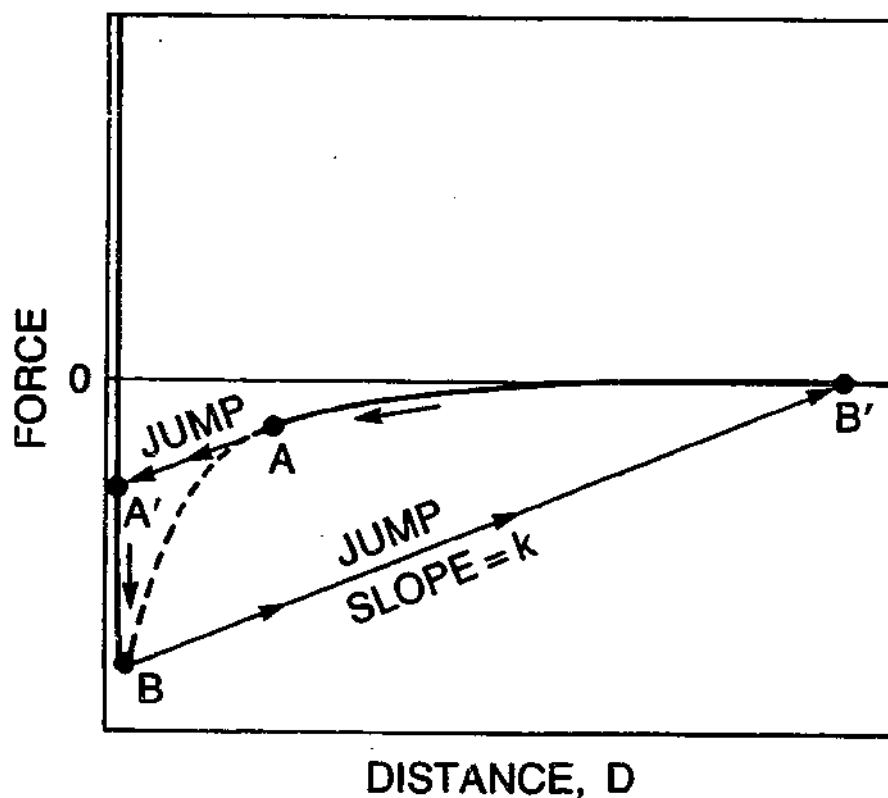


Figure 7.4: Illustration of "jump into contact" in a force versus probe-surface separation (Figure from Ref.[15])

7.3 EXPERIMENTAL

Solutions of different concentrations of Suwannee River fulvic acid (SRFA) were prepared using deionized water (Milli Q, Millipore). The pH was adjusted to ~6 by addition of NaOH. All glassware used in experiments was initially cleaned by soaking in 10% nitric acid and then subjected to ultrasonication for at least 1 hour in a 1% RBS / 20% ethanol solution. RBS-35 (Pierce Chemicals) is a commercial cleaning preparation consisting of a basic solution of anionic and non-ionic surfactants. The cleaned glassware was then rinsed with copious quantities of deionized water, prior to drying in a laminar flow clean air cabinet. The TEFLON® containers used in coating experiments were cleaned by soaking in 10% HCl overnight, followed by the procedure explained above.

Water used was obtained from a Milli-Q filtration system. Measured resistivity was not below 18.2 M Ω cm in any of the experiments. Other reagents were AR grade and used without further purification.

7.3.1 ATOMIC FORCE MICROSCOPY MEASUREMENTS

Atomic force microscope measurements were performed on a Digital Instruments Nanoscope IIIa AFM (Santa Barbara, CA). The spring constants of the gold coated silicon nitride cantilevers used in the AFM force measurement experiments were determined by the method of Cleveland *et al.*[16] which relies on monitoring the shifts in resonance frequency as a function of known attached masses to the cantilevers.

Colloidal silica was obtained from Allied Signal, Illinois, and was attached to the apex of the standard silicon nitride (NP-S) AFM cantilevers for use in direct force measurements.

The size of the spheres typically ranged from 4-6 μm in diameter. The properties of this silica and its preparation for use in direct force measurements are described in detail by Hartley *et al.* [17].

7.3.2 PREPARATION OF GOETHITE COATED MICA SURFACE

100 mL of deionized water was placed in a closed Teflon® container and bubbled with nitrogen gas for 20 minutes. The pH was lowered to 3-3.5 using 0.1 M HNO_3 . A sheet of freshly cleaved mica was immersed in the solution and 0.1 M $\text{Fe}(\text{NO}_3)_3$ solution was added gradually to the solution at constant temperature (20°C) to reach a final preset concentration of $\text{Fe}(\text{NO}_3)_3$. The pH was kept constant by adding 1 M NaOH using an autotitrator (Radiometer). When the addition of $\text{Fe}(\text{NO}_3)_3$ was complete the container was heated at 60 °C in an oven for 24 hours to allow formation of goethite.

The mica sheet was removed and rinsed with deionized water several times. This experiment was carried out at different pH values and different concentrations of Fe^{3+} and the AFM images of the surfaces were obtained. The experiment resulting in 10^{-3} M final concentration of $\text{Fe}(\text{NO}_3)_3 \cdot 9\text{H}_2\text{O}$ at pH 4 was found to have complete surface coverage. Therefore, this concentration of $\text{Fe}(\text{NO}_3)_3 \cdot 9\text{H}_2\text{O}$ and a solution pH of 4 was chosen for all further experiments.

7.3.3 ADSORPTION OF SRFA ON GOETHITE SURFACES FOR AFM FORCE MEASUREMENTS

The adsorption of SRFA onto goethite surfaces for AFM force measurements was performed *in situ* in the AFM fluid cell. 100 ppm SRFA in water was injected into the fluid cell and force measurements performed immediately. In some experiments the system was subsequently flushed with SRFA free solution and analysed further.

7.4 RESULTS AND DISCUSSION

7.4.1 CHARACTERISATION OF THE GOETHITE COATED MICA SURFACE

Figure 7.5 (a) shows a $1\ \mu\text{m} \times 1\ \mu\text{m}$ Tapping mode™ AFM image of the goethite coated mica surface recorded in air. It appears as if the goethite is deposited on the mica plate as discrete particles or that surface nucleation and crystal growth occur. The particles are fairly homogeneous in size and are quite regular in shape. The coverage of the underlying mica surface by the goethite coating is complete, as demonstrated by lower resolution scans of larger areas of the surface (Figure 7.5 (b)). From the section analysis of a 300 nm scan size image (Figure 7.5 (c)), the size of the goethite particles which comprise the coating may be estimated. The vertical dimensions of the particles appear to be $\sim 10\ \text{nm}$, whilst the horizontal dimensions appear to be $\sim 50\ \text{nm}$. This disparity in the dimensions might reflect the tip convolution in the horizontal distance measurements, but the possibility that the particles are not in fact spherical cannot be ruled out.

Roughness calculations based on the $1\ \mu\text{m} \times 1\ \mu\text{m}$ scan size image produce an RMS value for the surface of $\sim 3\ \text{nm}$ (Figure 7.5(c)). This is considerably rougher than the underlying mica surface (RMS roughness typically $< 0.1\ \text{nm}$).

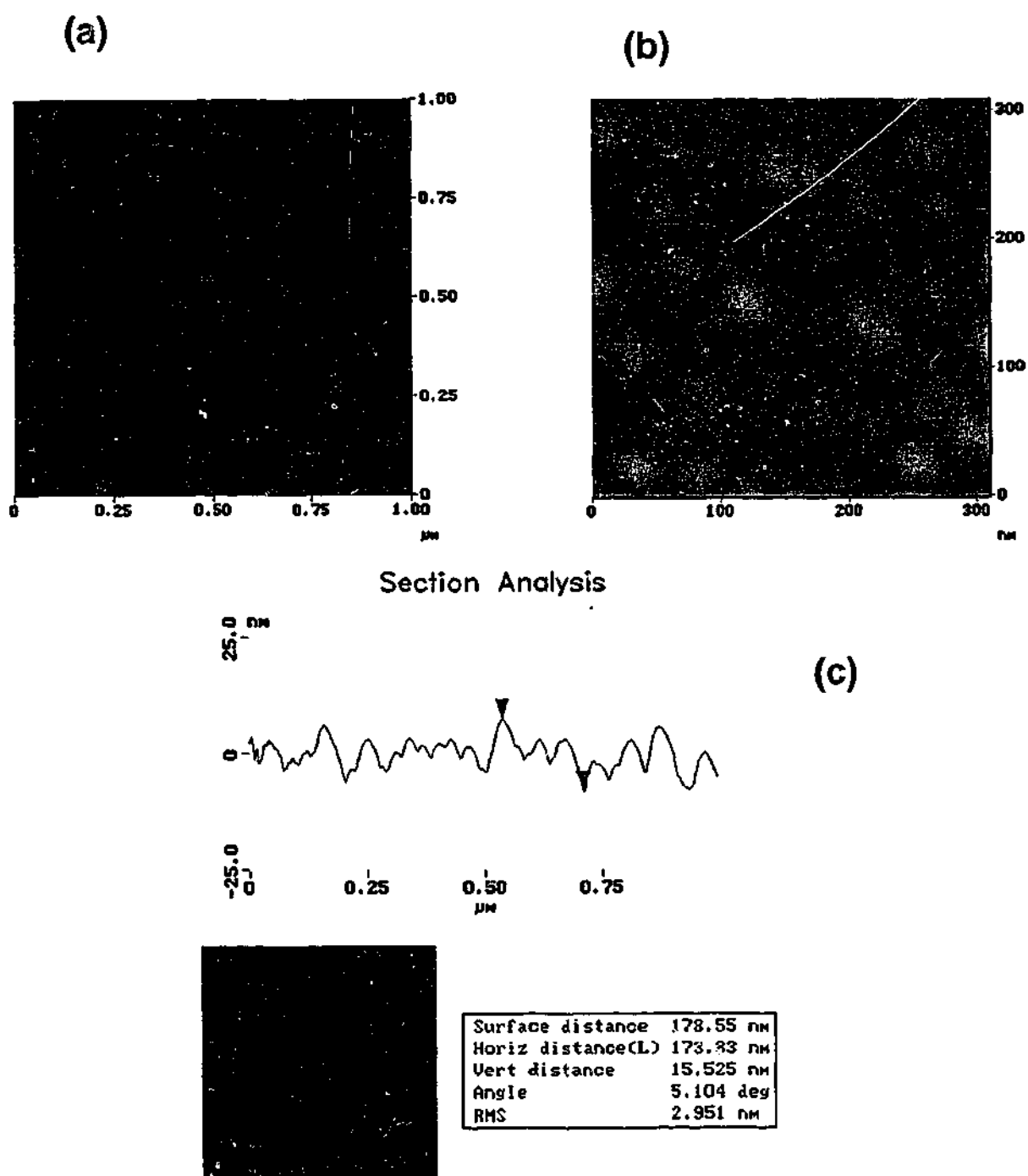


Figure 7.5: Tapping mode AFM image of the goethite coated mica surface. (a) scan size $1\ \mu\text{m} \times 1\ \mu\text{m}$, (b) scan size $300\ \text{nm} \times 300\ \text{nm}$ and (c) section analysis of the surface

Figure 7.6 shows data derived from AFM surface force measurements between a silica colloid probe and the goethite coated mica surface in solutions of different pH. Since the isoelectric point of the silica colloid probe attached to the AFM cantilever is below pH 3

[17], the probe is expected to carry a strongly negative surface charge at all the pH values shown in the figure. Thus, the AFM force measurements can give a direct indication of the surface charge of the goethite surface.

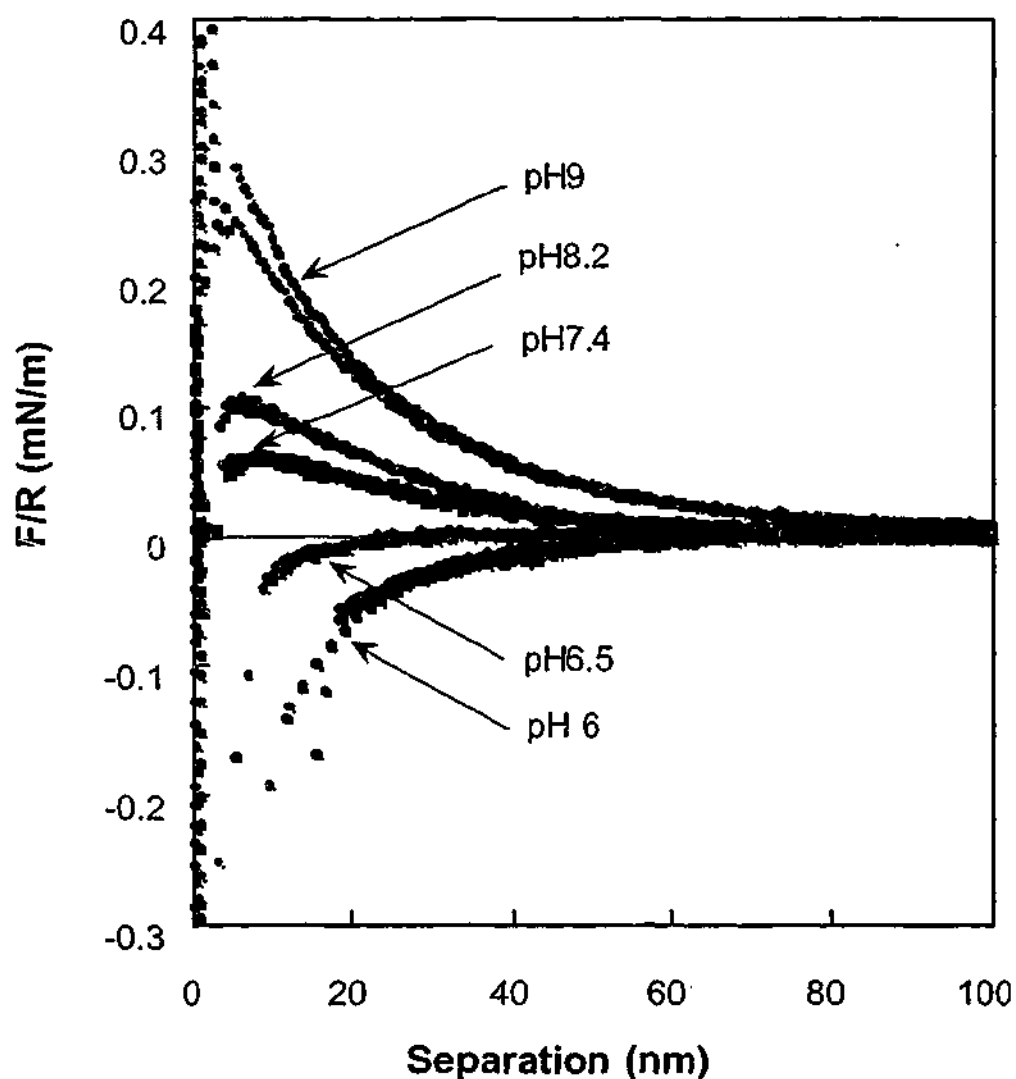


Figure 7.6: AFM force measurements between a silica colloid probe and goethite coated mica surface in different solution pH values.

As the data shows, at pH values greater than 7 a repulsive force dominates the interactions at surface separations greater than 10 nm. The decay length for these repulsions is found to be between 22 and 27 nm, which agrees well with the theoretical

Debye length of 30.5 nm for the simple 0.0001 M 1:1 electrolyte system studied here. These interactions may be attributed to an electrostatic repulsion operating between the silica and goethite surfaces, which indicates that the goethite surface is negatively charged at these pH values. Below pH 7.4, electrostatic attractive forces are observed, indicating that the goethite surface has reversed its surface charge, yielding a net positive surface. Thus, the isoelectric point of the goethite surface used in these studies might be deduced to be between pH 6.5 and 7.4. This is at the low end of the IEP range of 7-9.4 found for goethite using electrophoretic mobility measurements [2, 18], although synthetic goethite often has an IEP of around pH 7 [3, 19].

7.4.2 INCUBATION OF THE GOETHITE COATED MICA SURFACE IN 100 PPM SRFA

The impact of the introduction of fulvic acids on the surface forces between a silica colloid probe and the goethite surface is shown in Figure 7.7. The figure shows that after only a short period of incubation (~4 minutes) the interaction forces have been affected. After adsorption of SRFA there is a significant decrease in the decay length of interaction, indicating compression of the electrical double layer [13]. This would normally be the result of the addition of background electrolyte to the system. The conductivity of SRFA before freeze-drying has been reported as 50 μ S by the U.S Geological Survey[20].

A jump into contact, where short range van der Waals attractive forces dominate, can be observed in the uncoated goethite-silica interaction. Following addition of the SRFA, this jump is no longer apparent (Figures 7.7). Instead, a repulsive deviation from the curve expected for pure electrostatic interactions is observed. This suggests that an additional layer of fulvic acid is now present on one or both surfaces which masks the van der

Waals interaction by acting as a steric barrier. The effect of the adsorption of SRFA on the interactions between the silica and goethite surfaces is clearer following the removal of SRFA in solution by rinsing in SRFA free electrolyte at lower pH (pH 5.6, Figure 7.8). At this pH the non-SRFA treated silica and goethite interaction is purely attractive, since the goethite is positively charged and the silica negatively charged (see Figures 7.4 and 7.9).

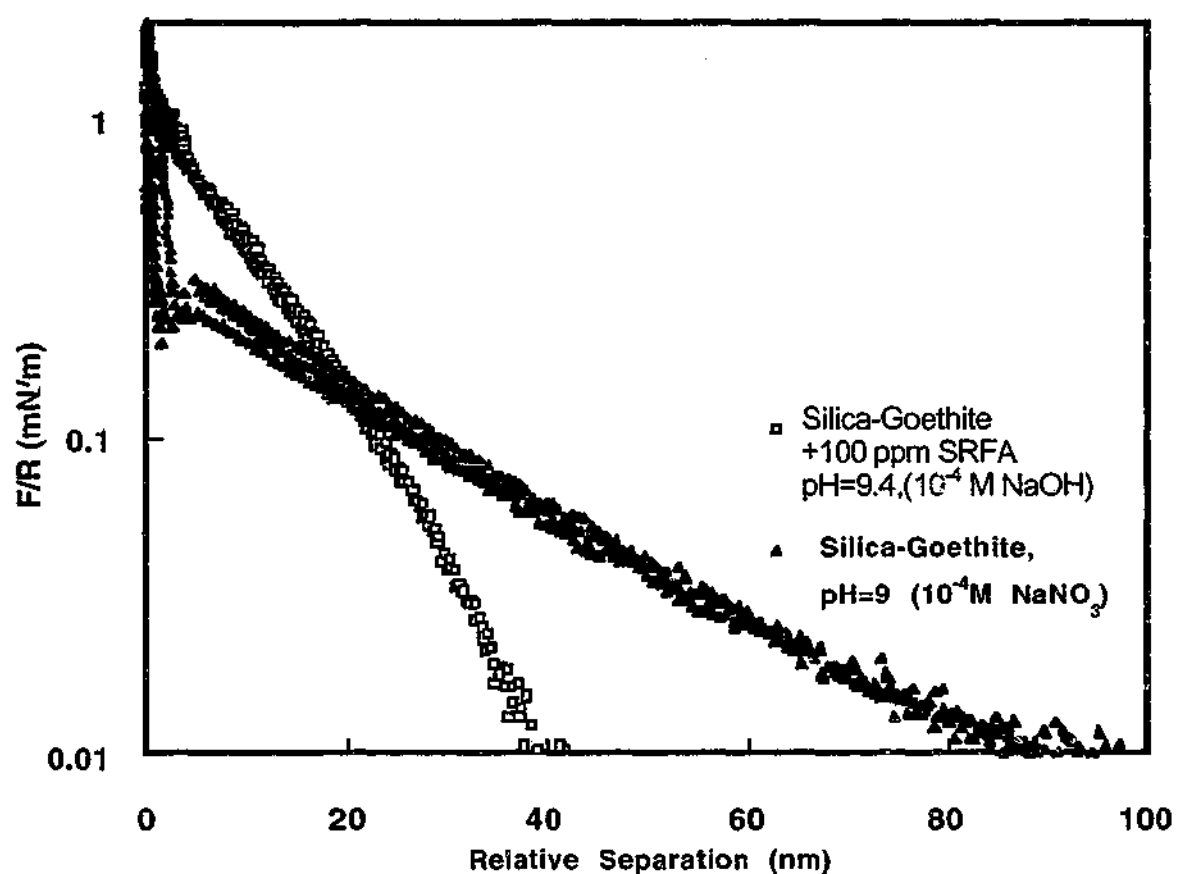


Figure 7.7: The effect of introduction of 100 ppm SRFA, on the electrostatic forces between the surface and the silica probe.

Incubation and subsequent removal of SRFA in solution, however, resulted in the interaction forces between the goethite surface and the silica probe becoming purely

repulsive. from both electrostatic and steric (electrosteric) interactions due to the negative charge and structure of the adsorbed SRFA layer.

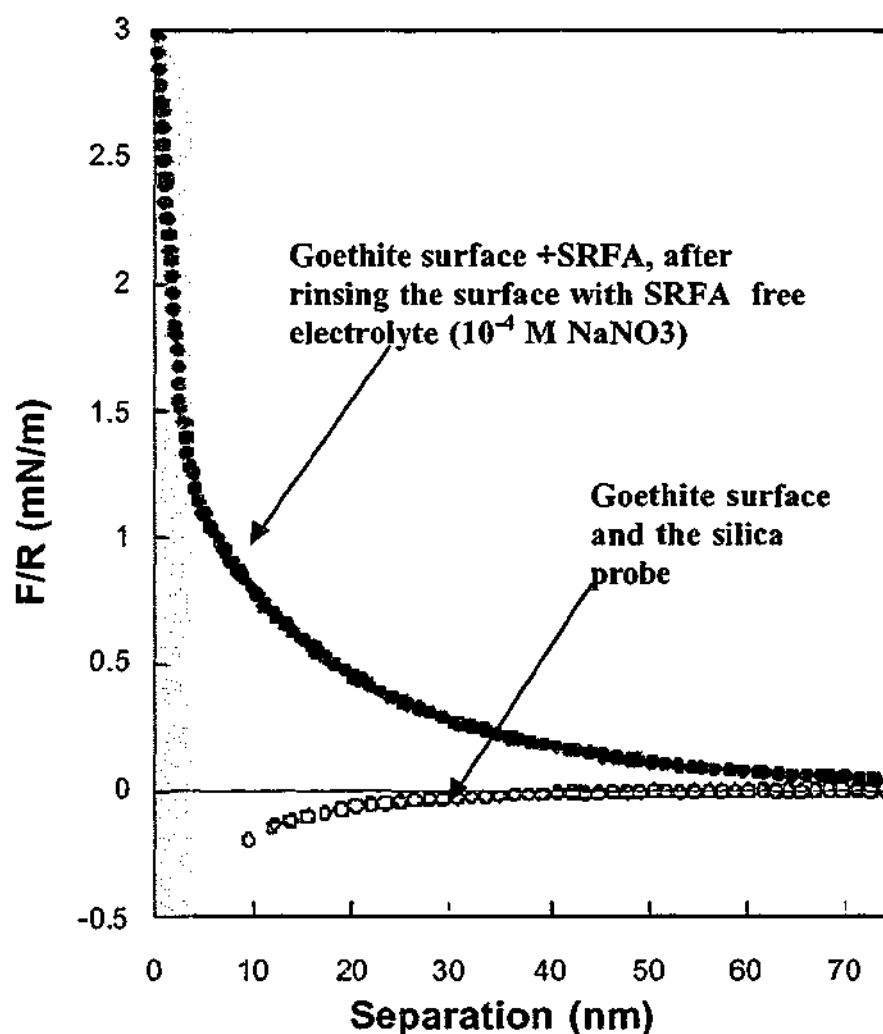


Figure 7.8: The electrostatic forces between the goethite surface and the silica probe as a result of introduction of SRFA at pH 5.6. The electrostatic repulsion in the absence of SRFA is replaced by attraction. The deviation from an exponential function at short separations suggest the presence of an steric layer in the repulsion case.

This, therefore, demonstrates that strong adsorption of SRFA onto goethite has occurred. Again, the presence of the steric layer is evidenced by deviation from a purely exponential

repulsion at short separations. The thickness of the steric barrier can be estimated at a minimum of ~ 5 nm. This thickness can be attributed to the adsorbed SRFA layer.

The interactions between the goethite coated surface with silica in the absence and presence of SRFA at $\text{pH} < 7$ are illustrated in figure 7.9:

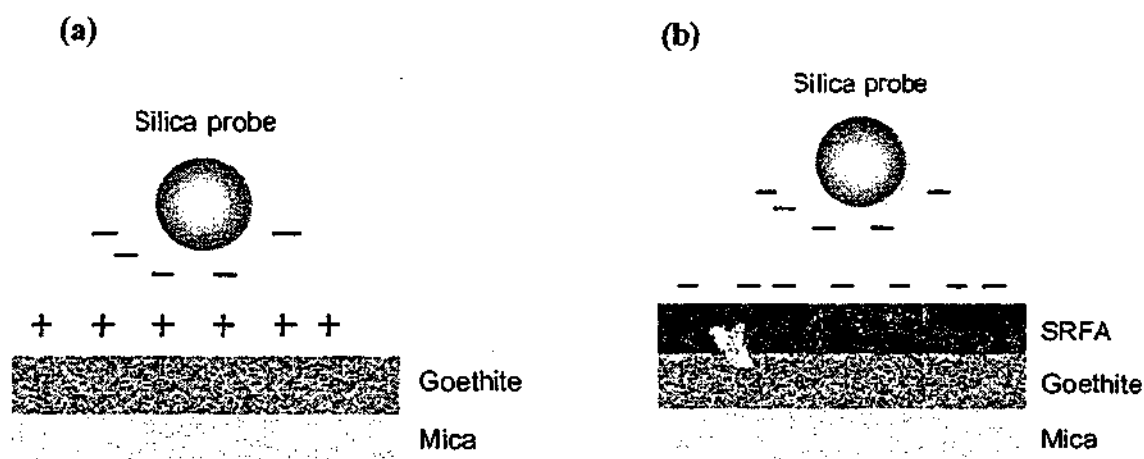


Figure 7.9: Illustration of the effect of introduction of SRFA on the interactions between goethite and the silica probe at pH below 7. (a) The goethite surface is positively charged and the silica probe is negatively charged ($\text{IEP} \sim \text{pH} 3$), resulting in attraction between the surfaces. (b) Coating goethite with SRFA, results in the surface being negatively charged and the electrostatic repulsion being the dominant force.

Figure 7.10 presents an initial attempt to gain insight into the kinetics of the SRFA adsorption process. At a relatively short incubation time (3 minutes) the "jump" to contact can still be observed. With further incubation, the "jump" disappears and the build up of a steric layer is observed. A concomitant increase in the magnitude of the exponential (electrostatic) repulsion may indicate a charging process on the surface as a result of the adsorption of SRFA. However, this may also be due to offsetting of the apparent zero separation from the true plane of charge position as a result of an increase in the thickness of the adsorbed layer.

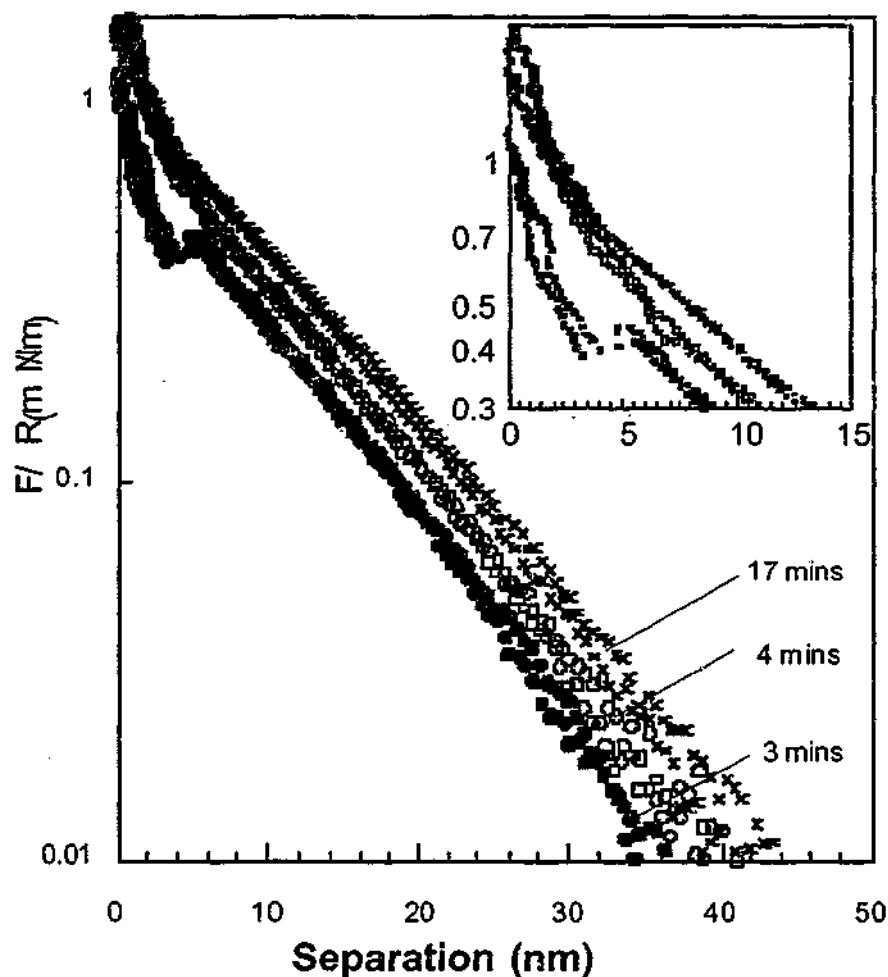


Figure 7.10: Effect of incubation time in 100 ppm SRFA on forces between silica probe and the goethite surface at pH 9.4.

7.4.3 IMAGE OF THE ADSORBED FULVIC ACID

The Tapping mode™ AFM image of the adsorbed fulvic acid on the goethite surface is given in Figure 7.11. The goethite structure can be seen underneath the partially filled adsorbed fulvic acid layer. This imaging has been done at pH 5.6 with the concentration of SRFA being about 100 ppm. The size of these adsorbed particles is about 4 nm when determined by FIFFF. This demonstrates that they are aggregates, either formed in solution, or during surface adsorption. The aggregation observed is probably due to the

low pH and high concentration of the fulvic acid, which is in agreement with other studies on SRFA using FIFFF (see Table 2.1, also chapters 4 and 5).

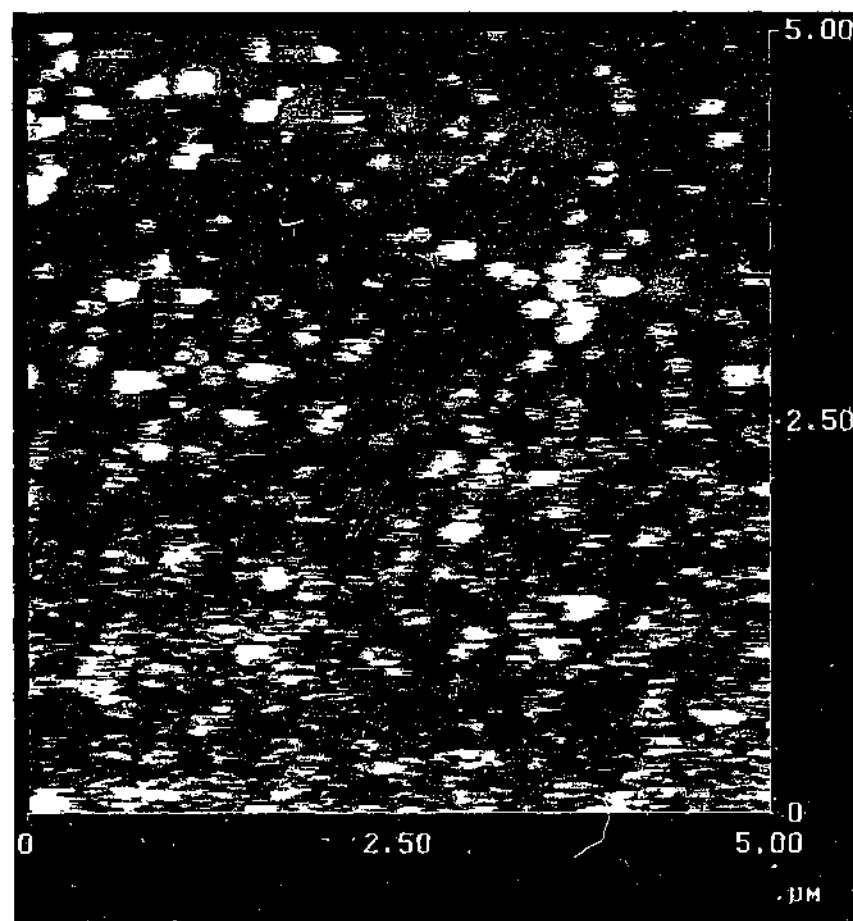


Figure 7.11: Tapping mode AFM image in fluid of SRFA adsorbed to the goethite coated mica surface. The goethite colloid is visible under the SRFA layer.

7.5 CONCLUSIONS

The aim of the study in this chapter was to use atomic force microscopy to obtain information about the size and charge characteristics of humic substances in solution and when adsorbed to surfaces. A goethite surface was developed for this purpose. Goethite has been used as a model environmental particle in earlier studies [1-3,5]. Humic substances can adsorb strongly to goethite and modify its charge. The extent of

adsorption increases with decreasing pH [2, 21]. This phenomenon has been used to explain the stability of suspended particulate matter in aquatic systems [5]. The goethite surface developed can be positive at pH values below its IEP (pH~7). The goethite surface is fairly smooth, but not as smooth as planar mica. Thus the smaller size HA or FA molecules will not be observed. On the other hand, because of its positive charge under pH=7, humic substances can easily be adsorbed to the surface. Sticking a silica sphere to the cantilever tip enabled the study of the effect of adsorption of SRFA on the goethite surface using force measurements.

The surface forces were radically altered by incubation in SRFA. This could be detected by the charge reversal of the surface before and after incubation in SRFA. The irreversible adsorption of SRFA on goethite could be detected when the surface remained negatively charged, even after washing with SRFA free electrolyte. The removal of "jump" into contact after incubation in SRFA indicated the presence of a steric layer of ~5 nm thickness. This steric layer can be attributed to the SRFA layer adsorbed on the goethite surface, assuming that no adsorption of SRFA has occurred on the tip.

This work shows the potential of a new and powerful method to obtain important information about the size and shape of humic substances in different solution conditions, as well as providing information about their interactive forces. The developed goethite surface can be useful in subsequent imaging studies.

7.6 REFERENCES

1. Hunter, K.A., Microelectrophoretic properties of natural surface-active organic matter in coastal seawater, *Limnology and Oceanography*, 25 (1980) 807-822.

2. Tipping, E., The adsorption of aquatic humic substances by iron oxides, *Geochimica et Cosmochimica Acta*, 45 (1981) 191-199.
3. Tipping, E., Adsorption by goethite (α -FeOOH) of humic substances from three different lakes, *Chemical Geology*, 33 (1981) 81-89.
4. Beckett, R., The composition and surface properties of suspended particulate matter, in B.T. Hart, (Ed.), *Water Quality Management: The role of particulate matter in the transport and fate of contaminants*, Chisholm Institute of Technology: Melbourne. 1986, 113-142 .
5. Beckett, R., and Le, N.P., The role of organic matter and ionic composition in determining the surface charge of suspended particles in natural waters, *Colloids and Surfaces*, 44 (1990) 35-49.
6. Binnings, G., Quate C.F. and Gerber, Ch., Atomic force microscope, *Physical Review Letters*, 56 (1986) 930-933.
7. Maurice, P.A., Applications of atomic force microscopy in environmental colloid and surface chemistry, *Colloids and Surfaces A: Physicochemical Engineering Aspects*, 107 (1996) 57-75.
8. Maurice, P.A., Scanning probe microscopy of environmental surfaces, in P.M. Huang, Senesi, N., and Buffle, J., (Eds.), *Structure and surface reactions of soil particles*, John Wiley & Sons, Baffins Lane, 1998, 109-153.
9. Maurice, P.A., and Namjesnik-Dejanovic, K, Aggregate structures of sorbed humic substances observed in aqueous solution., *Environmental Science & Technology*, 33 (1999) 1538-41 .
10. Widayati, S.a.T., K.H., Atomic force microscopy of humic acid, *Communications in Soil Science and Plant analysis*, 28 (1997) 189-196.

11. Plashke, M., Romer, J., Klenze, R., and Kim, I.J., In situ AFM study of sorbed humic acid colloids at different pH, *Colloids and Surfaces A*, 160 (1999) 269-279.
12. Lead, J.R., Balnois, M., Hosse, M., Menghetti, R., and Wilkinson, K.J., Characterization of Norwegian natural organic matter: size, diffusion coefficients, and electrophoretic mobilities, *Environment International*, 25 (1999) 245-258.
13. Ducker, W.A., Senden T.J, and Pashley R.M., Direct measurement of colloidal forces using an atomic force microscope, *Nature*, 353 (1991) 239-241.
14. Ducker, W.A., Senden, T.J., Pashley, R.M., Measurement of forces in liquids using a force microscope, *Langmuir*, 8 (1992) 1831-1836.
15. Burnham, N.A., and Colton, R.J., Force Microscopy, in D.A. Bonnel, (Ed.), *Scanning Tunneling Microscopy and Spectroscopy, Theory, Techniques and Applications*, VCH Publishers, Inc., New York, 1993, 191-249.
16. Cleveland, J.P., Manne, S., and Bocek, D., A nondestructive method for determining the spring constant of cantilevers for scanning force microscopy, *Review of Scientific Instruments*, 64 (1993) 403-405.
17. Hartley, P.G., Larson, I., Scales, P.J., Electrokinetic and direct force measurements between silica and mica surfaces in dilute electrolyte solutions, *Langmuir*, 13 (1997) 2207.
18. Hiemstra, T., and Van Riemsdijk, W.H., A surface structural approach to ion adsorption: The charge distribution (CD) model, *Journal of Colloid and Interface Science*, 179 (1996) 488-508.
19. Beckett, R., The surface chemistry of humic substances in aquatic systems. *Surface and Colloid Chemistry in* , R. Beckett (Ed.), *Natural Waters and Water Treatment* , Plenum Press, New York, 1990 .

20. Humic Substances in the Suwannee River, Georgia: Interactions, Properties, and Proposed Structures, Averett, R.C., Leeheer, J.A., McKnight, D.M., and Thorn, K.A (Eds.), Denver, 1995.
21. Day, G.M., Hart B., McKelvie, I.D., Beckett R., Adsorption of natural organic matter onto goethite, *Colloids and Surfaces A: Physicochemical and Engineering Aspects*, 89 (1994) 1-13.

CHAPTER 8

USE OF ^{31}P NMR IN INVESTIGATING THE BINDING OF ORTHOPHOSPHATE TO A HUMIC ACID

8.1 INTRODUCTION

Phosphorus is generally considered one of the limiting nutrients (with nitrogen) for primary producers in freshwater systems [1, 2]. Excess phosphorus from runoff, erosion or mineralisation can accelerate eutrophication and undesirable aquatic plant growth. Detrimental consequences of such plant proliferation can be a depletion of oxygen in the water column due to the heavy oxygen demand by microorganisms as they decompose the organic material. Also the decomposition of this plant material can result in undesirable color, odor and taste in drinking water.

Particulate phosphorus may accumulate in the sediments of lakes and streams where it may be recycled slowly or released more rapidly when the sediments are disturbed. One

of the parameters affecting dynamics of phosphorus in the environment is its interaction with the humic substances in soil, sediments and suspended particulate matter.

Interactions between humic substances and phosphorus compounds have been mainly attributed to bridging cations, such as Fe^{2+} and Al^{3+} [3-6]. The possibility of direct interactions have been excluded because humic substances and orthophosphate are considered to be negatively charged and are thus less likely to form a stable bond [6]. However, it is possible that orthophosphate can bind to the alcohol and carboxyl groups to form orthophosphate esters [7, 8]. This is the hypothesis to be tested in this study. A general scheme of the two possible ways that orthophosphate can bind to the humics is illustrated in Figure 8.1.

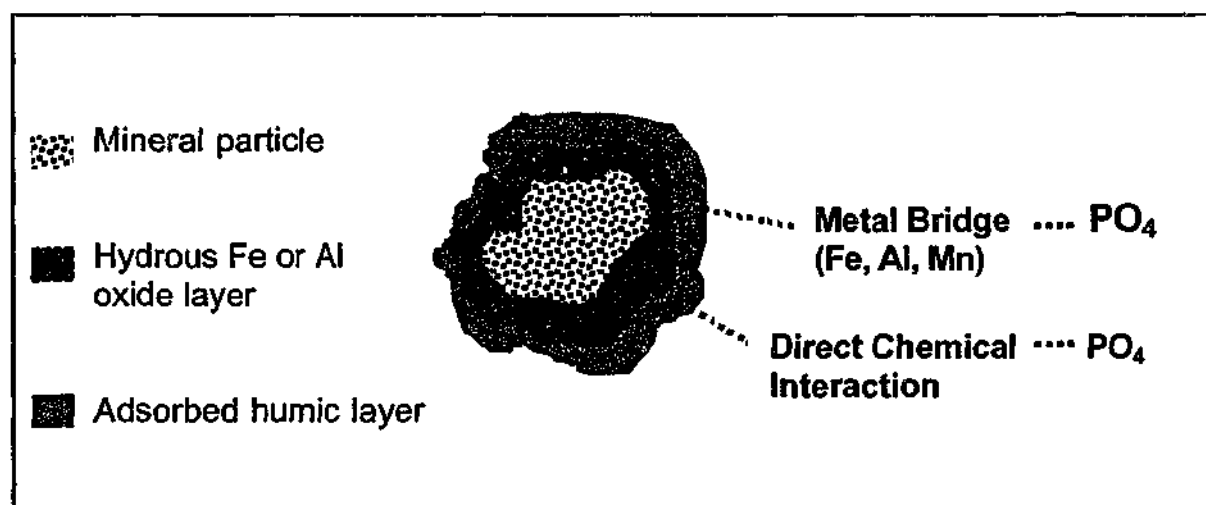


Figure 8.1: Schematic diagram illustrating the possible role of humic substances in binding orthophosphate.

These interactions are difficult to study by adsorption experiments, chiefly because both humic acid and orthophosphate are water soluble. NMR spectroscopy can be used for

this purpose because the chemical shift in NMR depends mainly on the chemical environment of the specific nuclei. In other words, any change in the chemistry of the sample will be reflected in the NMR spectrum of the species.

In this chapter the interactions between orthophosphate and a sediment humic acid have been studied using a combination of ^{13}C and ^{31}P NMR spectra before and after the addition of orthophosphate. The main objectives were to:

- explore whether there existed any direct interaction between orthophosphate and the humic acid used in this study
- identify the functional groups in the humic acid that were possibly involved in such binding
- study the effect of solution pH on the interaction.

8.1.1 PREVIOUS APPLICATION OF ^{31}P NMR TO HUMIC SUBSTANCES

^{31}P NMR can help identify a range of inorganic and organic phosphorus species in soil extracts and purified humic acids. These include: inorganic orthophosphate, orthophosphate monoesters, orthophosphate diesters and aromatic P-monoesters (which were observed more frequently in peat soils), prophosphates, phosphonates and polyphosphates [9-13]. A typical ^{31}P NMR spectrum of a humic acid with chemical shift assignments is illustrated in Figure 8.2.

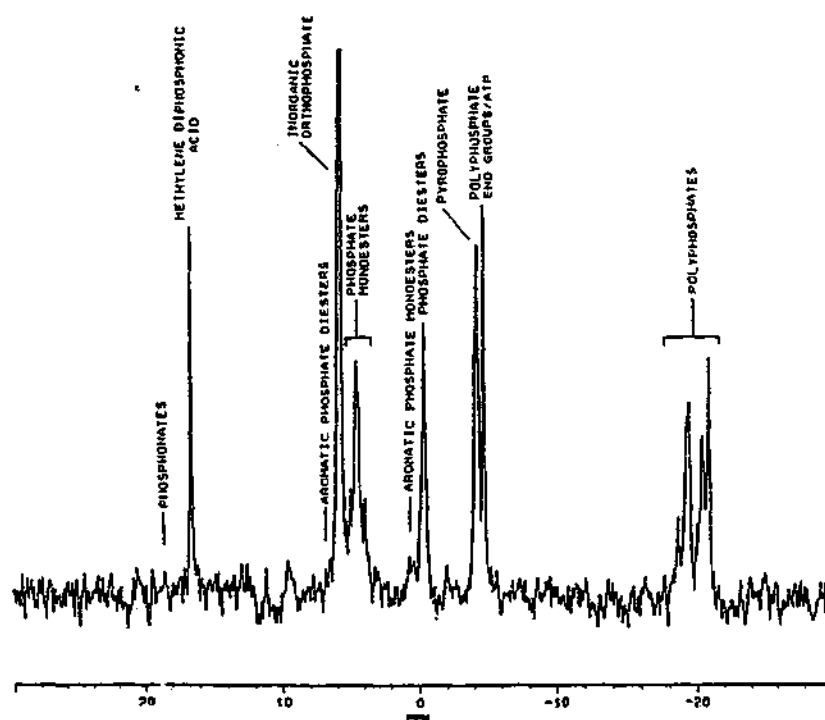


Figure 8.2: Chemical shift assignments for phosphorus forms present in peat, soil and humic acid. (Figure from Ref. [12])

^{31}P NMR has been employed to 0.5 M NaOH soil extracts to identify different phosphorus forms [9]. This includes comparison of the phosphate forms as a result of addition of fertilizer [10, 12] or a difference in climate and soil conditions [14]. Recently few experiments have been performed specifically on humic acids and their fractions [11, 15, 16].

Comparison of the different forms of phosphate after phosphate fertiliser treatment showed that addition orthophosphate or superphosphate produced an increase in phosphate monoester in soils [10, 12].

Another study on sludge amended soils revealed that whereas phosphate monoesters were more stable compared to phosphate diesters, which could be completely hydrolysed in

both acid and alkaline soils [17]. It was also observed that phosphate diesters could be affected by the climate and annual precipitation and become a ready supply of available phosphorus in the systems studied [14].

8.1.2 NMR SPECTROSCOPY

Nuclear magnetic resonance (NMR) is a very sensitive analytical technique that can provide information, which is difficult to obtain by chemical methods. This includes information on the quantity of the bound species, obtained from the peak areas provided that the data acquisition and data processing have been applied identically to all spectra. The chemical shift can give information on the functional groups involved in the binding.

^{13}C NMR is established as a standard method to investigate the functional groups of humic substances [18-23]. It was also mentioned in the previous section that ^{31}P NMR has been used to identify phosphorus forms in soil extracts [9, 10] and humic acid [11,13]. Simultaneous use of ^{13}C NMR and ^{31}P NMR can help identify the binding sites on the HA.

A brief overview of the general theory of NMR will be given in this section. More complete explanations can be found in standard text books on NMR spectroscopy [24-26]. There are also a few texts and review papers on specific applications of NMR spectroscopy on humic substances [18, 19, 27,28].

8.1.3 BRIEF OVERVIEW OF THE THEORY OF NMR SPECTROSCOPY

NMR is based on the measurement of absorption of electromagnetic radiation in the radio frequency range of about 4 to 600 MHz. Splitting of energy states of the nuclei is achieved by exposing the analyte to an intense magnetic field of several thousand hertz.

The difference between the energy levels (ΔE) is given by:

$$\Delta E = h\nu = \mu\beta \frac{H_0}{I} \quad (8.1)$$

where H_0 is the strength of external magnetic field (T), β is the nuclear magneton ($5.051 \times 10^{-24} \text{ J T}^{-1}$), μ is the magnetic moment of the particle (nuclear magneton), h is Planck's constant ($6.63 \times 10^{-34} \text{ J s}$) and I is the nuclear spin, and:

$$\mu = \frac{\gamma_n h I}{2\pi} \quad (8.2)$$

γ_n is called magnetogyric ratio and is a constant for a given nucleus.

Excitation to the higher nuclear magnetic quantum level can be brought about by absorption of a photon with energy that is equal to ΔE . This is called the resonance condition, which is satisfied by irradiating the sample with electromagnetic radiation at a frequency such that the photon energy is exactly ΔE . This leads to maximum absorption by the sample.

The factors affecting detection of a nucleus by NMR spectroscopy include: the natural

abundance of the isotope, concentration of the particular element in the sample, field strength and magnetogyric ratio of the element. The detectability is given as a comparison to proton. The detectability of ^{13}C is 1.76×10^{-4} and that of ^{31}P is 0.066. The natural abundance of ^{13}C is 1.1% and that of ^{31}P is 100%. The high abundance of ^{31}P makes this technique very useful in the study of orthophosphate-humic binding where the phosphate concentration is low.

THE CHEMICAL SHIFT

Structural information about the sample is obtained from the "Chemical Shift". The electrons around a nucleus alter the magnetic field experienced by it. It means that the actual magnetic field at the nucleus (H_{nucleus}) is different from that of the magnet (H_0) by a shielding factor (σ), Thus:

$$H_{(\text{nucleus})} = H_0 - \sigma H_0 \quad (8.3)$$

The shielding of a nucleus is a function of the chemical environment in the vicinity of that nucleus. Thus the resonance frequencies of the various nuclei in the chemical compound will give information on the chemical structure of the compound.

The NMR frequency of a given nucleus is generally measured relative to a suitable standard. This type of measurement gives rise to the so called Chemical shift (δ) and is defined as:

$$\delta = \frac{\nu_s - \nu_r}{\nu_r} \times 10^6 \quad (8.4)$$

Where ν_s and ν_r are the frequencies of the sample and reference. δ has a unit of parts per million (ppm). The chemical shift is based on difference from a standard and is independent of magnetic field [19, 24].

EXPERIMENTAL CONSIDERATIONS

The NMR spectrum for solids is generally broader than that obtained in solution. One of the main contributors to the line width in solid spectra is chemical shift anisotropy (anisotropic: having properties that differ according to the direction of measurement). The broadening results from changes in the chemical shift with the orientation of the molecule or part of the molecule, with respect to an external magnetic field. Line broadening due to chemical shift anisotropy can be removed by spinning the sample at 54.7° (magic angle spinning). The chemical shifts are isotropic in the liquid state NMR. The reason is that in liquid the disordered motion of a molecule caused by frequent and random collisions which includes rapid rotations, allows the sample to assume all possible orientations with equal probability, on the NMR time scale.

Static dipolar interaction (e.g. C-H bonds) can also contribute to the line width in the solid state NMR. In ^{13}C NMR, dipolar interactions can be removed by irradiating the sample at proton frequencies while collecting ^{13}C NMR spectra (dipolar decoupling).

Problems can also be caused by slow spin-lattice relaxation in solids. This can be overcome by a technique called cross polarization, which in principle uses a pulse technique to transfer the energy of the nuclei affected by the magnetic field (e.g. C), to another set of nuclei which are not under study (e.g. H) [19]. Several other techniques are used for signal enhancement and improving the spectrum resolution both in solid state

and liquid NMR spectroscopy. These can be found in standard NMR reference books [19, 24].

The presence of paramagnetic ions can effect the NMR spectra. For example carbons close to a paramagnetic centre may be undetectable. In the solid state, they can reduce the spin-lattice relaxation times. Therefore it is advised to reduce the concentration of paramagnetic ions in the sample as much as possible [27, 29].

Three sets of experiments have been carried out in this work. (1) solid state ^{31}P NMR was used in combination with solid state ^{13}C NMR to detect any irreversible binding between the humic acid and orthophosphate. For this purpose, orthophosphate was added to the Chaffey Reservoir humic acid and solid state ^{31}P NMR and ^{13}C NMR spectroscopy were used to detect the changes in the structure of humic acid as a result of addition of orthophosphate. (2) solution ^{31}P NMR spectra of the purified humic acid were collected before and after addition of orthophosphate at pH=8. (3) the pH was changed to see the effect of solution pH on the binding.

8.2 EXPERIMENTAL

8.2.1 SAMPLES

Orthophosphate in the form Na_2HPO_4 was used after drying at 110-130 °C for two hours. Millipore deionized water (Milli Q) was used in preparation of all samples. The NMR standard reference compounds, 85% H_3PO_4 and tetramethylsilane ($\text{Si}(\text{CH}_3)_4$) were used as obtained. All the plastic tubes and glassware used in the experiments were cleaned in 10% EXTRANTM overnight, followed by rinsing with deionized water, soaking

in 10% HCl bath overnight and rinsing with deionized water for several times.

Chaffey Reservoir humic acid (Chaffey HA) was isolated from Chaffey Reservoir sediment using the method recommended by the international humic substances society (IHSS) [30]. The total organic carbon was determined using a SHIMADZU™ TOC analyzer and the percentage of Fe was determined using a PERKIN-ELMER™ model 1100 flame atomic absorption spectrophotometer. Chaffey HA was used in the freeze-dried form for solid state NMR experiments. For solution NMR, a solution of about 2.3 mg dry weight of humic acid per mL of deionized water was prepared and concentrated to about 9.6 mg mL⁻¹ by stirring the sample under vacuum and condensing the vapor using liquid nitrogen.

8.2.2 NMR INSTRUMENT AND RUN CONDITIONS

NMR experiments were carried out by a Varian Unity Plus, 300 MHz instrument, using a frequency of 121.435 MHz for ³¹P NMR and 75.439 MHz for ¹³C NMR experiments. 85% H₃PO₄ was used as the external reference for ³¹P NMR and tetramethylsilane (TMS) for ¹³C NMR. Magic angle spinning and cross polarisation were regularly employed in obtaining solid state spectra. Solution experiments were performed using 10 mm NMR tubes. A D₂O field frequency lock was used. For solid state experiments 40-50 mg of the sample was packed in a Zirconia spinner with Kel-F turbines. The additional data processing were performed using Varian NMR data processing software, V-NMR, version 6.1. The concentrations of the material used either in solid state or solution state NMR experiments were kept relatively constant.

8.2.3 SAMPLE PREPARATION

SOLID-STATE ^{31}P AND ^{13}C NMR EXPERIMENTS

100 mg of freeze-dried Chaffey humic acid were mixed with 3 mL of deionized water containing 100 mg of Na_2HPO_4 ($[\text{PO}_4^{3-}] = 0.35 \text{ M}$) as an arbitrary excess amount. The mixture was shaken in a plastic tube for 48 hours and then freeze-dried. The freeze-dried sample was investigated by ^{31}P NMR and ^{13}C NMR spectroscopy.

DIALYSIS OF THE SAMPLE

60 mg of the freeze-dried HA sample with added orthophosphate were placed in a SPECTRAPOR™ dialysis bag with a nominal cutoff of 1000 daltons. The HA was dialyzed against deionised water until the free phosphate in the beaker was undetectable. The free phosphate concentration was measured by the ammonium molybdate method [31] using a flow injection analysis system (LCHAT QuickChem 8000™, USA).

SOLUTION NMR EXPERIMENTS

In these series of experiments, orthophosphate was added to the concentrated humic acid (about 5 mg C mL^{-1}) and ^{31}P NMR spectra of the concentrated pure sample and the sample plus phosphate in two different pH values of 9.3 and 4.6, were obtained in solution.

To observe the effect of Fe on the spectra, $\text{Fe}(\text{NO}_3)_3 \cdot 9\text{H}_2\text{O}$ was added to Na_2HPO_4 at the same proportion of the sample ($\text{Fe:P} = 10000$) and the ^{31}P NMR spectrum was collected using exactly the same NMR run conditions as used in the solution ^{31}P NMR of the HA sample.

8.3 RESULTS AND DISCUSSION

8.3.1 SOLID STATE ^{31}P OF CHAFFEY HUMIC ACID BEFORE AND AFTER ADDITION OF ORTHOPHOSPHATE

Addition of 0.35 M sodium orthophosphate to the Chaffey HA, resulted in a broad peak which is probably due to the added orthophosphate that masked the phosphate peak due to the humic acid (Figure 8.3(a)). Therefore not much information can be obtained from this spectrum. This sample was dialysed against deionized water and freeze dried again and the solid state ^{31}P NMR spectrum was collected (Figure 8.3 (b)). The spectrum is slightly broader than that of the same amount of pure humic acid. This might suggest a slight change in the phosphorus environment, which probably occurred during the dialysis and freeze drying processes.

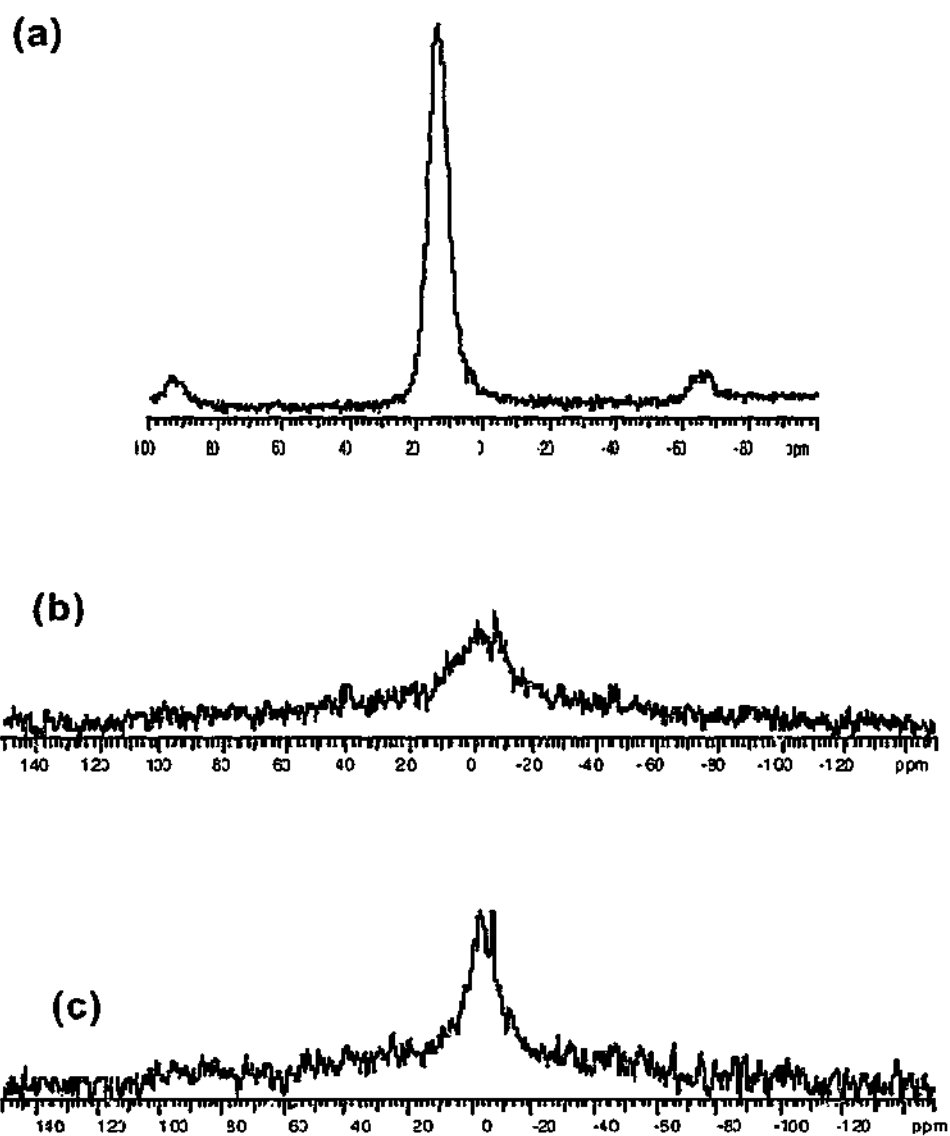


Figure 8.3: Solid state ^{31}P NMR spectra of (a) Chaffey HA with added orthophosphate (b) Chaffey HA with added orthophosphate and then dialysed, and (c) Pure Chaffey HA with the same amount as in (b).

8.3.2 SOLID STATE ^{13}C NMR OF SAMPLES BEFORE AND AFTER ADDITION OF ORTHOPHOSPHATE:

CPMAS (cross polarisation with magic angle spinning) solid state ^{13}C NMR spectra of pure HA and HA+ orthophosphate are presented in Figures 8.4(a) and (b). The features are similar to those reported in the literature [27, 32].

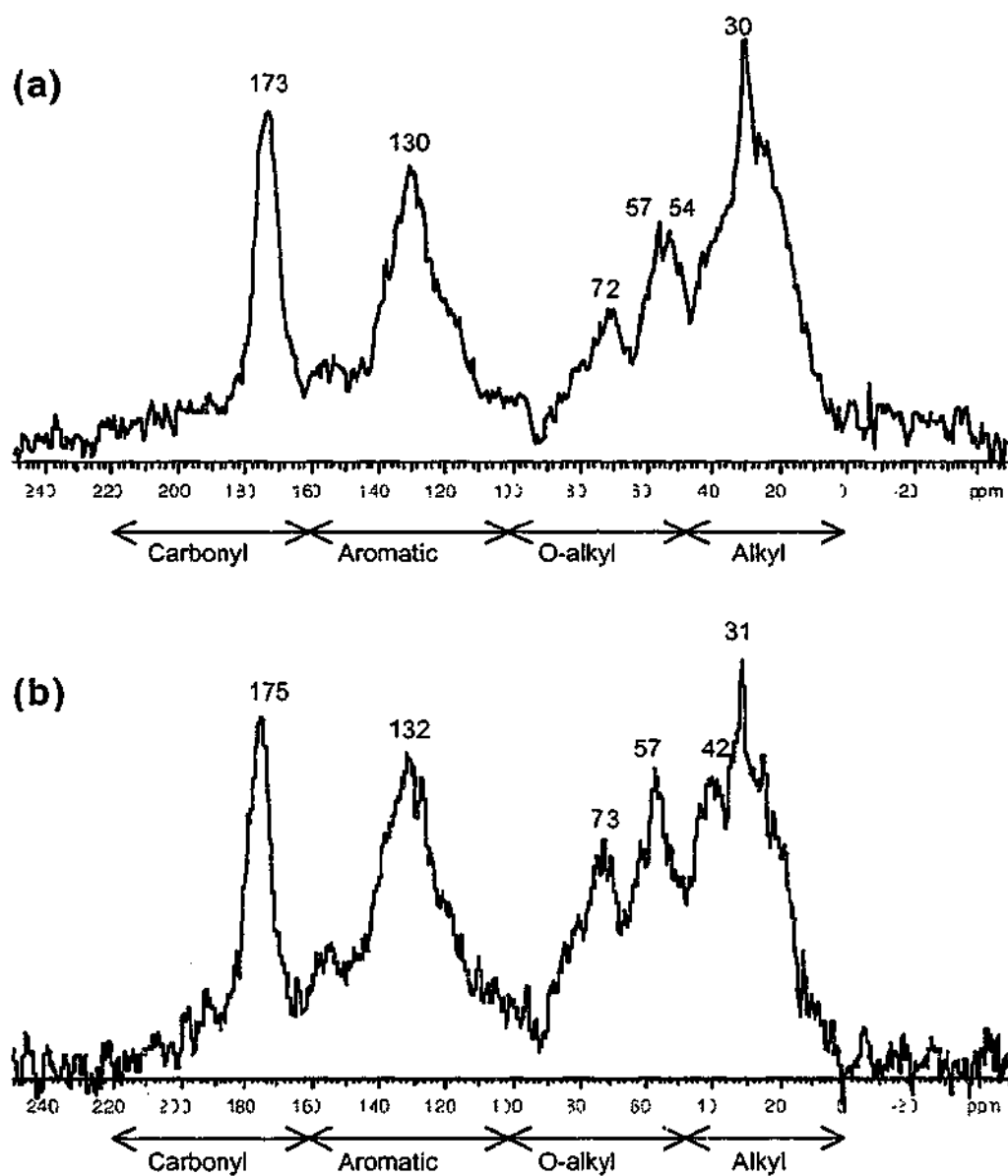


Figure 8.4: Solid state ^{13}C NMR spectrum of Chaffey humic acid (a) before and (b) after addition of orthophosphate

Comparison of the two spectra (Figure 8.4) shows that enhancement can be observed in the peak at about 40 ppm (aliphatic carbons). There is also a suggestion of changes in the region 50-60 ppm. Namely the change of the doublet peak to a singlet. These changes are associated with the alkyl and O-alkyl groups.

It can be suggested that a small amount of orthophosphate might have bound to the alkyl alcohol groups in the humic acid structure to produce a phosphate ester binding. Another possible reaction is the amidation reaction that can occur between orthophosphate and the amide groups. The esterification reaction is the more likely to happen because of the higher abundance of oxygen in the humic acid.

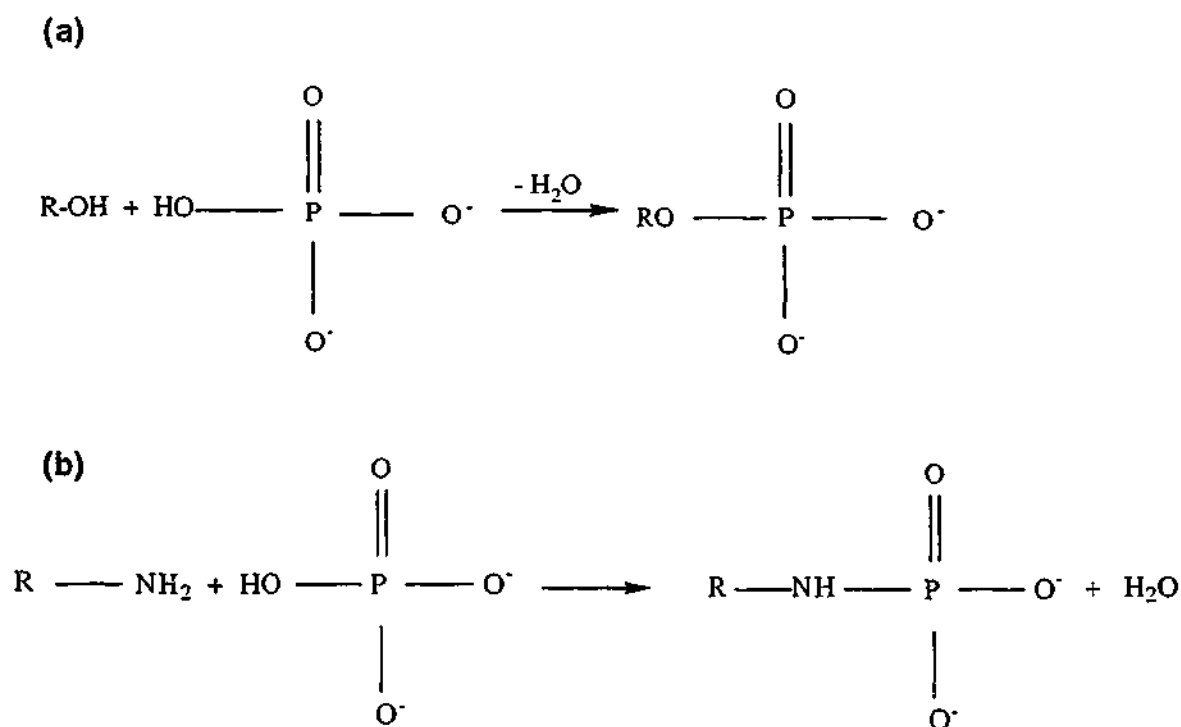


Figure 8.5 :Possible reactions that might have occurred between orthophosphate and some functional groups in Chaffey HA (a) reaction with alcohol groups to yield alkyl phosphates (b) reaction with amide groups [7].

8.3.3 SOLUTION ^{31}P NMR EXPERIMENTS:

More information on the forms of phosphates can be obtained from the solution ^{31}P NMR spectra. In this series of experiments, orthophosphate was added to the pure humic acid at pH=8 and the solution ^{31}P NMR spectrum was obtained before and after phosphate addition. The chemical shifts of the pure HA, HA after addition of 10^{-7} M orthophosphate at different pH values are summarized in Table 8.2.

Table 8.1: ^{31}P NMR chemical shifts of the pure HA and HA+ 10^{-7} M PO_4^{3-} at different solution pH. The chemical shifts have been assigned from the data available in the literature (references are given in brackets).

Peak Position (ppm)				Assignment
Pure HA (pH=8)	Pure HA + PO_4^{3-} (pH=8)	Pure HA + PO_4^{3-} (pH=9.3)	Pure HA + PO_4^{3-} (pH=4.6)	
-	-0.13	-0.12	-0.30	Phosphate diester[12]
0.42 2.04	1.48	1.51	0.8	Aromatic phosphate diester and nucleic acid[11]
3.83 5.03	3.00 4.94	3.36 3.95 4.84	4.95	Orthophosphate monoesters[12, 16]
6.72	6.20	6.20	6.08	Inorganic Orthophosphate [10]

EFFECT OF ADDITION OF ORTHOPHOSPHATE

Figure 8.6 (a) shows the ^{31}P NMR spectrum of concentrated HA ($\sim 5 \text{ mg C mL}^{-1}$) collected at pH ~ 8 . The spectrum displays five distinct peaks in the region of 0 - 6.6 ppm and is similar to the ^{31}P spectra presented by other researchers in the literature [12]. The peak at 20 ppm due to polyphosphate, reported by Newman *et al* [9] and Bedrock *et al.*[11] was not observed here. The absence of this peak can be explained in terms of the sample preparation. Purification of the humic acid sample by HCl and HF treatment has probably resulted in hydrolysis of the polyphosphate groups.

Figure 8.6 illustrates the solution ^{31}P NMR spectrum of Chaffey HA after addition of 10^{-7} M orthophosphate. pH of the HA (~ 8) did not change with addition of orthophosphate. Comparison of the two spectra (Figures 8.6 (a) and (b)) shows that the added orthophosphate is attached to the humic acid as three major groups: aromatic phosphate esters (1.5 ppm), orthophosphate monoesters (3.0-5.0 ppm) and inorganic orthophosphates (6.2 ppm). Attachment of the orthophosphate to the HA mostly in ester forms is consistent with the solid state ^{13}C NMR spectra that shows changes mainly due to the aliphatic and methoxyl carbons with addition of orthophosphate.

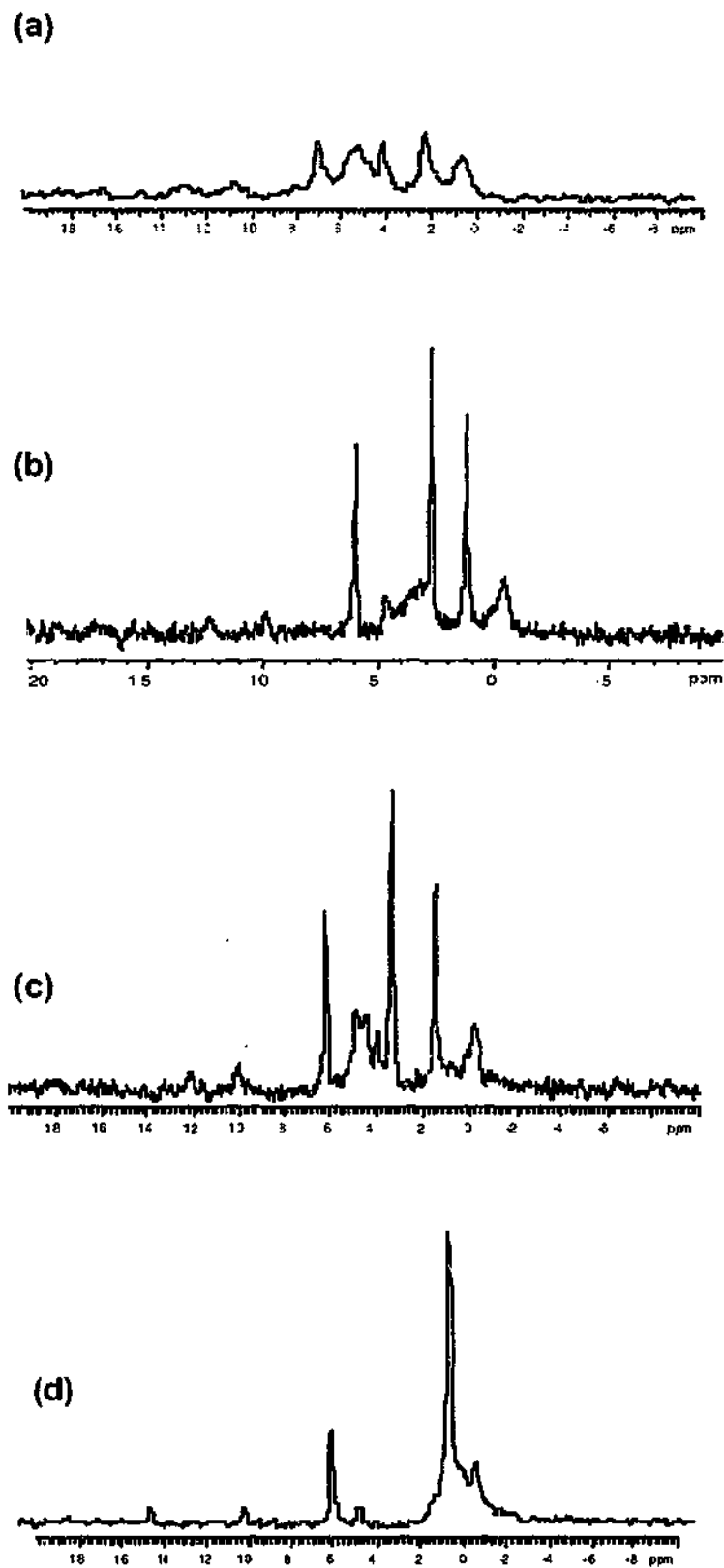


Figure 8.6: Solution ^{31}P NMR spectrum of Chaffey humic (a) Pure HA, pH=8 (b) HA after addition of 1×10^{-7} M orthophosphate pH=8, (c) HA after addition of 1×10^{-7} M orthophosphate pH=9.3 and (d) HA after addition of 1×10^{-7} M orthophosphate pH=4.6

The following paragraph should be read after the third paragraph in page 180.

This C/P ratio is very large compared to the C/P ratio of 1×10^3 - 1×10^4 normally found in humic substances [34-36]. This large difference indicates that although a direct bond may exist between the phosphorus and humic substances the amount of P bound in this way is probably negligible compared to the phosphate associated through bridging cations.

EFFECT OF CHANGE IN PH

Figure 8.6 (c) shows that changing the pH of the HA+orthophosphate solution from 8 to 9.3 resulted in an increase in the peak area in the region 3.3-5.0 ppm, which is assigned to the orthophosphate monoesters [9, 12].

When the pH was adjusted to 4.6 the spectrum changed significantly (Figure 8.6(d)). A major peak appeared in the 0-1 ppm which was assigned to phosphate diesters [9, 12]. The peak previously at 3.0 ppm due to orthophosphate monoesters is not observed in this spectrum. Two potential reasons can be suggested for this. Firstly, it is possible that bonding of humic acid to this particular phosphate group was affected by changing the solution pH for example hydrolysis as a result of acidification. The second reason could be the a decrease in the charge density of P and shift of the NMR peak towards 0 ppm, as a result of protonation of the P-O bond.

These results suggest that in this particular humic acid, orthophosphate is probably attached to the aliphatic sites in the HA structure, probably as orthophosphate esters. The ratio of the orthophosphate used to the amount of humic acid present may indicate the extent of orthophosphate binding to this humic acid. The total organic carbon of this particular humic acid was determined to be 56% (TOC and elemental analysis). From the concentrations of the humic acid and the added orthophosphate, the atomic ratio of carbon to phosphorus (C/P) can be calculated as approximately 5×10^6 .

8.3.4 EFFECT OF Fe

It is expected that the presence of paramagnetic ions would result in the peak broadening in NMR spectra. Therefore the peaks where P is attached to Fe (metal bridging [33]), should not be observed in the spectra presented here. Despite the careful sample purification used (0.3 M HF/0.1 M HCl treatment), the Chaffey HA contains about 0.2% Fe as determined

by atomic absorption spectroscopy. The molar ratio of added P to Fe present in the humic acid could therefore be estimated to be about 1:10000.

To observe whether or not any of the peaks observed in the previous spectra result from binding to Fe, ^{31}P NMR spectrum of a mixture of $\text{Fe}(\text{NO}_3)_3 \cdot 9\text{H}_2\text{O}$ and Na_2HPO_4 with P:Fe molar ratios of 1:10000 (same ratio as the added orthophosphate to the Fe present in the Chaffey HA sample), was collected under similar conditions (Figure 8.7). No peak was observed for orthophosphate after 3 days. This suggests that the Fe in the humic acid might have been bound in a manner that makes it unavailable for binding to the orthophosphate. If there is binding between the added orthophosphate and the Fe in the HA, then the peak due to the Fe bound orthophosphate would not be observed.

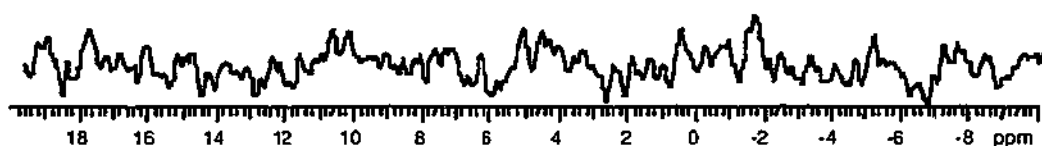


Figure 8.7: Solution ^{31}P NMR spectrum of a solution of 10^{-7} M PO_4^{3-} and 10^{-4} M Fe^{3+} (Fe:P ratio of 1:10000).

8.4 CONCLUSIONS

Interactions between natural organic matter and orthophosphate are generally explained in terms of a metal bridging. While this might be the dominant mechanism, other possibilities may also exist. In this work a humic acid sample was prepared with a relatively low amount of Fe, Al and Mn (0.19%, 0.03% and 0.27%, see Appendix 2) and it was then spiked with orthophosphate. The orthophosphate binding to the humic acid was detected by NMR spectroscopy. Solid state CPMAS ^{13}C NMR of the HA before and after addition of orthophosphate suggested binding in the aliphatic and O-alkyl groups as a

result of orthophosphate addition. Solution ^{31}P NMR experiments also suggested adsorption of orthophosphate by humic acid possibly in the forms of orthophosphate mono and diesters. Change of pH from 8 to 9.3 did not result in a significant change in the solution ^{31}P spectrum of the sample. But a change to 4.6 resulted in diminishing the peak due to orthophosphate monoesters. This was explained in terms of acid hydrolysis of the orthophosphate monoesters.

Solution ^{31}P NMR spectrum of a solution of iron and orthophosphate, made in the same ratio as the added orthophosphate to the iron present in the HA, showed no peak. This suggested that if orthophosphate was binding to the humic acid, via Fe ion, it could not be observed in the spectra obtained. Possibly the iron is already bound and is not available to the orthophosphate.

This work demonstrates the potential of combining ^{13}C and ^{31}P NMR in both solid and liquid states to study the interaction of orthophosphate with humic substances, even though the results did not provide evidence of the exact nature of the binding.

This series of NMR experiments was based on the hypothesis that orthophosphate can directly bind to humic substances. NMR spectroscopy was chosen to test this hypothesis because batch adsorption methods were not found to be suitable. Although a long acquisition time is required to obtain the NMR spectra with relatively good signal to noise ratios, NMR spectroscopy could provide information about both the nature of binding sites and the quantity of adsorption, without the necessity of phase separation.

This is a major limitation in those studies using other analytical techniques such as inductively coupled plasma mass spectroscopy (ICP-MS), atomic absorption spectroscopy (AAS) or flow injection analysis (FIA).

8.5 REFERENCES

1. Vollenweider, R.A., Scientific fundamentals of the eutrophication of lakes and flowing waters, with particular reference to nitrogen and Phosphorus as factors in eutrophication, 1968, OECD: Paris.
2. Harris, G.P., Phytoplankton Ecology., Chapman and Hall. London, 1986 .
3. Levesque, M., and Schnitzer, M., Organo-metallic interactions in soils: 6. Preparation and properties of fulvic acid-metal phosphates, Soil Science, 103 (1967) 183-190.
4. Minear, R.A., Characterisation of naturally occurring dissolved organophosphate compounds, Environmental Science and Technology, 6 (1972) 431-437 .
5. Sinha, M.K., Organo-metallic phosphates I, Interaction of phosphorus compounds with humic substances, Plant and soil, 35 (1971) 471-484.
6. Kastelan, M., and Petrovic M., Competitive sorption of phosphate and marine humic substances on suspended particulate matter, Water Science and Technology, 32 (1995) 349-355.
7. Solomons, T.W.G., Organic Chemistry. John wiley & Sons. New York. 1984.
8. Edmundson, R.S., Phosphoric acid derivatives, in I.O. Sutherland, (Ed.), Nitrogen Compounds, Carboxylic Acids, Phosphorus Compounds, Pergamon Press: Oxford. 1979, 1256-1300.

9. Newman, R.H., and Tate, K.R., Soil phosphorus characterisation by ^{31}P NMR, *Communications in Soil Science and Plant Analysis*, 11 (1980) 835-842.
10. Hawkes, G.E., Powlson, D.S., Randall E.W., and Tate, K.R., A ^{31}P nuclear magnetic resonance study of the phosphorus species in alkali extracts of soils from long-term field experiments, *Journal of Soil Science*, 35 (1984) 35-45.
11. Bedrock, C.N., Cheshire, M.V., Chudek, J.A., Goodman, B.A. and Shand, C.A., ^{31}P NMR studies of humic acid from a blanket soil, in N. Senesi, and Miano, T.M., (Eds.), *Humic Substances in the Global Environment and Implications on Human Health*, Elsevier Science, 1994, 227-232.
12. Bedrock, C.N., Cheshire M.V., Chudeck J.A., Goodman B.A., Shand C.A., Use of ^{31}P -NMR to study the forms of phosphorus in peat soils, *the Science of the Total Environment*, 152 (1994) 1-8.
13. Ogner, G., ^{31}P -NMR spectra of humic acids: a comparison of four different raw humus types in Norway, *Geoderma*, 29 (1983) 215-219.
14. Tate, K.R., and Newman, R.H., Phosphorus fractions of a climosequence of soils in New Zeland Tussock grassland, *Soil Biol. Biochem.*, 14 (1982) 191-196 .
15. Bedrock, C.N., Cheshire M.V., Chudeck J.A., Fraser A.R., Goodman B.A., Shand C.A., Effect of pH on precipitation of humic acid from peat and mineral soils on the distribution of phosphorus forms in humic and fulvic acids fractions, *Communications in Soil Science and Plant Analysis*, 26 (1995) 1411-1425.
16. Makarov, M.I., Phosphorus compounds of soil humic acid, *Eurasian Soil Science*, 30 (1997) 395-402.
17. Hinedi, Z.R., Chang, A.C. and Leem R.W., Mineralization of phosphorus in sludge-amended soils monitored by phosphorus- 31 nuclear magnetic resonance spectroscopy, *Soil Science Society America Journal*, 52 (1988) 1593-1596 .

18. Wershaw, R.L., and Mikita M.A., NMR of Humic Substances and Coal. Techniques, Problems and Solutions. Lewis Publishers, Chelsea, MI, 1987 .
19. Wilson, M.A., Techniques and Applications of Nuclear Magnetic Resonance Spectroscopy in Geochemistry and Soil Science. Pergamon Press. Oxford, 1987.
20. Steenlink, C., Wershaw, R.L., Thorn, K.A., Wilson, M.A., Application of Liquid-state NMR spectroscopy to humic substances, in M.H.B. Hayes, MacCarthy, P., Malcolm, R.L., and Swift, R., (Eds.), Humic Substances II, In search of structure, John Wiley & Sons: Chichester. 1989, 281-308.
21. Hatcher, P.G., Schnitzer, M., Dennis, L. W., and Maciel, G. E. Aromaticity of humic substances in soils, in Soil Science Society of America Journal, 45 (1981) 1089-94.
22. Krosshavn, M., Bjorgum, J.O, Krane, J., and Steinnes, E., Chemical structure of terrestrial materials formed from different vegetation characterized by solid-state ^{13}C NMR with CP-MAS techniques, Journal of Soil Science, 41 (1990) 371-377.
23. Preston, C.M. and M. Schnitzer, Carbon-13 NMR of humic substances: pH and solvent effects, Journal of Soil Science , 38 (1987) 667-78.
24. Becker, E.D., High Resolution NMR Theory and Chemical Applications. Academic Press. New York, 1980 .
25. Mason, J., Multinuclear NMR. Plenum Press. New York, 1987 .
26. Sanders, J.M., and Hunter, B.K., Modern NMR Spectroscopy, A Guide for Chemists. Oxford University Press. New York, 1990 .
27. Preston, C., Applications of NMR to soil organic matter analysis: History and prospects, Soil Science, 161 (1996) 144-166 .
28. Humic Substances II. In Search of Structure, Ed. M.B. Hayes, MacCarthy, P., Malcolm, R., and Swift, R., John Wiley & Sons, Chichester, 1989.

29. Wilson, M., Solid-State nuclear magnetic resonance spectroscopy of humic substances: basic concepts and techniques., in M.H.B. Hayes, MacCarthy, P., Malcolm, R.L., and Swift, R., (Eds.), Humic Substances II, In search of structure, John Wiley & Sons, Chichester, 1989, 309-338.
30. Swift, R.S., Organic matter characterisation, in D.L. Sparks, (Ed.), Methods of Soil Analysis, Soil Science Society of America and American Society of Agronomy: Madison, Wisconsin. 1996, pp. 1011-1069.
31. Freeman, P.R., McKelvie, I.D., Hart, B.T., and Caldwell, T.J., A flow injection analysis technique for the determination of low levels of phosphorus in natural waters, *Analytica Chimica Acta*, 234 (1990) 409-416.
32. Wershaw, R.L., Pinckney D.J., NMR characterization of humic acid fractions from different Philippine soils and sediments, *Analytica Chimica Acta*, 232 (1990) 31-42.
33. Gressel, N., McColl, J.G., Preston, C., Newman, R.H. and Powers R.F., Linkages between phosphorus transformations and carbon decomposition in a forest soil, *Biogeochemistry*, 33 (1996) 97-123.
34. Mills, M.S., Thurman, E.M., Ertel, J. and Thorn, K., Organic geochemistry and sources of natural aquatic foams, in Gaffney, J.S. et al (Eds.), Humic and Fulvic Acids: Isolation, Structure and Environmental Role, American Chemical Society 1996, pp 151-192.
35. Thurman, E.M., Organic Geochemistry of Natural Waters, Martinus Nijhoff/Dr W. Junk publishers, Dordrecht, 1985.
36. MacCarthy, P., and Malcolm, R.L., The nature of commercial humic acids, in Suffet, I.H. and MacCarthy, P. (Eds.), Aquatic Humic Substances, Influence on Fate and Treatment of Pollutants, American Chemical Society, Washington DC.1989, pp 55-63.

CHAPTER 9

CONCLUSIONS AND RECOMMENDATIONS FOR FUTURE WORK

Humic substances are stated to be "nature's least understood materials" [1]. Their complexity is the reason why the subject of characterization of humic substances is so exciting and challenging. One of the key parameters for understanding the reactions of humic substances is the knowledge of their average molecular parameters like size and molecular weight. Many methods have been used for this purpose. They either need calibration (HPSEC, UF) or require long acquisition times (UC). The majority (except for equilibrium UC) can estimate one average parameter and an indication of the polydispersity. The only way to obtain the distribution of the molecular parameters is to use a separation technique.

FIFFF is a separation technique. Acquisition time is not long, it does not involve interaction with a stationary phase and it can give the diffusion coefficient and hydrodynamic diameter of the sample species without calibration. This technique also gives

a distribution of the preceding parameters, from which different averages can be calculated. FIFFF instruments are now available commercially and are equipped with data processing software. They are easier to use than the laboratory research versions. FIFFF has been used to characterize humic substances since 1987 [2].

9.1 MAJOR OUTCOMES OF THE THESIS:

One of the outcomes of this thesis is that the results obtained from FIFFF fall in the same range as those obtained from methods like FCS, PFG-NMR, AFM and HPSEC. This strengthens the degree of confidence that can be placed on the analysis of molecular parameters of humic substances using FIFFF.

Chapter 6 explains the application of FIFFF controversial issue; Separation of humic substances by membrane ultrafiltration (UF). UF is an attractive separation method, since it can isolate large volumes of humic substances with relative ease. The results of this chapter suggest that separation by some commonly used UF membranes are probably based more on structure than size, and one should be very cautious, when handling data generated by UF.

A major outcome of this thesis is the application of the force measurement aspect of AFM in the characterization of humic substances. It was seen earlier in Chapter 7, that AFM was used for the measurement of forces between a goethite surface and a silica probe. The effect of the introduction of humic substances to the goethite substrate was also studied. This research has demonstrated the enormous potential of AFM, not only as an imaging tool for humic substances, but also as a means to measure their interactive forces.

The adsorption of orthophosphate onto humic substances is an important environmental issue as explained in Chapter 8. Direct orthophosphate adsorption experiments on humic

acid are very tedious, if not impossible, because of the major problems of species phase separation and detection. The combined ^{13}C , ^{31}P NMR study could help identify the orthophosphate binding sites on the humic acid.

9.2 RECOMMENDATIONS FOR FUTURE WORK:

A detailed characterisation of humic substances can be carried out using a combination of FIFFF and HPSEC (performed in optimised conditions of carrier and column packing). Fractions can be obtained from HPSEC runs and analysed for size by FIFFF. Each fraction can then be further analysed for functional groups by ^{13}C NMR spectroscopy, metal contents by ICP-MS and ICP-AES and surface charge using zeta potential measurements or atomic force microscopy. The fractions can be used for batch metal and contaminant adsorption experiments.

AFM can be used to measure the interactive forces between humic substances in different pH and salt concentrations and also in the presence of contaminants in solution. The goethite surface developed in Chapter 7 can be used as a substrate to immobilise humic substances. It is possible to modify the system here, so that the interactive forces between two humic surfaces can be measured.

The computer simulation used in Chapter 5 can be used to study the effect of solution conditions on the conformation of different model humic substances in solution.

The study of the humic-orthophosphate binding using combined ^{31}P and ^{13}C NMR spectroscopy can be advanced by performing experiments in the same condition and by addition of orthophosphate. Integration of the ^{31}P NMR peak area should give a quantitative estimate of orthophosphate binding to the humic acid.

Thermal FFF can be used to determine the size distribution of humin. Thermal FFF yields the ratio of the diffusion coefficient to the thermal diffusion coefficient.

9.3 OVERVIEW OF THESIS

This thesis has presented FIFFF as a major technique to investigate molecular parameters of humic substances and the environmental issues related to their size and molecular weight (where FIFFF is applicable). These subjects include a study of the aggregation of humic substances, the characterisation of humic substances which have been separated by methods such as UF and HPSEC and the validation of other measurement techniques including FCS and PFG-NMR. The advantages and limitations and of FIFFF have been explored and discussed throughout.

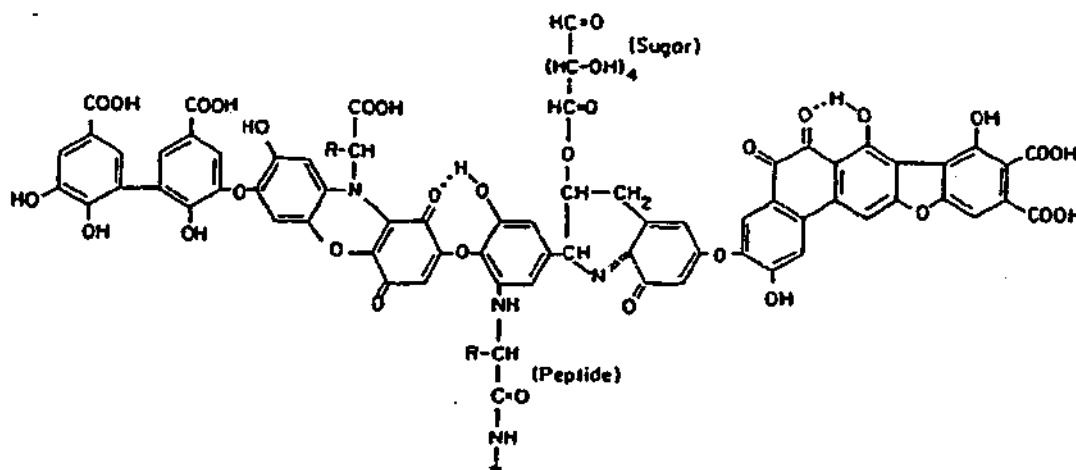
AFM and NMR have also been used in studying the environmental interactions of humic substances. Some new approaches have been introduced; the use of AFM for the measurement of interactive forces between humic substances and model minerals, development of a goethite surface for imaging of humic substances in solution and the combined use of ^{13}C and ^{31}P NMR in investigation of orthophosphate adsorption onto pure humic substances.

I hope that the research presented in this thesis has introduced some approaches that could help in a better understanding of the mysterious world of humic substance. In particular I would anticipate that FIFFF could be used with more ease and confidence to measure the molecular parameters of humic substances.

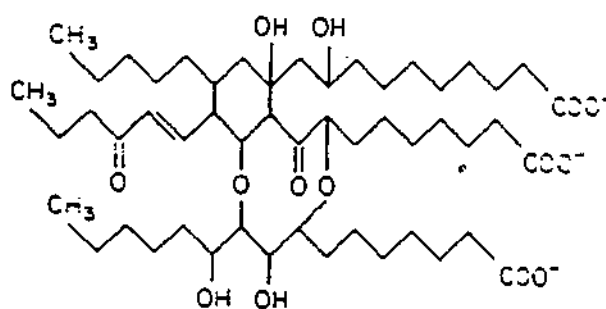
9.4 REFERENCES

1. Davis, G. and Ghabour, E.A, Preface, in Davis, G., and Ghabour, E.A. (Eds.), *Humic Substances: Structures, Properties and Uses*, The Royal Society of Chemistry, Cambridge. 1998.
2. Beckett, R., Zhang J., and Giddings C., Determination of molecular weight distributions of fulvic and humic acids, using flow field-flow fractionation, *Environmental Science and Technology*, 21 (1987) 289-295.

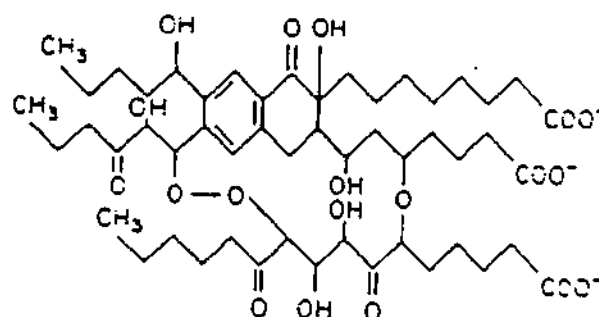
Stevenson: 1982 [4]:



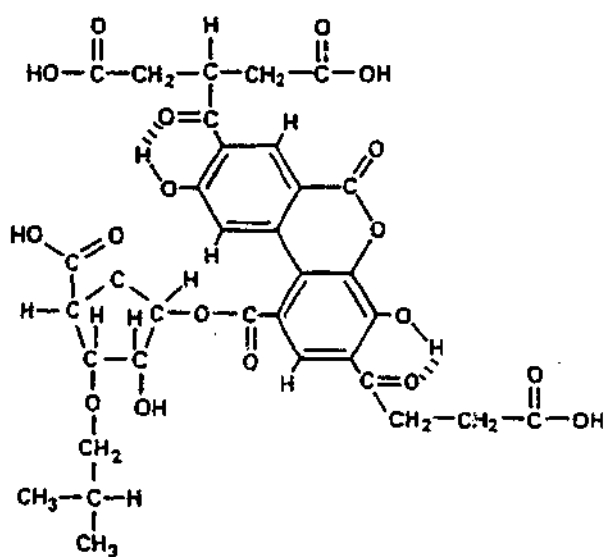
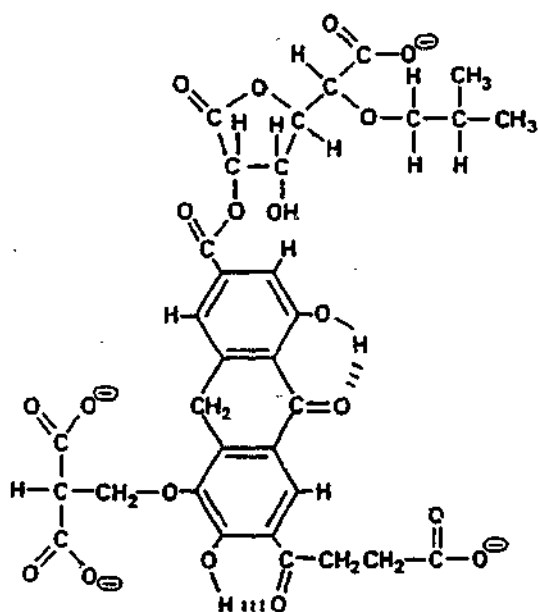
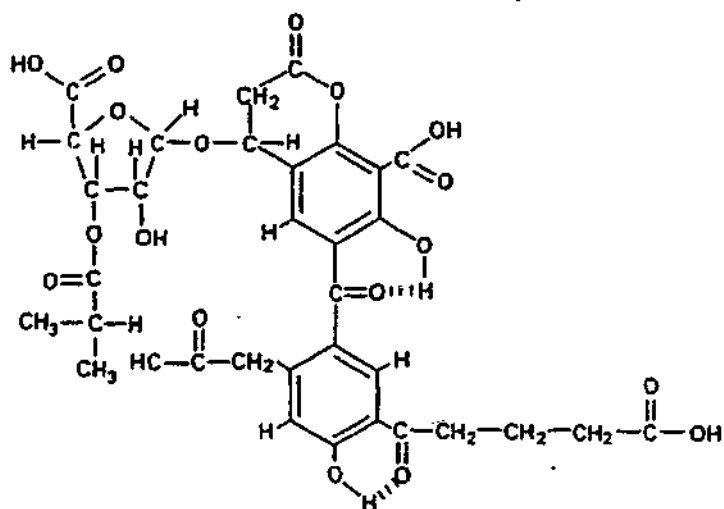
Harvey 1983 [5]:

Marine
Fulvic Acid

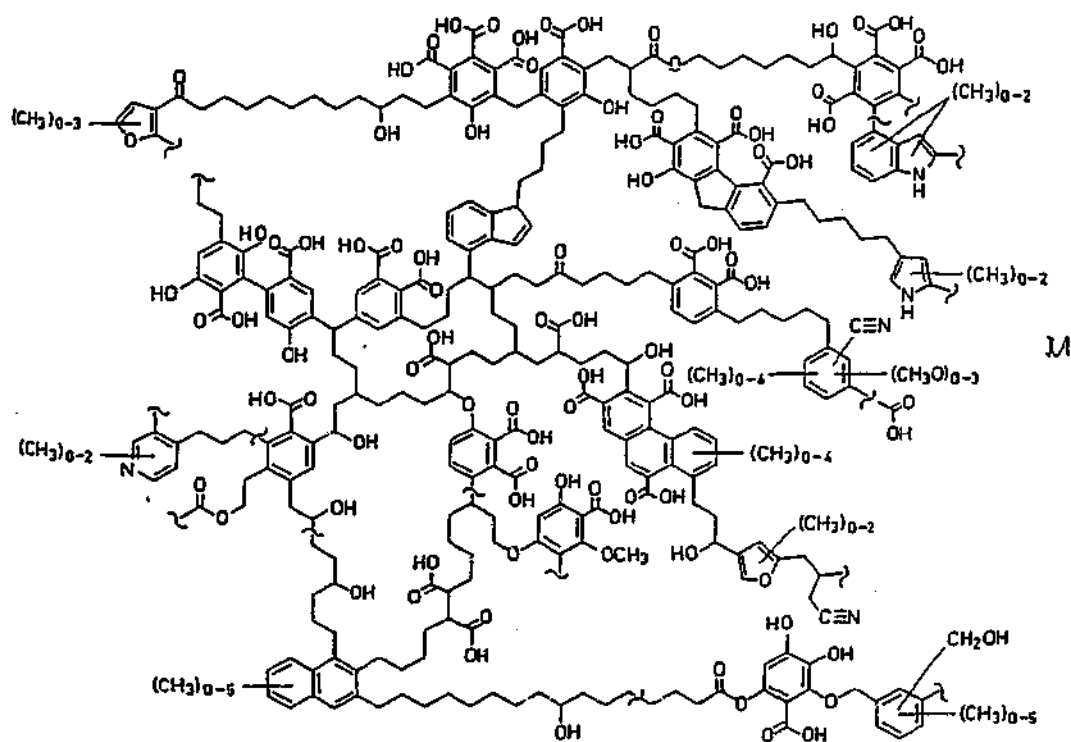
↓ ETC.

Marine
Humic Acid

Leenheer 1995 [6]:



Schulten 1993 [7]:



References:

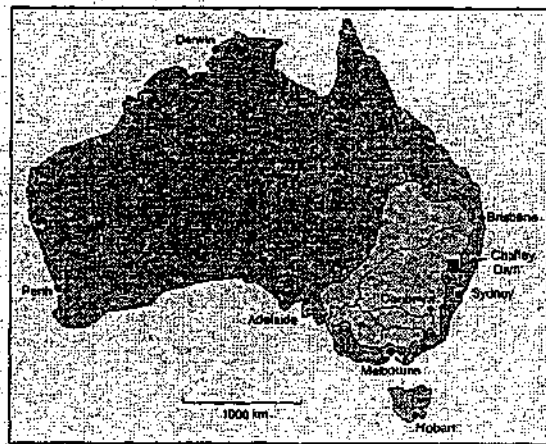
1. Flaig, W., Comparative chemical investigations on natural organic compounds and their model substances, *Scientific Proceedings of Royal Dublin Society*, 4 (1960) 49-62 .
2. Buffle, J., Gerter, F.L., and Haredi, W., Measurement of complexation properties of humic and fulvic acids in natural waters with lead and copper ion-selective electrodes, *Analytical Chemistry*, 49 (1977) 216-222 .
3. Schnitzer, M., and Khan ,S.U., *Soil Organic Matter*, Elsevier Scientific Publication Company, (1978) .
4. Stevenson, I.L. and M. Schnitzer, Transmission electron microscopy of extracted fulvic and humic acids, *Soil Science*, 133 (1982) 179-85 .

5. Harvey, G.R., Boran, D.A., Chesal, L.A., and Tokar, J.M., The structure of marine fulvic and humic acids, *Marine Chemistry*, 12 (1983) 119-132 .
6. Leenheer, J.A., McKnight, D.M., Thurman, E.M., MacCarthy, P., Humic Substances in the Suwannee River, Georgia: Interactions, properties and proposed structures, . 1995, US Geological Survey: Denver.
7. Shulten, H.R., and Schnitzer, M., A state of the Art structural concept for humic substances, *Naturwissenschaften*, 80 (1993) 29-30 .

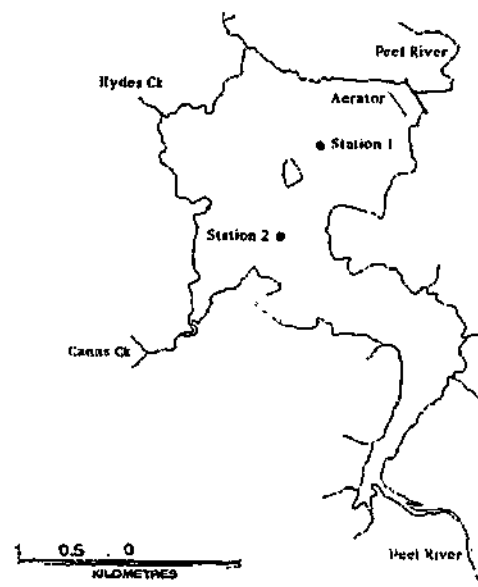
APPENDIX 2

ISOLATION AND CHARACTERISATION OF CHAFFEY HA:

The Chaffey sediment was collected by Jason van Berkel from Chaffey dam Reservoir which is located on the Peel River in northern NSW, Australia. Chaffey Reservoir supplies water for irrigation and to the city of Tamworth from about 16 meters deep. The location of the dam and the sampling station is given below:



Position of Peel River and Chaffey dam.



Position of the sampling stations in Chaffey Reservoir.

The humic acid was isolated from Chaffey sediment using the procedure recommended by the International Humic Substances Society (IHSS)[1]:

ISOLATION AND PURIFICATION OF CHAFFEY HA AND FA:

The air-dried sediment was crushed and passed through 500 μm sieve. The sample was extracted with a volume of 0.1 M HCl equal to ten times the weight of the sample. The pH of the solution was adjusted between 1 and 2 using 1 M HCl.

The sediment-HCl mixture was shaken for 1 hour and the suspension was allowed to settle. The mixture was centrifuged at 3500 rpm for one hour and the supernatant was separated. The sediment was neutralised with 1 M NaOH to pH 7 under nitrogen gas and a volume of 0.1 M NaOH equal to ten times the weight of the sample was added under nitrogen. The mixture was shaken for 4 hours and was allowed to settle overnight.

The supernatant was then separated from the sediment by centrifugation. The pH of supernatant was adjusted to 1.0 with 6 M HCl and allowed to stand overnight. The sediment was separated by centrifugation and redissolved in 0.1M KOH under nitrogen. The K^+ concentration was adjusted to 0.3 M with KCl to solubilise the humic fraction.

The solution was again centrifuged. The supernatant was acidified to pH 1 using 6 M HCl and allowed to stand overnight. The sediment (humic acid), was then separated by centrifugation. The humic acid was suspended in a solution of 0.1 M HCl and 0.3 M HF overnight, to remove the mineral matter. The mixture was centrifuged and the precipitated humic acid was dialysed against deionised water until a negative chloride test was obtained with AgNO_3 .

The fulvic acid fraction was purified by passing it through XAD-8 resin, eluting with NaOH and passing through a cation exchange resin.(Bio-Rad AG-MP-50).

CHARACTERISATION OF CHAFFEY HUMIC AND FULVIC ACIDS:

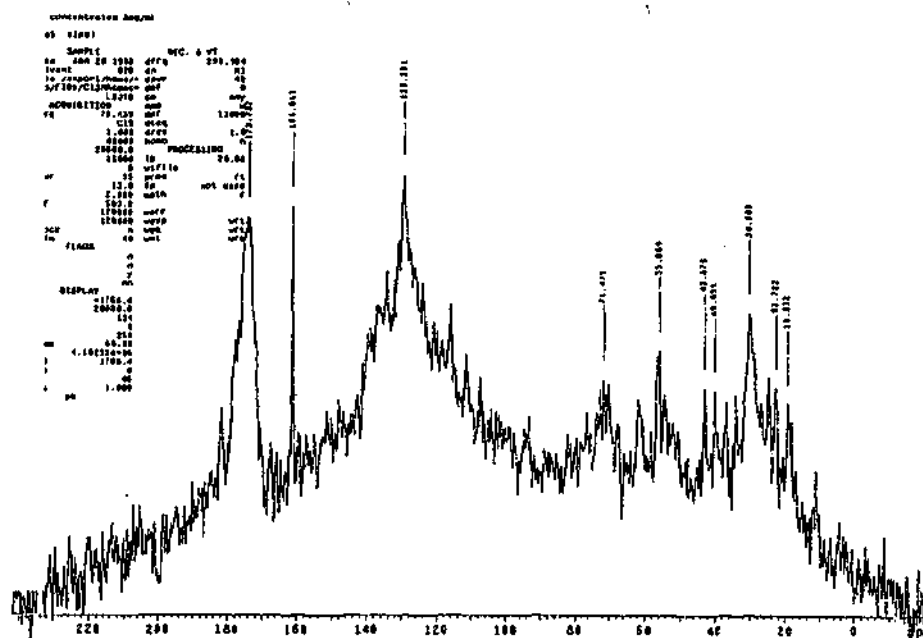
The purified humic and fulvic acid samples were characterised by elemental analysis. The metal contents were determined using a PERKIN-ELMER™ model 11100 flame atomic absorption spectrophotometer, after digestion in HNO₃. The humic acid fraction was further analysed by ¹³C NMR, ¹H NMR and ³¹P NMR.

ELEMENTAL AND METAL PERCENTAGE ANALYSIS:

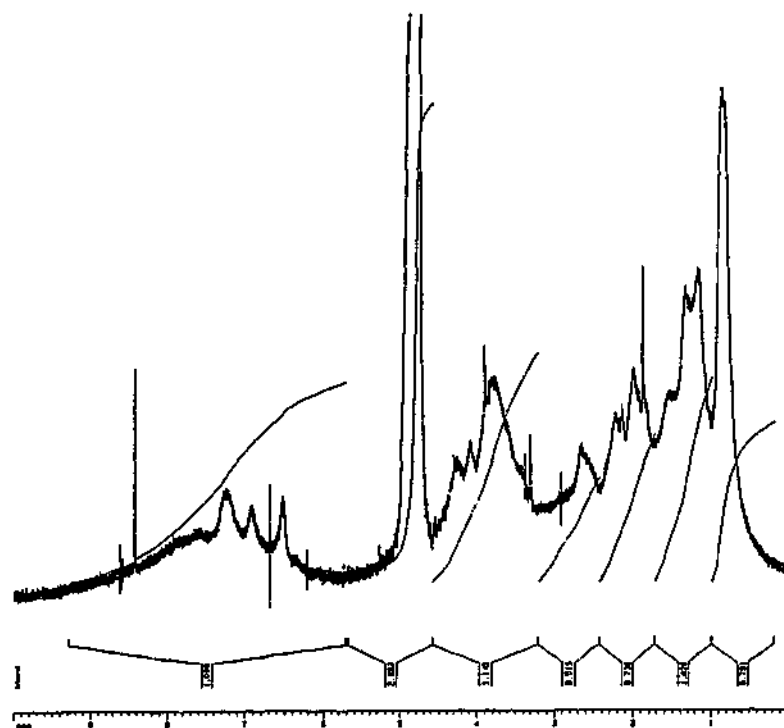
Table A2-1: Results of the elemental analysis and percentage of metals in Chaffey HA:

Sample	%C	%H	%N	%Fe	%Al	%Mn
Chaffey HA	50.0	5.1	5.1	0.19	0.28	0.003

NMR SPECTRA OF CHAFFEY HA:



Solution ¹³C NMR spectrum of Chaffey HA:



^1H NMR spectrum of Chaffey HA:

References:

1. Swift, R.S., Organic matter characterisation, in D.L. Sparks, (Ed.), *Methods of Soil Analysis*, Soil Science Society of America and Am. Soc. Agronomy: Madison, Wisconsin. 1996, 1011-1069 .

APPENDIX 3:

SPECIFICATIONS OF SOME COMMONLY USED ULTRAFILTRATION MEMBRANES

The membranes used in the literature reviewed, together with their nominal molecular weight cut off (MWCO) and some specifications [1-4].

Membrane	Nominal MWCO (K daltons)	Specifications*
YCO5	0.5	Hydrophilic
YM2	1	Hydrophilic, Regenerated Cellulose, Probably IEP* pH~4
YM5	5	
YM10	10	
YM50	50	
YM100	100	
UM05	0.5	Polyelectrolyte Complex Cellulosic IEP* pH~4
UM2	1	
UM10	10	
UM20	10	
UM20E	20	
XM50	50	Hydrophobic, (moderately hydrophilic) Acrylic Copolymer, poly (acrylonitrile-co-vinyl Chloride),
XM100	100	
XM100A	100	
XM300	300	
PM10	10	Hydrophobic, Polysulfone IEP*: pH 8
PM30	30	
SPS 20	APD† = 14 nm	Sulphonated Polysulfone
SPSB/50	APD† = 13 nm	
GR 61	20K, APD† = 4-12nm	Polysulfone, hydrophobic, non ionic, IEP: pH 3.7
GS 61		Sulfonate Polysulfone, hydrophilic, ionic,
FS 61	20K, APD† = 4- 12nm	Modified polyvinylidene Fluoride, slightly hydrophilic, IEP: pH 3.3
	20K, APD† = 4- 12nm	

† APD= Average Pore Diameter , *IEP=Isoelectrical point

References:

1. McGregor, W.C., Membrane Separations in Biotechnology. Bioprocess Technology, W.C. McGregor. (Ed.), Vol. 1. Marcel Dekker. New York, 1986 .
2. Amicon Co., Membrane Filtration Chromatography Catalogue, (1993) .
3. Nystrom, M., Lindstrom M., and Matthiasson, E., Streaming potential as a tool in the characterisation of ultrafiltration membranes, Colloids and Surfaces, 36 (1989) 297-312 .
4. Kabsch-Korbutowicz, M. and Winnicki, T., Application of modified polysulfone membranes to the treatment of water solutions containing humic substances and metal ions, Desalination, 105 (1996) 41-49 .